A Thesis
entitled

Curvilinear Extension to the Giles Non-reflecting Boundary Conditions for Wall-bounded Flows

by

Shivaji Medida

Submitted as partial fulfillment of the requirements for the
Master of Science Degree in Mechanical Engineering

Advisor: Dr. Ray Hixon

Graduate School

The University of Toledo
August 2007

An Abstract of

Curvilinear Extension to the Giles Non-reflecting Boundary Conditions for Wall-bounded Flows

Shivaji Medida

Submitted in partial fulfillment
of the requirements for the
Master of Science Degree in Mechanical Engineering

The University of Toledo
August 2007

In the present work, the Giles non-reflecting boundary conditions have been extended to Curvilinear co-ordinates for wall-bounded flows. In addition to the non-reflecting boundary conditions, wall boundary conditions have been derived and implemented for inflow/outflow-wall corners (grid points common to the inflow/outflow and wall boundaries) so that the flow solution at the corner points satisfies both the inflow/outflow boundary conditions and the wall boundary conditions. Two-dimensional, wall-bounded, Ringleb flow configurations (with non-orthogonal grids and curved boundary geometries) were used as test cases to validate the non-reflecting boundary conditions and the wall corner conditions. The wall corner conditions for the Cartesian Giles boundary conditions were sufficient to eliminate the flow through wall at inflow and outflow corners. However, the Cartesian Giles boundary conditions along with the wall corner conditions could not solve the corner problem in the Ringleb flow test cases and eventually caused the flow solution to diverge. Two-dimensional Curvilinear Giles boundary conditions derived from the Curvilinear form

of the linearized Euler equations resulted in additional terms that were not present in the chain rule form of Cartesian Giles boundary conditions. These additional terms contained the factor $(\xi_x\eta_x + \xi_y\eta_y)$ which becomes zero for an orthogonal grid. The Curvilinear Giles boundary conditions, when implemented without the additional terms, displayed the same corner problem that was encountered with the chain rule form of Cartesian Giles boundary conditions, proving the significance of the additional orthogonal terms. In order to completely eliminate flow through the wall and obtain the correct solution at the corners, the Curvilinear boundary conditions with the additional terms and the wall corner conditions were required. The Curvilinear Giles boundary conditions along with the wall corner conditions were successfully tested on various Ringleb flow geometries and grid densities. However, a long-term instability was noticed for all the Ringleb flow configurations beyond a certain number of grid points. This was eliminated by stretching the grid towards the inflow and outflow boundaries. Converged solutions were obtained for all the test cases with acceptable L2 errors.

Acknowledgments

I would like to express my sincere gratitude to Dr. Ray Hixon for his invaluable guidance and support throughout the course of my Masters research work at The University of Toledo. I have greatly benefited from the meaningful discussions I had with Dr. Hixon on relevant research topics such as computational physics and boundary conditions. I have learned much about insightful and fundamental research under his guidance.

I would like to thank Dr. Abdollah Afjeh and Dr. Sorin Cioc for serving on my thesis defense committee.

This research was funded by the **NASA Glenn Research Center contract NNC06GA07G**, supervised by the technical monitor, Dr. Edmane Envia.

Financial support during my graduate study was provided also by the MIME Department at The University of Toledo.

Contents

List of Figures

List of Tables

Nomenclature

η	Curvilinear co-ordinate corresponding y-direction
γ	Ratio of specific heats
Λ	Diagonal matrix of eigenvalues
μ	$\xi_x\eta_x + \xi_y\eta_y$
ν	$\xi_x\eta_y - \xi_y\eta_x$
ω	Wave frequency
$\overline{\rho}$	Mean density
$\overline{p}$	Mean pressure
$\overline{U}$	Contravariant mean velocity in $\xi -$ direction
$\overline{u}$	Mean flow speed in x-direction
$\overline{V}$	Contravariant mean velocity in $\eta -$ direction
$\overline{v}$	Mean flow speed in y-direction
$\overline{v}_n^L$	First order approximation to the left eigenvector corresponding to λ_n

$\overline{w}$	Mean flow speed in z-direction
$\overrightarrow{c_g}$	Group velocity column matrix
$\overrightarrow{m}$	Unit vector tangent to the non-reflecting boundary
$\overrightarrow{N_w}$	Unit vector normal to the wall boundary
$\overrightarrow{n}$	Unit vector normal to the non-reflecting boundary
Φ	$\sqrt{\eta_x^2 + \eta_y^2}$
Ψ	$\sqrt{\xi_x^2 + \xi_y^2}$
ρ	Instantaneous density
ξ	Curvilinear co-ordinate corresponding x-direction
$\xi_x, \xi_y, \eta_x, \eta_y$	Grid metrics
C	Matrix of reflection co-efficients
c	Speed of sound
C_i	Characteristic variables of Euler equations
k	Wavenumber in x-direction
l	Wavenumber in y-direction
m	Wavenumber in z-direction
p	Instantaneous pressure

u	Instantaneous flow speed in x-direction
u_n^L	Left eigenvector of the dispersion relation, corresponding to the eigenvalue λ_n
u_n^R	Right eigenvector of the dispersion relation, corresponding to the eigenvalue λ_n
v	Instantaneous flow speed in y-direction
v_n^L	Alternate definition of the Left eigenvector of the dispersion relation, corresponding to the eigenvalue λ_n
w	Instantaneous flow speed in z-direction
w_n^L	Left eigenvector of the dispersion relation, corresponding to the eigenvalue $\lambda_n = 0$
w_n^R	Right eigenvector of the dispersion relation, corresponding to the eigenvalue $\lambda_n = 0$

The University of Toledo

College of Engineering

I HEREBY RECOMMEND THAT THE THESIS PREPARED UNDER MY SUPERVISION BY Shivaji Medida

ENTITLED Curvilinear Extension to the Giles Non-reflecting Boundary Conditions for Wall-bounded Flows

BE ACCEPTED IN PARTIAL FULFILLMENT OF THE REQUIREMENTS FOR THE DEGREE OF Master of Science in Mechanical Engineering

---

Thesis Advisor: Dr. Ray Hixon

Recommendation concurred by

_____ Committee

Dr. Abdollah Afjeh on

_____ Final Examination

Dr. Sorin Cioc

Dean, College of Engineering

Chapter 1

Introduction

1.1 Motivation

Numerical modeling often involves solution of a given set of governing equations over a finite computational domain. While the domain could be naturally bounded by physical boundaries such as a solid wall, an artificial free-surface boundary is sometimes introduced in order to limit the extent of the domain and make the modeling feasible. Examples of such situations include limited-area problems in oceanography and meteorology and the modeling of fluid flows in exterior domains. The governing equations for these physical problems (such as the Euler equations of gas dynamics, the shallow water equations, Maxwell's equations, the equations of magnetohydrodynamics, the classical wave equation and, the elastic wave equation) are all hyperbolic systems of partial differential equations. From a mathematical point of view, in order to determine a unique solution to a given set of hyperbolic partial differential equations, it is necessary to specify an *Initial Solution* and impose conditions on the

solution at the non-physical and/or physical boundaries. These imposed conditions are commonly known as *Boundary Conditions*. The resulting problem is called an *Initial-Boundary Value Problem* (IBVP). To formulate a well-posed IBVP, the correct number of boundary conditions must be specified. Over-specification or under-specification of boundary conditions will lead to an ill-posed problem. In some cases, the correct boundary conditions to be imposed can be easily identified from physical considerations. At a solid wall boundary, it is trivial that there is no flow passing through the wall and hence the normal component of flow momentum must be set to zero. In case of a viscous flow, the tangential component of momentum is also set to zero (the no-slip boundary condition). But, at artificial boundaries, the choice of boundary conditions is not so obvious since the boundaries do not correspond to anything physical. From a numerical implementation point of view, at any interior grid point, if there are no source terms, the flow variables are computed directly using the data at the neighboring grid points. The need for boundary conditions arises at grid points on the boundaries (both physical and non-physical), where sufficient information for such computations is not available to the flow solver. These boundary conditions are very important since they are used to inform the interior flow solver of what is occurring outside the computational domain, and thus set the problem definition correctly.

1.2 The Physical Problem

We are interested in solving unsteady fluid flow problems which are governed by hyperbolic system of equations. A hyperbolic system of equations represents waves propagating in various directions. These waves carry information about the flow through the flow domain under consideration. At a domain boundary, some of these waves propagate into the computational domain and some of them propagate outwards. One of the primary goals of artificial boundary conditions should be to ensure that no waves enter the computational domain except for those specified by the user and that the outgoing waves do not produce any spurious reflections back into the domain. The resulting boundary conditions are known as *Non-reflecting Boundary Conditions.* When solving a steady flow problem, any change in the flow variables is considered as an error. It is desirable to quickly get past the initial transient phase during a steady flow simulation and obtain convergence. Reflecting boundary conditions are sufficient to solve steady flow problems. However, they require longer computational duration since they cause spurious reflections back into the domain and might allow undesirable waves to enter the domain through the boundaries. Non-reflecting boundary conditions are more accurate and obtain a converged steady flow solution much faster than reflecting boundary conditions.

To specify characteristic based non-reflecting boundary conditions, the waves must be grouped into two distinct sets of incoming and outgoing waves. To demonstrate the characteristic analysis to identify the waves represented by the hyperbolic governing equations, a brief discussion of the Thompson characteristic boundary conditions [1],

[2] is provided here.

Fig (1-1) shows a simple two dimensional computational domain.

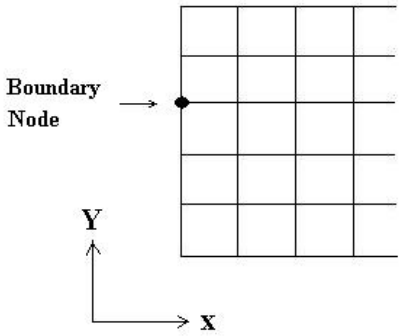

Figure 1-1: **2D Computational Domain**

The two dimensional Euler equations in non-conservative form can be written as

$$\frac{\partial Q}{\partial t} + [A]\frac{\partial Q}{\partial x} + [B]\frac{\partial Q}{\partial y} = 0 \tag{1.1}$$

where,

Q is a column matrix of the primitive variables (ρ, u, v, p), A and B are 4x4 matrices. At the boundary whose normal is in the x-direction, the $y-$derivative term in Eq. (1.1) can be calculated from the existing data from neighboring points using the interior flow equations. But we need to specify additional conditions to compute the x-derivative at the boundary node. For nodes at intersection of two boundaries (corners), conditions must be specified to compute both the x and the y derivative terms.

Eqn. (1.1) can be re-written as

$$\frac{\partial Q}{\partial t} + [A] \underbrace{\frac{\partial Q}{\partial x}}_{\text{needs BC}} = -[B] \underbrace{\frac{\partial Q}{\partial y}}_{\text{known}} = S \tag{1.2}$$

Now,

$$[A] = [T][\Lambda][T]^{-1} \tag{1.3}$$

where,

columns of $[T]$ are the right eigenvectors of $[A]$,

rows of $[T]^{-1}$ are the left eigenvectors of $[A]$, and

$[\Lambda]$ is a diagonal matrix of eigenvalues of $[A]$. The eigenvalues $[\Lambda]$ are,

$$[\Lambda] = \begin{pmatrix} u & 0 & 0 & 0 \\ 0 & u & 0 & 0 \\ 0 & 0 & u+c & 0 \\ 0 & 0 & 0 & u-c \end{pmatrix} \tag{1.4}$$

where $c = \sqrt{\gamma RT}$ is the speed of sound, and the corresponding left eigenvectors are,

$$\begin{aligned} l_1 &= \begin{pmatrix} c^2 & 0 & 0 & -1 \end{pmatrix} \\ l_2 &= \begin{pmatrix} 0 & 0 & 1 & 0 \end{pmatrix} \\ l_3 &= \begin{pmatrix} 0 & \rho c & 0 & 1 \end{pmatrix} \\ l_4 &= \begin{pmatrix} 0 & -\rho c & 0 & 1 \end{pmatrix} \end{aligned} \tag{1.5}$$

Substituting $[A]$ in Eq. (1.2),

$$\frac{\partial Q}{\partial t} + [T][\Lambda][T]^{-1}\frac{\partial Q}{\partial x} = S \tag{1.6}$$

Pre-multiply by $[T]^{-1}$ to obtain:

$$[T]^{-1}\frac{\partial Q}{\partial t} + [\Lambda][T]^{-1}\frac{\partial Q}{\partial x} = [T]^{-1}S \tag{1.7}$$

Define a new function $dC_i = l_i dQ - l_i S dt$, then Eq. (1.7) becomes:

$$\frac{\partial C_i}{\partial t} + [\lambda_i]\frac{\partial C_i}{\partial x} = 0 \tag{1.8}$$

which is a set of wave equations whose characteristic velocities are the elements of λ_i. Each wave amplitude C_i is constant along a curve in the $x - t$ plane with a slope $dx/dt = \lambda_i$.

Each one of the eigenvalues and eigenvectors is related to the physical flow properties. For a subsonic flow,

1. l_1 corresponds to a downstream-running entropy wave propagating at the flow speed $\lambda_1 = u$,

2. l_2 corresponds to a downstream-running vorticity wave propagating at the flow speed $\lambda_2 = u$,

3. l_3 corresponds to a downstream-running acoustic wave propagating at a speed $\lambda_3 = u + c$,

4. l_4 corresponds to a upstream-running acoustic wave propagating at a speed $\lambda_3 = u - c$.

Fig (1-2) shows the one-dimensional characteristics and their direction of propagation at a subsonic outflow boundary.

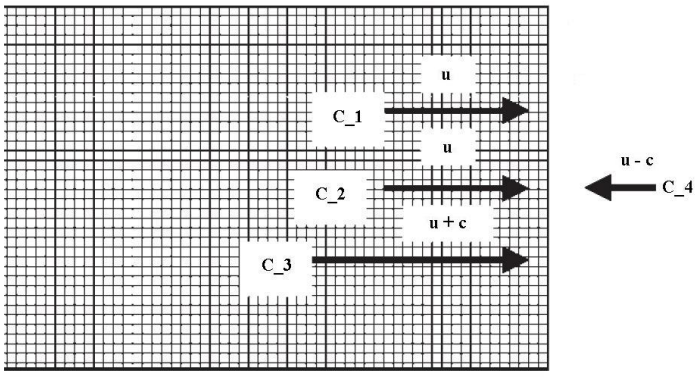

Figure 1-2: **Characteristics at a Subsonic Outflow Boundary**

Hedstrom's [45] definition of a non-reflecting boundary condition can be stated as: *The amplitude of the incoming waves are constant, in time, at the boundaries.* This statement is equivalent to saying that there are no incoming waves, as it is the change in the amplitude which indicates a wave. A mathematical representation of this condition for the incoming waves is

$$\left.\frac{\partial C_i}{\partial t}\right|_{\text{boundary}} = 0, \tag{1.9}$$

in terms of the wave amplitude C_i, or

$$\left.\left(l_i \frac{\partial Q}{\partial t} + l_i \frac{\partial Q}{\partial y}\right)\right|_{\text{boundary}} = 0 \tag{1.10}$$

The direction of propagation determines whether the interior flow solution should set the amplitudes of these eigenvectors or whether the user must. For example, if the boundary is a subsonic grid boundary with the outgoing normal pointing in the positive x-direction ($u > 0, u + c > 0, u - c < 0$), then the interior flow would be used to set the entropy, vorticity and downstream-running acoustic waves (C_1, C_2, C_3) and the user must specify the incoming acoustic wave C_4. Note that the incoming waves that must be specified by the user at a grid point depend on the grid and flow geometry as well as the local velocity direction and magnitude. Once the amplitudes of these waves are specified, the values of the derivatives normal to the boundary can be calculated and used in the governing equations.

At a two-dimensional, subsonic outflow, there is one incoming characteristic C_4 and three outgoing characteristics C_1, C_2, and C_3. According to the Thompson boundary conditions, the boundary condition at the outflow would be $\frac{\partial C_4}{\partial t} = 0$. Specification of constant pressure at the outflow boundary as $\frac{\partial p}{\partial t} = 0$, results in a perfectly reflecting boundary condition. In terms of $\frac{\partial C_i}{\partial t}$,

$$\frac{\partial p}{\partial t} = \frac{1}{2}\left(\frac{\partial C_3}{\partial t} + \frac{\partial C_4}{\partial t}\right) \tag{1.11}$$

If $\frac{\partial p}{\partial t} = 0$, the incoming characteristic would then be,

$$\frac{\partial C_4}{\partial t} = -\frac{\partial C_3}{\partial t} \tag{1.12}$$

as opposed to the non-reflecting condition $\frac{\partial C_4}{\partial t} = 0$.

Clearly, a non-physical acoustic wave is being reflected back into the domain in the form of $\frac{\partial C_3}{\partial t}$ due to the application of the classical constant pressure boundary condition.

Define vector L as,

$$L = [\Lambda][T]^{-1}\frac{\partial Q}{\partial x} = \begin{pmatrix} \lambda_1\left(c^2\frac{\partial \rho}{\partial x} - \frac{\partial p}{\partial x}\right) \\ \lambda_2\left(\frac{\partial v}{\partial x}\right) \\ \lambda_3\left(\frac{\partial p}{\partial x} + \rho c\frac{\partial u}{\partial x}\right) \\ \lambda_4\left(\frac{\partial p}{\partial x} - \rho c\frac{\partial u}{\partial x}\right) \end{pmatrix}$$

A general form of the boundary condition for incoming and outgoing waves as given by Thompson [1] is

$$\left(l_i\frac{\partial Q}{\partial t} + L_i + l_i\frac{\partial Q}{\partial y}\right)\Big|_{boundary} = 0, \tag{1.13}$$

where

$$L_i = \begin{cases} \lambda_i l_i\frac{\partial Q}{\partial x} & \text{for outgoing waves,} \\ 0 & \text{for incoming waves.} \end{cases} \tag{1.14}$$

1.3 Problem Statement

It is important to note that in the characteristic analysis presented in the previous section, waves are treated as one-dimensional and propagating normal to the boundary (by ignoring the tangential derivative terms), which is not the case in realistic flows. This approximation results in partial reflection of waves incident at an angle

and perfect reflection of the waves propagating tangential to the boundaries. Hence the boundary conditions based on one-dimensional characteristics are generally not accurate. The work of Giles [46] shows that the Thompson boundary conditions are a zeroth order Taylor series approximation to the exact non-reflecting boundary conditions which is less accurate than the higher order approximations. However, Giles [46] showed that the first order Taylor series approximation results in an ill-posed set of boundary conditions for the Euler equations. Another serious problem of concern is that at wall corners (in two-dimensional domains) and edges (in three-dimensional domains) the non-reflecting boundary conditions are most reflecting. Also they may not be compatible with the wall boundary conditions and cause a non-physical flow normal to the wall. As it will be shown in the present work, this corner problem leads to divergence of the flow solution in many cases when the Giles boundary conditions are used. In the present work, the instability of Giles boundary conditions [46] due to incompatibility of boundary conditions at corners and edges is of concern. To fix this problem, compatibility conditions that blend the non-reflecting boundary conditions with the wall boundary conditions are required at wall corners and edges. Most of the artificial boundary conditions are developed in Cartesian or polar co-ordinate systems, including Giles boundary conditions. Unlike the Thompson boundary conditions, the Giles boundary conditions require characteristics of neighboring points to compute the characteristics at a given point on the boundary. Since the Giles boundary conditions were derived from the Cartesian form of Euler equations, it is essential for the characteristics at every grid point to be at the same angle (normal to the boundary) for consistency, thus restricting the boundary shapes to straight lines (in

two-dimensional problems) and planes (in three-dimensional problems). It is desirable to construct these boundary conditions in Curvilinear co-ordinates for problems involving irregular boundary geometries. The boundary conditions in Curvilinear co-ordinates implicitly account for the curvature of the boundary.

1.4 Background

Several researchers have been working on the development of non-reflecting boundary conditions since the early 1970s. Review articles by Givoli [5], Tam [7],[8], Lele[9], Tsynkov[10], Hagstrom[6], Colonius [11], and Hixon [12] discuss the formulation, implementation, and performance of various non-reflecting boundary conditions applicable to acoustics, electrodynamics and fluid mechanics. More recently, Caraeni and Fuchs [13] analyzed a series of the existing non-reflecting boundary conditions (with an emphasis on boundary conditions for turbulent flows) and proposed an improved outflow boundary condition for simulation of sound produced by turbulence. Givoli[5] summarizes the following goals that one should keep in mind when developing a new set of boundary conditions:

- *The problem together with the boundary conditions is mathematically well-posed.*
- *The problem together with the boundary conditions is a good approximation of the original problem in the infinite domain*
- *The boundary conditions are highly compatible with the numerical scheme used.*

- *The numerical scheme employed together with the boundary conditions must result in a stable numerical scheme.*
- *The amount of spurious reflection generated by the boundary conditions is small.*
- *The use of the boundary conditions does not involve a large computational effort.*
- *In time-dependent scheme where only the steady state solution is sought, the numerical scheme should reach the steady state rapidly.*

Inflow and outflow boundary conditions can broadly be classified into two types: (1) non-local boundary conditions, and (2) local boundary conditions. The exact boundary conditions are non-local in space for steady problems and in both space and time for unsteady problems (that is, they are not expressed as differential equations, but as integrals over space and time). Formulation of non-local boundary conditions involves integral transforms along the boundaries and pseudo-differential operators which can be quite complicated to obtain for irregular boundary geometries. Moreover, the non-locality of the boundary conditions makes them computationally inefficient in spite of the numerical accuracy they provide (with minimal or no spurious reflections) since they require a knowledge of flow history over the entire computational time and space to be implemented at a particular grid point.

Local boundary conditions are obtained by approximating the exact boundary conditions using polynomial (Taylor series) [46], rational functional (Padé series) approximations [64] or asymptotic expansions [22].The resulting boundary conditions are geometrically universal (readily applicable to the various irregular geometries

encountered in practical applications), simpler to implement, and computationally inexpensive. However, local boundary conditions are inaccurate and produce more spurious reflections compared to the non-local boundary conditions. Also, most of the local boundary conditions have been constructed so that spurious reflections are kept very small (or vanish entirely) only in certain modes, or at certain angles of incidence, or for a certain range of frequencies. The choice of boundary conditions is essentially a compromise between accuracy and computational efficiency with ease of implementation.

There are several approaches to the construction of non-reflecting boundary conditions. Each of these approaches is essentially a result of a different assumption used to localize the exact boundary conditions. In general, the available methods can be divided into three distinct groups.

1.4.1 Boundary Conditions based on 1-D Characteristics or Riemann Invariants

These boundary conditions are based on grouping the wave modes supported by a system of hyperbolic equations into incoming and outgoing waves with respect to their direction of propagation. As mentioned earlier, at any given boundary, some of the waves are propagating into the computational domain while others are propagating out of it. The outward propagating waves have their behavior defined entirely by the solution at and within the boundary, and no boundary conditions can be specified for them. The inward propagating waves depend on the solution exterior to the

domain and therefore require boundary conditions to complete the specification of the behavior. Exact boundary conditions are hence obtained by setting the amplitudes of incoming waves to zero while the amplitudes of the outgoing waves are computed based on interior flow solution using one-sided boundary stencils. Engquist and Majda [40] developed a systematic method for obtaining a hierarchy of non-local boundary for general classes of wave equations by applying the theory of reflection of singularities for solutions of differential equations ([41], [42], [43]). They derived approximate local boundary conditions from the the exact boundary conditions using Taylor and Padé series approximations. Hedstrom[45] developed boundary conditions based on an eigenvector approach for one-dimensional non-linear Euler equations. Thompson ([1], [2]) extended Hedstrom's work to multi-dimensional problems and developed a general boundary condition formalism for all types of boundary conditions to which hyperbolic systems are subject. These boundary conditions are developed for multi-dimensional problems by performing a local analysis normal to the far-field boundary and ignoring all tangential derivatives. This approach (referred to as the quasi-one-dimensional or characteristic based boundary conditions) remains the most commonly used for unsteady flow calculations. The Thompson boundary conditions [2] were later extended to Curvilinear co-ordinates by Rodman [44].

As mentioned earlier, one of the most important issues to deal with when developing a new set of boundary conditions is their well-posedness. The work of Kreiss [3] which examined the problem of well-posedness of IBVPs for hyperbolic systems in multiple dimensions formed a firm theoretical foundation for later research. Well-posedness is the requirement that a solution exists, is unique, and is bounded in the

sense that the magnitude of the solution (defined using an appropriate norm) divided by the magnitude of the initial and boundary data (defined using some other norm) is less than some function which depends on time but not on the initial and boundary data. Any hyperbolic system arising from a physical problem ought to be well-posed and so it is critical that any far-field boundary conditions which are used to truncate the solution domain must result in a well-posed problem. Higdon[4] has written an excellent review of the work of Kreiss and others, and in particular gives a physical interpretation of the theory in terms of wave propagation.

Giles ([46]) developed a unified theory for the construction of steady-state and unsteady boundary conditions (both exact and approximate forms) for two-dimensional linearized Euler equations based on the theoretical work of Engquist and Majda [40] to construct both exact and approximate boundary conditions, and the well-posedness theory of Kreiss [3]. His approach is based upon Fourier analysis and eigenvectors (similar to Hedstrom's work [45]). Giles used Taylor series to obtain non-local first and second order boundary conditions from exact boundary conditions. Complete details of the formulation of Giles boundary conditions can be found in [47]. These boundary conditions have been implemented for steady and unsteady turbomachinery flow calculations and the precise numerical details are given in [49]. A significant original contribution of Giles work is the analysis of well-posedness of boundary conditions for Euler equations. Kreiss [3] and subsequent investigators assumed for simplicity that there is no degeneracy in the eigenvalues of the hyperbolic system under consideration. Trefethen and Halpern [48] show that the approximate boundary conditions for the scalar wave equation are ill-posed if a second or higher order Taylor series

approximation is used. The Euler equations have a multiple root with distinct eigenvectors, and at a particular complex frequency there is an eigenvalue/eignevector coalescence. Also, an unexpected result is that the outflow boundary condition is well-posed, whereas the inflow boundary conditions are found to be ill-posed. Giles derived modified well-posed inflow boundary conditions using an *ad hoc* method based on the order of reflection co-efficients. Later, he extended these boundary conditions to steady-state quasi-three-dimensional boundary conditions [50]. Banica et al. [51] extended the 2D boundary conditions developed by Giles to non-uniform mean velocity inflow and outflow boundaries. They report that these boundary conditions lead to low frequency-instabilities due to the way the mean flow was being calculated and updated.

Viscous flow problems require more number of boundary conditions than inviscid flows ([53], [52]). Although exact boundary conditions can be derived for Euler equations as discussed earlier, the problem is much more complicated for Navier-Stokes (N-S) equations. Well-posedness analysis of boundary conditions for N-S equations can be performed only in certain simple cases ([52], [53]). While most of the boundary conditions are derived for Euler equations, Poinsot and Lele [54] developed procedures to define NRBCs for N-S equations. They derived a new formulation using the 1D characteristic wave relations for the Euler equations and generalized them to the Navier-Stokes equations. A brief discussion of the boundary treatment of edges and corners is also provided in their work. Apart from Poinsot and Lele, a few other researchers ([55], [56], [57], [58], [59], [60])have also developed non-reflecting boundary conditions for N-S equations. The main criteria for formulation of boundary condi-

tions for N-S equations are: (1) they must reduce to boundary conditions for Euler equations when the viscous terms vanish to avoid creation of viscous boundary layers, (2) they must represent a well-posed problem in the continuous form and must be stable in the discrete form.

1.4.2 Boundary Conditions based on Asymptotic Expansions

This technique is based on taking an asymptotic expansion of the solution for large distances from the source region. The flow equations are reduced to a simpler form in the far field. The particular form of the reduced equations depends on the geometry of the computational domain; thus, there are two main types of boundary conditions based on asymptotic expansions.

The first boundary condition is for external flows in which the flow equations are reduced to a convective wave equation form in the far field. Bayliss and Turkel ([14] , [15], [16]) introduced this method for time dependent problems (wave equation and Euler equations). The authors developed a series of higher-order operators, requiring higher-order derivatives, by which the accuracy of the boundary conditions can be increased. Higdon ([17], [18]) reduced the higher-order operators to a series of 1-D operators that are applied at various angles to the boundary. Using a series of auxiliary functions, Hagstrom and Hariharan devised a method to apply the higher-order operators while only requiring low-order derivatives ([19], [20], [21], [22], [23]). Roe [24] suggested using the asymptotic solution to set only the acoustic disturbances, while allowing entropy and vorticity waves to be set separately. The wave-equation-based

boundary conditions were also derived by Tam and Webb [65] through a different approach. In their work, they took a Fourier-Laplace transform of the linearized Euler equations and determined the form of the solution at infinity. They have also extended the outflow radiation condition to allow vortical and entropy waves to exit the boundary. Tam and Dong [25] and Dong [27] extended the acoustic radiation condition of Tam and Webb to allow for non-uniform mean flows.

A second type of asymptotic boundary condition is for two-dimensional flows such as ducts or cascades. In these boundary conditions, from Tam et al. [26] for application to an axisymmetric duct geometry and a 2-D flat-plate cascade, the outgoing solution is assume to be composed of a small number of propagating modes. At each time step, a least square fit is used to find the amplitude and phase of each outgoing mode, and this information is used to update the solution at the inflow and outflow boundaries and thus eliminate any spurious incoming modes.

1.4.3 Absorbing Layers

Most of the boundary conditions discussed in the above sections are developed for uniform mean flow problems and are designed to let the waves leave the domain boundaries without reflection. In principle, these boundary conditions can be applied to non-uniform mean flows provided that the variation of the mean flow is long compared to the length scale of the disturbances. Although useful in many flows of practical interest, this high frequency approximation is not accurate at inflow and outflow boundaries of turbulent shear flows, where the largest vortical structures are on the same scale as variation of the mean flow and peak acoustic radiation is at longer wavelengths. The problem is that acoustic, vortical, and entropic modes lose their distinct identity in the presence of arbitrary mean flow gradients. This section discusses the techniques to deal primarily with the problem of large errors caused due to nonlinear effects in linearized boundary conditions. One such technique is called absorbing layers where the flow physics are modified in a finite region upstream of the outflow boundary. This method attempts to damp the waves before reaching the boundary rather than letting them pass through the boundary without reflections. Several absorbing layers have been suggested to either enhance the efficacy of the non-reflecting boundary conditions or to obviate the need for any non-reflecting boundary conditions. Absorbing layers typically provide for damping of disturbances prior to interaction with a non-reflection boundary condition. Some obvious ways to do this are to introduce artificial dissipation, to increase the value of physical viscosity etc. The basic problem with this approach is that the internal boundary of the absorbing

layer is itself reflective. Without further modification, the only way to obtain a satisfactory result is to gradually increase the damping from zero over a relatively long distance, which results in thick, computationally inefficient layers.

Perfectly Matched Layer

Perfectly Matched Layer is a relatively new technique for construction of absorbing boundary conditions. It was first proposed by Berenger [28] for absorbing electromagnetic waves in unbounded two-dimensional electromagnetic problems governed by the Maxwell equations (solved using the finite difference method). This method is based on the use of an absorbing layer of a certain depth adjacent to the artificial boundary of a computational domain. The equations for the PML medium are designed such that the outgoing electromagnetic waves are absorbed with no reflection (theoretically). A small amount of numerical reflection occurs in practical computations, but with a magnitude that can be reduced by tuning some parameters of the layer, especially it's thickness and absorption co-efficients. Berenger [29] later extended this technique to three-dimensional electromagnetic problems. Since it's introduction in the early 90's, the PML technique has found widespread applications in elastic wave propagation, computational aeroacoustics and many other areas. Based on Berenger's work, Hu [30] first proposed a Perfectly Matched Layer to absorb the outgoing waves in a uniform mean flow governed by the linearized Euler equations. The absorbing layer equations were obtained by splitting the governing equations in the co-ordinate directions and introducing absorbing co-efficients in each direction. To apply the PML technique, the computational domain is divided into an interior domain, where

the Euler equations are used, and PML domains adjacent to artificial boundaries, where the proposed PML equations are to be used. Hu showed that the theoretical reflection co-efficients at an interface between the Euler and PML domains are zero, independent of the angle of incidence and frequency of waves. However, he reports instability of his technique and found that filtering was necessary in order to avoid temporal instabilities. Hesthaven [31] showed the strong loss of well-posedness due to the nonphysical splitting of variables, hence explaining the instabilities reported by Hu [30] as well as illustrating why the application of filters has a stabilizing effect. Hu extended his PML equations to non-uniform mean flow and non-linear Euler equations [32]. In a later work, Hu et al. [33] demonstrated the effectiveness of absorbing layers for the Euler equations by applying the methodology to three different physical problems - shock-vortex interactions, a plane free shear flow, and an axisymmetric jet - with empasis on acoustic wave propagation. Abarbanel and Gottlieb [34] performed a detailed mathematical analysis of the PML method for electromagnetic equations and showed that the PML formulation of Berenger [28] for electromagnetic equations is not strongly well-posed and that for a highly refined grid or very long time of computations, the PML method might not yield appropriate results. Qi and Geers [35] evaluated the performance of the perfectly matched layer (PML), first formulated by Berenger for the time-domain, finite-difference solution of Maxwells equations, has been evaluated for computational acoustics. They found that, while the PML constitutes an excellent absorbing boundary for plane waves incident upon a planar interface, its performance in non-planar geometries is not always satisfactory.

A second PML formulation was given by Abarbanel et al. [36] in which the

physical variables were unsplit, but instead the Euler equations were augmented with additional terms so that all the waves decayed exponentially inside the PML domain. Though Abarbanel's new formulation was well-posed, he still used artificial damping terms to suppress the exponentially growing solutions. Tam et al. [37] analyzed the dispersion relations of the linear waves and found that the PML equations of Hu [30] have unstable solutions whenever the mean flow has a component normal to the PML domain interface. They suggested the use of artificial selective damping for the suppression of instability waves, since the unstable modes were associated with high wave numbers. In a more recent work, Hu [38] developed a new stable PML formulation for linearized Euler equations. This formulation addressed the issue of well-posedness (using unsplit physical variables) and the exponentially growing solutions of earlier PML techniques without using any additional damping terms. In his work, Hu found that in the presence of a mean flow, there exist acoustic waves that have a positive group velocity but a negative phase velocity in the direction of the mean flow and these waves become actually amplified in the previous formulation [30], thus giving rise to the instability. It employed a spacetime transformation before applying the PML technique so that in the transformed coordinates all waves have consistent phase and group velocities. Hu later extended this new stable PML to linearized Euler equations with a parallel non-uniform mean flow [39].

1.5 Purpose

The primary focus of the present work is on the development of *Wall Corner Compatibility Conditions* for the non-reflecting boundary conditions developed by Giles [46], based on one-dimensional characteristics. Although no mathematical proof of stability of the compatibility conditions is provided here, they have been successfully applied to various flow and geometry configurations. Another objective of this work is to extend the two-dimensional, Cartesian, Giles boundary conditions [46] to three-dimensional Cartesian and two-dimensional Curvilinear boundary conditions with corresponding wall corner compatibility conditions. Proof of well-posedness is also provided for the extended boundary conditions. The boundary conditions along with the wall corner compatibility conditions have been validated for several test cases of the *Ringleb Flow*.

1.6 Outline of Thesis

To address the problems mentioned above, the thesis is organized as follows: Chapter 2 presents a step-by-step procedure that Giles adopted to construct non-reflecting boundary conditions for the linearized Euler equations in Cartesian co-ordinates [47], including the general theory of Fourier analysis to obtain one and two-dimensional, local, unsteady boundary conditions, analysis of well-posedness and an ad-hoc method to overcome the ill-posedness of boundary conditions. Chapter 3 develops the wall corner compatibility conditions for the two-dimensional Cartesian Giles boundary conditions at inflow and outflow boundaries. Chapter 4 begins with the construc-

tion of Giles boundary conditions in two-dimensional Curvilinear co-ordinates and moves on to the derivation of the corresponding wall corner compatibility conditions. Chapter 5 presents the extension of Giles boundary conditions to three-dimensional linearized Euler equations. Chapter 6 describes the theoretical background of Ringleb flow which is the primary test case in this work. Chapter 7 discusses the details of flow solver and numerical implementation of the boundary conditions. Chapter 8 presents and discusses the results of test cases for the wall corner compatibility conditions and Curvilinear boundary conditions. Conclusions and recommendations for future work are given in Chapter 9. Flow contours of a sample Ringleb flow test case are provided in Appendix A.

Chapter 2

Giles Boundary Conditions for 2D Euler Equations in Cartesian Co-ordinates

This chapter presents the work of Giles [46] in detail and the same methodology is adopted to derive the three dimensional boundary conditions (in Cartesian co-ordinates) and the two-dimensional Curvilinear boundary conditions for Euler equations in subsequent chapters. The entire text of this chapter is taken from the detailed report by Giles [47].

2.1 General Theory

2.1.1 Fourier Analysis

Consider a general two-dimensional unsteady system of N hyperbolic partial differential equations given by:

$$\frac{\partial U}{\partial t} + A\frac{\partial U}{\partial x} + B\frac{\partial U}{\partial y} = 0 \tag{2.1}$$

U is vector of N components and A and B are N x N constant matrices.

To perform Fourier analysis, a wave like solution of the form

$$U(x, y, t) = ue^{i(kx+ly-\omega t)} \tag{2.2}$$

where k and l are wave numbers in x and y directions respectively.

The dispersion relation is obtained by substituting this wave like solution into (2.1)

$$(-\omega I + kA + lB)\, u = 0 \tag{2.3}$$

$$\Longrightarrow det\,(-\omega I + kA + lB) = 0 \tag{2.4}$$

This dispersion relation is a polynomial of degree N in each of ω, k, and l.

To construct the boundary conditions, it is essential to group the waves into incoming and outgoing modes based on their direction of propagation. If ω is complex with $Im\,(\omega) > 0$ (giving an exponential growth in time), then the right propagating waves are those for which $Im(k) > 0$. This is because the amplitude of the waves

is proportional to $e^{Im(\omega)(t-x/c)}$ where $c = Im(\omega)/Im(k)$ is the apparent velocity of propagation of the amplitude.

If ω and k are real then a standard result in the analysis of dispersive wave propagation [61] is that the velocity of energy propagation is given by the group velocity:

$$\overrightarrow{c_g} = \begin{pmatrix} \dfrac{\partial\omega}{\partial k} \\ \dfrac{\partial\omega}{\partial l} \end{pmatrix} \tag{2.5}$$

Hence for real ω the incoming waves are those which either have $Im(k) > 0$, or have real k and $\dfrac{\partial\omega}{\partial k} > 0$.

2.1.2 Eigenvectors

The right and left eigenvectors of an N x N matrix C are defined by

$$Cu_n^R = \lambda u_n^R, \quad u_n^L C = \lambda u_n^L \tag{2.6}$$

where λ_n is the corresponding eigenvalue. The right eigenvectors are column vectors, whereas the left eigenvectors are row vectors. An equivalent definition of eigenvectors is that they are the null vectors of the singular matrix $C - \lambda_n I$.

$$(C - \lambda_n I)\, u_n^R = 0, \quad u_n^L\, (C - \lambda_n I) = 0 \tag{2.7}$$

An important property of the eigenvectors is that when the eigenvalues are dis-

tinct, each left eigenvector is orthogonal to all of the right eigenvectors except to the one corresponding to the same eigenvalue. The proof is as follows:

$$\begin{aligned}(\lambda_n - \lambda_m)\, v_n^L u_m^R &= \left(v_n^L C\right) u_m^R - v_n^L \left(C u_m^R\right) \\ &= 0 \end{aligned} \tag{2.8}$$

If $m \neq n$ then $\lambda_m \neq \lambda_n$ and hence $v_n^L u_m^R = 0$. If the system has repeated eigenvalues then provided there is a complete set of N eigenvectors, v_n^L and u_m^R can still be constructed using the Gram-Schmidt orthogonalization method [62], so that $v_n^L u_m^R = 0$ if $m \neq n$.

For construction of boundary conditions the right eigenvectors we require are the null-vectors) of $(-\omega I + kA + lB)$.

$$(-\omega I + kA + lB)\, u^R = 0 \tag{2.9}$$

u^R is a right eigenvector of $(kA + lB)$ with eigenvalue ω. By pre-multiplying Eq.(2.9) by A^{-1} we obtain

$$\left(-\omega A^{-1} + kI + lA^{-1}B\right) u^R = 0 \tag{2.10}$$

From the above equation, it is obvious that u^R is also a right eigenvector of $(-\omega A^{-1} + lA^{-1}B)$ with eigenvalue $-k$.

There are two different sets of left eigenvectors which are important in this problem. The first set, labelled u^L, are the left eigenvectors of $(kA + lB)$ which are also

the null-vectors of $(-\omega I + kA + lB)$.

$$u^L \left(-\omega I + kA + lB\right) = 0 \tag{2.11}$$

The second set, labelled v^L, are the left eigenvectors of $(-\omega A^{-1} + lA^{-1}B)$ which are also the null-vectors of $(-\omega A^{-1} + kI + lA^{-1}B) = A^{-1}\left(-\omega I + kA + lB\right)$.

$$v^L A^{-1} \left(-\omega I + kA + lB\right) = 0 \tag{2.12}$$

By comparing Eq. (2.11) and (2.12), it is clear that the two sets of left eigenvectors u^L and v^L are related, with $v^L A^{-1}$ equal to (or a multiple of) u^L, or alternatively v^L equal to (or a multiple of) $u^L A$.

The difference between the two sets of left eigenvectors lies in their orthogonality relations with the right eigenvectors. Since u^L is a left eigenvector of $(kA + lB)$, it is orthogonal to all of the right eigenvectors of the same matrix, except for the one with the same eigenvalue ω. The key point here is that the orthogonality is for the *same* k and l and *different* ω. Thus if ω_n and ω_m are two different roots of the dispersion relation for the same values of k and l, then the orthogonality relation is $u^L\left(\omega_n, k, l\right) u^R\left(\omega_m, k, l\right) = 0$.

In contrast, since v^L is a left eigenvector of $(-\omega A^{-1} + lA^{-1}B)$, it is orthogonal to all of the right eigenvectors u^R with the *same* k and l and *different* ω. Thus if k_n and k_m are two different roots of the dispersion relation for the same values of ω and l, then the orthogonality relation is $v^L\left(\omega, k_n, l\right) u^R\left(\omega, k_m, l\right) = 0$.

Normally in discussing wave motion, one is concerned with propagation on an infinite domain, and so usually one considers a group of waves with the same values of k and l and different values of ω, in which case u^R and u^L would be the relevant right and left eigenvectors. In analyzing boundary conditions however, a general solution U at the boundary $x = 0$ can be decomposed into a sum of Fourier modes with different values of ω and l. Each of these modes is then a collection of waves with the same values ω and l and different values of k. Hence, for the purpose of constructing non-reflecting boundary conditions it is u^R and v^L which are important.

u^L is still useful in this approach as a convenient way to construct v^L. Direct construction of v^L involves calculation of A^{-1} which could be a laborious process. An easier way is to use the result obtained earlier that v^L is a multiple of $u^L A$. Let k_n be the n^{th} root of the dispersion relation for a given value of ω and l, and ${u_n}^L$ be the corresponding left eigenvector of $(k_n A + lB)$. Then ${v_n}^L$ can be defined by

$$v_n^L = \left.\frac{k_n}{\omega}\right|_{l=0} u_n^L A \tag{2.13}$$

The reason for choosing the constant of proportionality as $\left.\frac{k_n}{\omega}\right|_{l=0}$ is that when $l = 0$, $u_n^L A = \frac{\omega}{k}_n u_n^L$ and hence $u_n^L = v_n^L$.

An observation is that by dividing the dispersion relation in Eq. (2.4) by ω we obtain

$$det\left(-I + \frac{k_n}{\omega}A + \frac{l}{\omega}B\right) = 0 \tag{2.14}$$

and so it is clear that $k_n/\omega, u^R, u^L$, and v^L are all functions of l/ω. Thus the variable

$\lambda = l/\omega$ will play a key role in the construction of all the boundary conditions.

2.1.3 Exact One-dimensional Non-reflecting Boundary Conditions for a Single Fourier mode

Suppose that the system of differential equations is to be solved in the domain $x > 0$, and one wants to construct non-reflecting boundary conditions at $x = 0$ to minimize or ideally prevent the reflection of outgoing waves. At the boundary at $x = 0$, U can be decomposed into a sum of Fourier modes with different ω and l, so the analysis begins by considering just one particular choice of ω and l. In this case the most general form for U is

$$U(x, y, t) = \left[\sum_{n=1}^{N} a_n u_n^R e^{ik_n x} \right] e^{i(ly - \omega t)} \tag{2.15}$$

k_n is the n^{th} root of the dispersion relation for the given values of ω and l, and u_n^R is the corresponding right eigenvector.

The ideal non-reflecting boundary conditions would be to specify that $a_n = 0$ for each n that corresponds to an incoming wave. Because of orthogonality,

$$\begin{aligned} v_n^L U &= v_n^L \left[\sum_{m=1}^{N} a_m u_m^R e^{ik_m x} \right] e^{i(ly - \omega t)} \\ &= a_n \left(v_n^L u_n^R \right) e^{ik_n x} e^{i(ly - \omega t)} \end{aligned} \tag{2.16}$$

and so an equivalent specification of non-reflecting boundary condition is

$$v_n^L U = 0 \tag{2.17}$$

for each n corresponding to an incoming mode. v_n^L is the left eigenvector defined in the last section. This use of the left eigenvector illustrates its physical significance; because of the orthogonality relations, when applied to a general solution it "measures" the amplitude of a particular wave component. The significance of the right eigenvector is apparent in Eq. (2.15); it shows the variation in the primitive variables caused by a particular wave mode.

In principle these exact boundary conditions can be implemented in an numerical method. The problem is that v_n^L depends on ω and l and so the implementation would involve a Fourier transform in y and a Laplace transform in t. Computationally this is both difficult and expensive to implement and so instead four simpler variations which use different assumptions and approximations are considered here.

2.1.4 One-dimensional, Unsteady Boundary Conditions

The one dimensional, non-reflecting boundary conditions are obtained by ignoring all variations in y-direction and setting $\lambda = 0$. The corresponding right and left eigenvectors are important in defining and implementing the other boundary conditions, and so they are labeled w.

$$w_n^R = u_n^R\big|_{\lambda=0} \tag{2.18}$$

$$w_n^L = u_n^L\big|_{\lambda=0} = v_n^L\big|_{\lambda=0} \tag{2.19}$$

The boundary condition, expressed in terms of the primitive variables, is

$$w_n^L U = 0 \tag{2.20}$$

for all n corresponding to incoming waves.

If the right and the left eigenvectors are normalized so that

$$w_m^L w_n^R = \delta_{mn} \equiv \begin{cases} 1, \ m = n \\ 0, \ m \neq n \end{cases} \tag{2.21}$$

then they can be used to define a transformation between the primitive variables and the one-dimensional characteristic variables.

$$U = \sum_{n=1}^{N} c_n w_n^R, \tag{2.22}$$

where

$$c_n = w_n^L U \tag{2.23}$$

Expressed in terms of the characteristic variables, the boundary condition is simply

$$c_n = 0 \tag{2.24}$$

for all n corresponding to incoming waves.

Numerical implementations of these boundary conditions usually extrapolate the

outgoing characteristic variables, in addition to setting the incoming characteristic variables to zero. This gives a complete set of equations for the solution on the boundary using Eq. (2.22).

An observation, which will be needed for the well-posedness analysis, is that

$$(-\omega I + k_n A)\, w_n^R = 0 \tag{2.25}$$

so

$$A w_n^R = \frac{\omega}{k_n} w_n^R = \alpha_n w_n^R \tag{2.26}$$

Thus w_n^R is an eigenvector of A with eigenvalue $\alpha_n = \dfrac{\omega}{k_n}$. Furthermore,

$$w = \alpha_n k_n \Rightarrow \vec{c_g} = \begin{pmatrix} \alpha_n \\ \\ 0 \end{pmatrix}, \tag{2.27}$$

so the incoming waves are those for which $\alpha_n > 0$.

2.1.5 Approximate, Two-dimensional, Unsteady Boundary Conditions

By dividing the dispersion relation by ω it is clear that k_n/ω, u_n^R, u_n^L, v_n^L are all functions of l/ω. Thus a sequence of approximations can be obtained by expanding v_n^L in a Taylor series as a function of $\lambda = l/\omega$.

$$v_n^L(\lambda) = v_n^L\big|_{\lambda=0} + \lambda \left.\frac{dv_n^L}{d\lambda}\right|_{\lambda=0} + \frac{1}{2}\lambda^2 \left.\frac{d^2 v_n^L}{d\lambda^2}\right|_{\lambda=0} + \ \ldots \tag{2.28}$$

The first order approximation obtained by just keeping the leading term gives the one-dimensional boundary conditions which have already been discussed. The second order approximation is

$$\begin{aligned} \overline{v}_n^L(\lambda) &= v_n^L\big|_{\lambda=0} + \frac{l}{\omega}\left.\frac{dv_n^L}{d\lambda}\right|_{\lambda=0} \\ &= u_n^L\big|_{\lambda=0} + \frac{l}{\omega}\left.\left[\frac{k_n}{\omega}\frac{du_n^L}{d\lambda}A\right]\right|_{\lambda=0} \end{aligned} \tag{2.29}$$

The overbar denotes the fact that $\overline{v}$ is an approximation to v. This produces the boundary condition

$$\left(u_n^L\big|_{\lambda=0} + \frac{l}{\omega}\left.\left[\frac{k_n}{\omega}\frac{du_n^L}{d\lambda}A\right]\right|_{\lambda=0}\right)U = 0 \tag{2.30}$$

Multiplying by ω, and replacing ω and l by $i\dfrac{\partial}{\partial t}$ and $-i\dfrac{\partial}{\partial y}$ respectively gives,

$$u_n^L\big|_{\lambda=0}\frac{\partial U}{\partial t} - \left.\left[\frac{k_n}{\omega}\frac{du_n^L}{d\lambda}A\right]\right|_{\lambda=0}\frac{\partial U}{\partial y} = 0 \tag{2.31}$$

This is a local boundary condition (meaning that it does not involve any global decomposition into Fourier modes) and so can be implemented without difficulty. As the equation is similar in nature to the original differential equation, having first order derivatives in both y and t, the numerical algorithm used for the interior equations can probably also be used for the boundary conditions.

2.1.6 Analysis of Well-posedness

One-dimensional Boundary Conditions

It is relatively easy to prove that the one-dimensional boundary conditions are always well-posed, by using an energy analysis method. A key step in the proof is that because the system is hyperbolic there exists a transformation of variables under which the transformed A and B matrices are symmetric, and so without loss of generality we can assume that A and B are symmetric. The 'energy' is defined by

$$E(t) = \int_{-\infty}^{\infty} \int_{0}^{\infty} |u|^2 \, dx \, dy \tag{2.32}$$

To ensure that this integral remains finite it will be assumed that u is zero outside some distance from the origin. The rate of change of the energy is given by

$$\begin{aligned}
\frac{dE}{dt} &= 2 \int_{-\infty}^{\infty} \int_{0}^{\infty} u^T \, \frac{\partial u}{\partial t} \, dx \, dy \\
&= -2 \int_{-\infty}^{\infty} \int_{0}^{\infty} u^T \left(A \frac{\partial u}{\partial x} + B \frac{\partial u}{\partial y} \right) \, dx \, dy \\
&= -\int_{-\infty}^{\infty} \int_{0}^{\infty} u^T A \frac{\partial u}{\partial x} + \frac{\partial u^T}{\partial x} A^T u + u^T B \frac{\partial u}{\partial y} + \frac{\partial u^T}{\partial y} B^T u \, dx \, dy \\
&= -\int_{-\infty}^{\infty} \int_{0}^{\infty} \frac{\partial}{\partial x} \left(u^T A u \right) + \frac{\partial}{\partial y} \left(u^T B u \right) \, dx \, dy \qquad \left(\text{since A} = \text{A}^{\text{T}} \text{ and B} = \text{B}^{\text{T}} \right) \\
&= -\int_{-\infty}^{\infty} \left(u^T A u \big|_{x=\infty} - u^T A u \big|_{x=0} \right) \, dy - \int_{0}^{\infty} \left(u^T B u \big|_{y=\infty} - u^T B u \big|_{y=-\infty} \right) \, dx \\
&= \int_{-\infty}^{\infty} u^T A u \big|_{x=0} \, dy
\end{aligned} \tag{2.33}$$

The evaluation of this integral requires some earlier results.

$$\begin{aligned} u^T A u &= \left(\sum_{n=1}^{N} c_n w_n^R\right)^T A \left(\sum_{n=1}^{N} c_n w_n^R\right) && \text{(usingEq.(2.22))} \\ &= \sum_{n=1}^{N} \alpha_n c_n^2 && \text{(usingEq.(2.26))} \end{aligned} \tag{2.34}$$

where, as defined earlier, α_n is the n^{th} eigenvalue of A, w_n^R is the corresponding right eigenvector which is also the transpose of the left eigenvector w_n^L since A is symmetric, and $c_n = w_n^L u$.

The final step is to note that the one-dimensional boundary condition states that $c_n = 0$ for incoming waves, which are those for which $\alpha_n \geq 0$. Thus each term in the above sum is either zero or negative, and hence $u^T A u$ is non-positive and the energy is non-increasing, proving that the IBVP is well-posed.

Approximate, Two-dimensional Boundary Conditions

To analyze the well-posedness of the approximate, two-dimensional boundary conditions, one must use the theory developed by Kreiss [3]. As explained by Trefethen [48] and Higdon [4], the aim is to verify that there is no incoming mode which exactly satisfies the boundary condition.

As explained earlier, an incoming mode is a solution of the interior differential equation which *either* is growing exponentially in time but decaying exponentially in space away from the boundary, *or* has a real frequency and a group velocity which is incoming. If this incoming mode also satisfies the boundary condition then in the first case there is an exponentially growing energy and in the second case there is a

linear growth as the incoming mode moves into the interior.

If there are N' incoming waves then the generalized incoming mode may be written as

$$U(x,y,t) = \left[\sum_{n=1}^{N'} a_n u_n^R e^{ik_n x}\right] e^{i(ly-\omega t)} \tag{2.35}$$

with $Im(\omega) \geq 0$. Substituting this into the N' non-reflecting boundary conditions produces a matrix equation of the form

$$C \begin{pmatrix} a_1 \\ \vdots \\ a_{N'} \end{pmatrix} = 0 \tag{2.36}$$

where C is a N x N' matrix whose elements are the products of the approximate left eigenvectors and the exact right eigenvectors.

$$C_{mn} = \overline{v}_m^L u_n^R \tag{2.37}$$

Provided that the right eigenvectors are linearly independent, the requirement that there is no non-trivial incoming mode satisfying the boundary conditions is equivalent to the statement that there is no non-trivial solution to the above matrix equation. Thus the IBVP is well-posed if it can be proved that the determinant of C is non-zero for all real l and complex ω with $Im(\omega) \geq 0$.

If the right eigenvectors are linearly dependent then the theory needs to be modified. Suppose for simplicity that there are just two incoming waves and that $k_1 = k_2$

and $u_1^R = u_2^R$ at $\omega = \omega_{crit}$. A general incoming mode may be written as the sum of two incoming modes with amplitudes a_1', a_2'.

$$U(x,y,t) = \left[a_1' u_1^R e^{ik_1 x} + a_2' \frac{1}{\omega - \omega_{crit}} \left(u_1^R e^{ik_1 x} - u_2^R e^{ik_2 x} \right) \right] e^{i(ly - \omega t)} \tag{2.38}$$

By construction, the second mode is finite in the limit $\omega \to \omega_{crit}$, and so if the limit is defined to be the value at $\omega = \omega_{crit}$ then this expression is the correct general solution to the eigenvalue problem

$$\omega U = A \frac{\partial U}{\partial x} + lBU \tag{2.39}$$

subject to the condition $U \to 0$ as $x \to \infty$.

The amplitudes $a_{1,2}$ and $a_{1,2}'$ are related by

$$\begin{pmatrix} a_1 \\ \\ a_2 \end{pmatrix} = T \begin{pmatrix} a_1' \\ \\ a_2' \end{pmatrix} \tag{2.40}$$

where

$$T = \begin{pmatrix} 1 & 1/\left(\omega - \omega_{crit}\right) \\ \\ 0 & -1/\left(\omega - \omega_{crit}\right) \end{pmatrix} \tag{2.41}$$

Substituting this into the boundary conditions gives

$$CT \begin{pmatrix} a_1' \\ \\ a_2' \end{pmatrix} \tag{2.42}$$

By continuity, the requirement for well-posedness is that $\det(CT) = \det(C)\det(T) \nrightarrow 0$ as $\omega \rightarrow \omega_{crit}$. Since $\det(T) = O(\omega - \omega_{crit})^{-1}$, this requires that $\det(C) = O(\omega - \omega_{crit})$, or equivalently that

$$\frac{\partial}{\partial \omega} det(C)\Big|_{\omega_{crit}} \neq 0 \tag{2.43}$$

More generally, we conjecture that if the N' right eigenvectors collapse to N" linearly independent eigenvectors at some ω_{crit} then the requirement for well-posedness is that $\det(C) = O(\omega - \omega_{crit})^{N'-N"}$, or equivalently that

$$\frac{\partial^{N'-N"}}{\partial \omega^{N'-N"}} det(C)\Big|_{\omega_{crit}} \neq 0 \tag{2.44}$$

Engquist and Majda conjectured that the second approximation is always well-posed. Giles [46] showed that this is not true for Euler equations. Trefethen and Halpern have proved that the boundary conditions for the scalar wave equation which come from the second and higher order Taylor series expansions l^2/ω^2 are ill-posed [48]. Thus it seems likely that for the differential system of equations which are going to be considered here, the Taylor series approximations may be ill-posed.

2.1.7 Reflection Co-efficients

The calculation of reflection co-efficients is very similar to the well-posedness analysis. A general solution with a given frequency ω and wavenumber l can be written as a sum of incoming and outgoing modes.

$$U(x,y,t) = \left[\sum_{n=1}^{N'} a_n u_n^R e^{ik_n x} + \sum_{n=N'+1}^{N} a_n u_n^R e^{ik_n x} \right] e^{i(ly-\omega t)} \tag{2.45}$$

Substituting this into the approximate non-reflecting boundary conditions gives

$$C \begin{pmatrix} a_1 \\ \vdots \\ a_{N'} \end{pmatrix} + D \begin{pmatrix} a_{N'+1} \\ \vdots \\ a_N \end{pmatrix} = 0 \tag{2.46}$$

where C is the same matrix as in the well-posedness analysis and D is defined by

$$D_{mn} = \overline{v}_m^L u_{N'+m}^R \tag{2.47}$$

If the IBVP is well-posed C is non-singular and so Eq. (2.46) can be solved to obtain

$$\begin{pmatrix} a_1 \\ \vdots \\ a_{N'} \end{pmatrix} = -C^{-1} D \begin{pmatrix} a_{N'+1} \\ \vdots \\ a_N \end{pmatrix} \tag{2.48}$$

This equation relates the amplitudes of the incoming waves to the amplitude of the outgoing waves, so $-C^{-1}D$ is the matrix of the reflection co-efficients.

Since $v_m^L u_n^R = 0$ if $m \neq n$, the off-diagonall elements of C and the elements of D can be re-written as

$$C_{mn} = \left(\overline{v}_m^L - v_m^L\right) u_n^R, \qquad m \neq n \tag{2.49}$$

$$D_{mn} = \left(\overline{v}_m^L - v_m^L\right) u_{N'+n}^R \tag{2.50}$$

Because the elements on the diagonal of C are $O(1)$, C^{-1} is $O(1)$ and hence the order of magnitude of the reflection co-efficients for $l/\omega \leq 1$ depends solely on the order of magnitude of D. Using the one-dimensional approximation $w_m^L - v_m^L = O(l/\omega)$. Hence $D = O(l/\omega)$ in general and the reflection co-efficients will be $O(l/\omega)$. Similarly, using the approximate two-dimensional boundary conditions gives reflection co-efficients which are $O(l^2/\omega^2)$.

2.2 Application to Euler Equations

2.2.1 Non-dimensional Linearized 2D Euler equations in Cartesian Co-ordinates

The two-dimensional Euler equations which describe an instead, inviscid, compressible flow are usually expressed in the following form based upon the conservation of mass, momentum and energy.

$$\frac{\partial}{\partial t}\begin{pmatrix} \rho \\ \rho u \\ \rho v \\ E_{total} \end{pmatrix} + \frac{\partial}{\partial x}\begin{pmatrix} \rho u \\ \rho u^2 + p \\ \rho uv \\ u\left(E_{total} + p\right) \end{pmatrix} + \frac{\partial}{\partial y}\begin{pmatrix} \rho v \\ \rho uv \\ \rho v^2 + p \\ v\left(E_{total} + p\right) \end{pmatrix} = 0 \qquad (2.51)$$

ρ is the density, u and v are the two velocity components, and E_{total} is the total internal. To complete the system of equations an equation of state is needed to define the pressure p. For an ideal gas this is

$$p = (\gamma - 1)\left(E_{total} - \frac{1}{2}\rho\left(u^2 + v^2\right)\right) \qquad (2.52)$$

with γ being the ratio of specific heats which is a constant.

Using Eq. (2.52) to eliminate E_{total} from Eq. (2.51), and rearranging substantially,

yields the following 'primitive' form of the Euler equations.

$$\frac{\partial}{\partial t}\begin{pmatrix}\rho\\ u\\ v\\ p\end{pmatrix}+\begin{pmatrix}u & \rho & 0 & 0\\ 0 & u & 0 & \frac{1}{\rho}\\ 0 & 0 & u & 0\\ 0 & \gamma p & 0 & u\end{pmatrix}\frac{\partial}{\partial x}\begin{pmatrix}\rho\\ u\\ v\\ p\end{pmatrix}+\begin{pmatrix}v & 0 & \rho & 0\\ 0 & v & 0 & 0\\ 0 & 0 & v & \frac{1}{\rho}\\ 0 & 0 & \gamma p & v\end{pmatrix}\frac{\partial}{\partial y}\begin{pmatrix}\rho\\ u\\ v\\ p\end{pmatrix}=0 \tag{2.53}$$

This equation is still nonlinear. The next step is to consider small perturbations from a uniform, steady flow, and neglect all but the first order linear terms. This produces a linear equation of the form analyzed in the theory section,

$$\frac{\partial U}{\partial t}+A\frac{\partial U}{\partial x}+B\frac{\partial U}{\partial y}=0 \tag{2.54}$$

where U is the vector of perturbation variables

$$U=\begin{pmatrix}\rho'\\ u'\\ v'\\ p'\end{pmatrix} \tag{2.55}$$

and the co-efficient matrices A and B are constant matrices based on the uniform,

steady variables.

$$A = \begin{pmatrix} \overline{u} & \overline{\rho} & 0 & 0 \\ 0 & \overline{u} & 0 & \frac{1}{\overline{\rho}} \\ 0 & 0 & \overline{u} & 0 \\ 0 & \gamma\overline{p} & 0 & \overline{u} \end{pmatrix}, \qquad B = \begin{pmatrix} \overline{v} & 0 & \overline{\rho} & 0 \\ 0 & \overline{v} & 0 & 0 \\ 0 & 0 & \overline{v} & \frac{1}{\overline{\rho}} \\ 0 & 0 & \gamma\overline{p} & \overline{v} \end{pmatrix} \tag{2.56}$$

The analysis is greatly simplified if the unsteady perturbations and the steady variables in A and B are all non-dimensionalized using the steady density and speed of sound. With this choice of non-dimensionalization the final form of the matrices A and B is

$$A = \begin{pmatrix} \overline{u} & 1 & 0 & 0 \\ 0 & \overline{u} & 0 & 1 \\ 0 & 0 & \overline{u} & 0 \\ 0 & 1 & 0 & \overline{u} \end{pmatrix}, \qquad B = \begin{pmatrix} \overline{v} & 0 & 1 & 0 \\ 0 & \overline{v} & 0 & 0 \\ 0 & 0 & \overline{v} & 1 \\ 0 & 0 & 1 & \overline{v} \end{pmatrix} \tag{2.57}$$

and the variables $\overline{u}$ and $\overline{v}$ in the above matrices are now the Mach numbers in x and y directions.

It should be mentioned that a number of approximation errors are being introduced in converting the nonlinear Euler equations into the linearized equations. For steady state calculations the error will be proportional to the square of the steady state perturbation at the inflow and the outflow. These should be very small and may well be unnoticeable except for the case of an oblique shock at the outflow. For unsteady calculations there are two sources of error. The first which is similar to the steady state error is proportional to the square of the unsteady perturbation. The

second is due to the possible non-uniformity of the underlying steady state solution to which the unsteady perturbation is being added. For the Fourier analysis to be valid it requires that the matrices A and B are constant, and so they must be based on some average of the steady state solution at the inflow and outflow. Thus there will be an error which is proportional to the product of the unsteady perturbation and the steady state non-uniformity. This will usually be negligible at the inflow where the steady state solution is almost uniform, but it may be dominant error at the outflow where there are steady state non-uniformities due to wakes and shock losses. A final note is that these approximation errors are all second order effects and so are much smaller than the first order improvements that are obtained with the non-reflecting boundary conditions. In fact they are probably similar in magnitude to the approximation errors involved in formulating the approximate non-reflecting boundary conditions for the general, unsteady, multi-frequency, two-dimensional problems.

2.2.2 One-dimensional, Unsteady Boundary Conditions

Using Fourier analysis to obtain the right and left eigenvectors and grouping the waves into incoming and outgoing modes as described in the theory section Giles obtained the following one-dimensional unsteady inflow and outflow boundary conditions.

If the computational domain is $0 < x < 1$, and $0 < u < 1$, then the boundary at $x = 0$ is an inflow boundary with incoming waves corresponding to the first three roots of the dispersion relation, and the boundary at $x = 1$ is an outflow boundary

with just one incoming wave due to the fourth root.

The transformation to, and from, 1-D characteristic variables is given by the following two matrix equations.

$$\begin{pmatrix} C_1 \\ C_2 \\ C_3 \\ C_4 \end{pmatrix} = \begin{pmatrix} -1 & 0 & 0 & 1 \\ 0 & 0 & 1 & 0 \\ 0 & 1 & 0 & 1 \\ 0 & -1 & 0 & 1 \end{pmatrix} \begin{pmatrix} \rho' \\ u' \\ v' \\ p' \end{pmatrix} \tag{2.58}$$

$$\begin{pmatrix} \rho' \\ u' \\ v' \\ p' \end{pmatrix} = \begin{pmatrix} -1 & 0 & \frac{1}{2} & \frac{1}{2} \\ 0 & 0 & \frac{1}{2} & \frac{1}{2} \\ 0 & 1 & 0 & 0 \\ 0 & 0 & \frac{1}{2} & \frac{1}{2} \end{pmatrix} \begin{pmatrix} C_1 \\ C_2 \\ C_3 \\ C_4 \end{pmatrix} \tag{2.59}$$

ρ', u', v' and p' are the perturbations from the uniform flow about which the Euler equations were linearized, and C_1, C_2, C_3, C_4 are the amplitudes of the four characteristic waves. At the inflow boundary the correct unsteady, non-reflecting, boundary conditions are

$$\begin{pmatrix} C_1 \\ C_2 \\ C_3 \end{pmatrix} = 0 \tag{2.60}$$

while at the outflow boundary the correct non-reflecting boundary condition is

$$C_4 = 0 \tag{2.61}$$

The standard numerical method for implementing these is to calculate or extrapolate the outgoing characteristic values from the interior domain, and then use Eq. (2.67) to reconstruct the solution at the boundary.

2.2.3 Approximate, Two-dimensional, Unsteady Boundary Conditions

Following the theory presented earlier, the second order non-reflecting boundary conditions are obtained by taking the second-approximation to the left eigenvectors v^L in the limit $\lambda \simeq 0$. This gives the inflow boundary conditions

$$\begin{pmatrix} -1 & 0 & 0 & 1 \\ 0 & 0 & 1 & 0 \\ 0 & 1 & 0 & 1 \end{pmatrix} \frac{\partial U}{\partial t} + \begin{pmatrix} 0 & 0 & 0 & 0 \\ 0 & \overline{u} & \overline{v} & 1 \\ 0 & \overline{v} & -\overline{u} & \overline{v} \end{pmatrix} \frac{\partial U}{\partial y} = 0, \tag{2.62}$$

and the outflow boundary condition

$$\begin{pmatrix} 0 & -1 & 0 & 1 \end{pmatrix} \frac{\partial U}{\partial t} + \begin{pmatrix} 0 & -\overline{v} & \overline{u} & \overline{v} \end{pmatrix} \frac{\partial U}{\partial y} = 0 \tag{2.63}$$

The well-posedness of the second approximation non-reflecting boundary conditions was analyzed using the theory discussed earlier and it was found that the inflow boundary conditions were ill-posed with one ill-posed mode and the outflow boundary

condition was well-posed.

To overcome the ill-posedness of the inflow boundary condition, the third inflow boundary condition was modified using an *ad hoc* procedure to obtain the following modified set of boundary conditions at the inflow

$$\begin{pmatrix} -1 & 0 & 0 & 1 \\ 0 & 0 & 1 & 0 \\ 0 & 1 & 0 & 1 \end{pmatrix} \frac{\partial U}{\partial t} + \begin{pmatrix} 0 & 0 & 0 & 0 \\ 0 & \overline{u} & \overline{v} & 1 \\ 0 & \overline{v} & \frac{1}{2}(1-\overline{u}) & \overline{v} \end{pmatrix} \frac{\partial U}{\partial y} = 0, \tag{2.64}$$

There is also a corresponding modified well-posed outflow boundary condition which is

$$\begin{pmatrix} 0 & -1 & 0 & 1 \end{pmatrix} \frac{\partial U}{\partial t} + \begin{pmatrix} 0 & -\overline{v} & \frac{1}{2}(1+\overline{u}) & \overline{v} \end{pmatrix} \frac{\partial U}{\partial y} = 0 \tag{2.65}$$

2.2.4 Reflection Co-efficients for 2D Euler Equations in Cartesian Co-ordinates

Calculation of reflection co-efficients for the well-posed inflow boundary conditions shows that the outgoing pressure wave produces no reflected entropy or vorticity waves. Also, the reflected pressure wave has an amplitude which is $O(l/\omega)^4$.

For the second order outflow boundary condition, the outgoing entropy and vorticity waves produce no reflection but the outgoing pressure wave produces a second order reflection.

The modified outflow boundary condition differs from the second order outflow condition in that now the outgoing pressure wave produces a fourth order reflection,

but the outgoing vorticity wave produces a first order reflection. Thus this boundary condition is preferable only in situations where it is known that there is no outgoing vorticity wave. As an example, in the far-field of an oscillating transonic airfoil there will be an outgoing vorticity wave only at the outflow boundary directly behind the airfoil because the only vorticity generation mechanisms are a shock and the unsteady Kutta condition. Thus one might use the second order boundary condition directly behind the airfoil, and the modified boundary condition on the remainder of the outflow far-field boundary.

2.2.5 Dimensional Boundary Conditions for 2D Euler Equations in Cartesian Co-ordinates

This section lists the one-dimensional and two-dimensional approximate unsteady boundary conditions in the original dimensional variables, developed by Giles.

a) Transformation to, and from, one-dimensional characteristic variables.

$$\begin{pmatrix} C_1 \\ C_2 \\ C_3 \\ C_4 \end{pmatrix} = \begin{pmatrix} -\overline{c}^2 & 0 & 0 & 1 \\ 0 & 0 & \overline{\rho c} & 0 \\ 0 & \overline{\rho c} & 0 & 1 \\ 0 & -\overline{\rho c} & 0 & 1 \end{pmatrix} \begin{pmatrix} \rho' \\ u' \\ v' \\ p' \end{pmatrix} \tag{2.66}$$

$$\begin{pmatrix} \rho' \\ u' \\ v' \\ p' \end{pmatrix} = \begin{pmatrix} \frac{-1}{\overline{c}^2} & 0 & \frac{1}{2\overline{c}^2} & \frac{1}{2\overline{c}^2} \\ 0 & 0 & \frac{1}{2\overline{\rho c}} & \frac{1}{2\overline{\rho c}} \\ 0 & \frac{1}{\overline{\rho c}} & 0 & 0 \\ 0 & 0 & \frac{1}{2} & \frac{1}{2} \end{pmatrix} \begin{pmatrix} C_1 \\ C_2 \\ C_3 \\ C_4 \end{pmatrix} \tag{2.67}$$

b) One-dimensional, Unsteady Boundary Conditions.

Inflow:

$$\begin{pmatrix} C_1 \\ C_2 \\ C_3 \end{pmatrix} = 0 \tag{2.68}$$

Outflow:

$$C_4 = 0 \tag{2.69}$$

c) Fourth order, Two-dimensional, Unsteady, Inflow Boundary Conditions.

$$\frac{\partial}{\partial t} \begin{pmatrix} C_1 \\ C_2 \\ C_3 \end{pmatrix} + \begin{pmatrix} 0 & 0 & 0 & 0 \\ 0 & \overline{v} & \frac{1}{2}(\overline{c}+\overline{u}) & \frac{1}{2}(\overline{c}-\overline{u}) \\ 0 & \frac{1}{2}(\overline{c}-\overline{u}) & \overline{v} & 0 \end{pmatrix} \frac{\partial}{\partial y} \begin{pmatrix} C_1 \\ C_2 \\ C_3 \\ C_4 \end{pmatrix} = 0 \tag{2.70}$$

d) Second order, Two-dimensional, Unsteady, Outflow BC.

$$\frac{\partial C_4}{\partial t} + \begin{pmatrix} 0 & \overline{u} & 0 & \overline{v} \end{pmatrix} \frac{\partial}{\partial y} \begin{pmatrix} C_1 \\ C_2 \\ C_3 \\ C_4 \end{pmatrix} = 0 \tag{2.71}$$

e) First/fourth order, Two-dimensional, Unsteady, Outflow BC.

$$\frac{\partial C_4}{\partial t} + \begin{pmatrix} 0 & \frac{1}{2}(\overline{c} + \overline{u}) & 0 & \overline{v} \end{pmatrix} \frac{\partial}{\partial y} \begin{pmatrix} C_1 \\ C_2 \\ C_3 \\ C_4 \end{pmatrix} = 0 \tag{2.72}$$

Chapter 3

Wall Corner Compatibility Conditions for 2D Cartesian Giles Boundary Conditions

The inviscid solid wall boundary condition is easily formulated: there is no flow through the wall

$$\vec{V} \bullet \vec{n} = 0 \tag{3.1}$$

CFD codes, which were originally designed to compute steady-flows, usually do not update the wall boundary points using the interior equations; instead, the flow variables at the wall are updated by extrapolating data from the interior points and setting the normal velocity at the wall to zero. This method is acceptable for steady-state flow problems, but introduces a nonphysical propagating speed from the interior to the wall when an unsteady flow is calculated.

For a time-accurate problem, it is thus preferable to compute the wall surface as an interior point in the domain, setting the wall boundary conditions using the normal derivatives at the wall surface. An example of this approach, introduced by Tam and Dong [75] for linearized flow equations on Cartesian grids, is briefly summarized below.

For an unsteady flow, not only is the flow through the wall in the normal direction zero, but its time derivative is as well:

$$\overrightarrow{V} \bullet \overrightarrow{n} = 0, \quad \frac{\partial}{\partial t}\left(\overrightarrow{V} \bullet \overrightarrow{n}\right) = 0. \tag{3.2}$$

Consider a wall that lies at the $y = 0$ plane, with its normal pointing in the positive y direction. The linearized Euler equations at the wall for $\overline{v} = 0$ are:

$$\begin{aligned} \rho_t + \overline{u}\rho_x + \overline{\rho}\left(u_x + v_y\right) &= 0 \\ u_t + \overline{u}u_x + \frac{1}{\overline{\rho}}\left(p_x\right) &= 0 \\ v_t + \frac{1}{\overline{\rho}}\left(p_y\right) &= 0 \\ p_t + \overline{u}p_x + \overline{\rho c}^2\left(u_x + v_y\right) &= 0 \end{aligned} \tag{3.3}$$

Since the normal derivatives of the density and tangential velocity at the wall do not appear in the equations, this leaves the possibility of setting the normal derivatives of pressure and normal velocity at the wall.

The Tam and Dong approach proposes that the boundary condition specify the minimum amount of exterior data required to set the analytic boundary condition.

Since only the normal derivative of the pressure at the wall appears in the normal velocity equation, the analytic boundary condition $v_t = 0$ can be enforced by setting $p_y = 0$ (using a "ghost point" outside of the computational domain), and calculating v_y at the wall by using only interior information (using a fully one-sided boundary stencil). Looking back to the section "The Physical Problem" in chapter 1, an interesting result from the Thompson-type analysis is that the time derivative of the normal velocity at the wall would be set by combining an outgoing acoustic wave from the interior of the computational domain with an incoming acoustic wave specified by the boundary condition. Since, in the Thompson 1-D characteristics, the incoming acoustic wave contains both pressure and normal velocity derivatives, most of the wall conditions given may be incorrectly specifying the wall boundary by not specifying the normal derivative of the normal velocity at the wall in addition to the normal derivative of pressure at the wall. However, the wall boundary conditions specifying the normal pressure derivative alone have been applied to a wide range of linear and nonlinear flow problems with great success.

Treating the grid points on a wall boundary as interior points of the domain raises the question of what needs to be done at the interface of a wall boundary and an inflow or outflow boundary. At the intersection of a wall and inflow/outflow boundary, the flow solution should satisfy both the boundary conditions. To deal with this issue, a set of compatibility conditions are required to blend the differing boundary conditions at intersection of boundaries. Collino [63] developed a set of compatibility conditions at boundary intersections for the wave equation. In the corner treatment proposed by Rowley and Colonius [64], the boundary conditions are written in terms of spatial

derivatives normal to the boundary (using the full governing equations), thus applying the boundary conditions as closures for the derivatives. Then at the corner point, the BC for both the derivatives is specified.

In the present work, a new compatibility condition is derived for calculations at wall corners for the Giles non-reflecting boundary conditions. The wall condition developed in this work is based on Tam and Dong's approach [75] by setting the pressure derivative normal to the wall (using a "ghost point" outside of the computational domain) such that there is no flow through the wall at the corner.

Wall boundary condition for the 2D Cartesian Giles boundary conditions are derived for a simple 2D Cartesian domain shown in Fig 3-1.

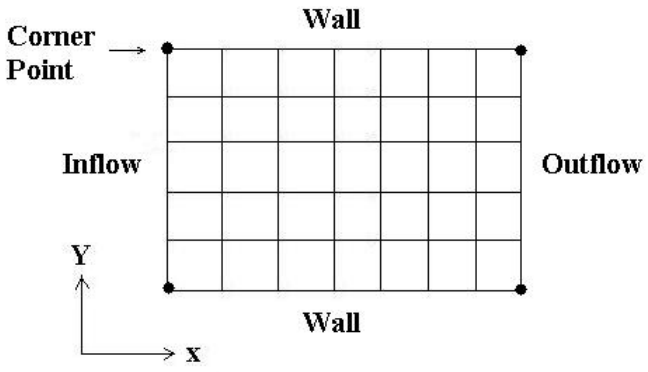

Figure 3-1: **2D Computational Domain with Wall Corners**

3.1 Giles Inflow-Wall Corner Condition

The time derivatives of the incoming characteristics $(C_1)_t, (C_2)_t, (C_3)_t$ are first computed on the inflow boundary using the Giles boundary conditions. These time derivatives must be corrected such that they result in a flow solution that satisfies

the unsteady wall boundary condition at the corner points.

The unsteady wall boundary condition can be written in terms of the time derivatives of the inflow boundary characteristics as:

$$\left.\frac{\partial}{\partial t}\left(\overline{\rho}\overline{c}v'\right)\right|_{\text{corner}} = 0 = \left.\frac{\partial C_2}{\partial t}\right|_{\text{corner}} \tag{3.4}$$

We need to write the unsteady wall boundary condition in terms of the normal pressure derivative p'_y in order to implement the pressure-derivative correction based wall boundary condition discussed earlier. From the 2D Cartesian Giles inflow boundary conditions, $(C_2)_t$ is a function of $(C_2)_y, (C_3)_y, (C_4)_y$ which in turn are functions of u'_y, v'_y, and p'_y.

$$\Rightarrow \quad \left.\frac{\partial}{\partial t}\left(\overline{\rho}\overline{c}v'\right)\right|_{\text{corner}} = -\overline{v}\frac{\partial C_2}{\partial y} - \frac{1}{2}\left(\overline{c}+\overline{u}\right)\frac{\partial C_3}{\partial y} - \frac{1}{2}\left(\overline{c}-\overline{u}\right)\frac{\partial C_4}{\partial y} \tag{3.5}$$

Since the desired value of time derivative of flow through the wall is zero, the required change would be:

$$\Delta\frac{\partial}{\partial t}\left(\overline{\rho}\overline{c}v'\right) = -\left.\frac{\partial}{\partial t}\left(\overline{\rho}\overline{c}v'\right)\right|_{\text{corner}} \tag{3.6}$$

$$\Rightarrow \quad \left.\Delta\frac{\partial}{\partial t}\left(\overline{\rho}\overline{c}v'\right)\right|_{\text{corner}} = -\overline{v}\Delta\left(\frac{\partial C_2}{\partial y}\right) - \frac{1}{2}\left(\overline{c}+\overline{u}\right)\Delta\left(\frac{\partial C_3}{\partial y}\right) - \frac{1}{2}\left(\overline{c}-\overline{u}\right)\Delta\left(\frac{\partial C_4}{\partial y}\right) \tag{3.7}$$

From the 1D characteristics,

$$\begin{aligned}
\Delta\frac{\partial C_2}{\partial y} &= \overline{\rho c}\Delta\left(\frac{\partial v'}{\partial y}\right) \\
\Delta\frac{\partial C_3}{\partial y} &= \overline{\rho c}\Delta\left(\frac{\partial u'}{\partial y}\right) + \Delta\left(\frac{\partial p'}{\partial y}\right) \qquad (3.8)\\
\Delta\frac{\partial C_4}{\partial y} &= \overline{\rho c}\Delta\left(\frac{\partial u'}{\partial y}\right) - \Delta\left(\frac{\partial p'}{\partial y}\right) \qquad (3.9)\\
& \qquad (3.10)
\end{aligned}$$

We do not wish to set the normal derivatives of u', and v'. Therefore,

$$\Delta\left(\frac{\partial u'}{\partial y}\right) = \Delta\left(\frac{\partial v'}{\partial y}\right) = 0 \qquad (3.11)$$

Substituting $(C_2)_y, (C_3)_y, (C_4)_y$ into Eq. (3.7) we get an expression for the required change in normal derivative of pressure at the wall corner in order for the time derivative of flow through wall to be zero:

$$\Delta\left(\frac{\partial p'}{\partial y}\right)_{\text{corner}} = \frac{1}{\overline{c}}\frac{\partial}{\partial t}\left(\overline{\rho c}v'\right) \qquad (3.12)$$

Once the normal pressure derivative correction is obtained at the wall corner point, the change is applied to the derivative of the boundary point and the interior points by modifying the value of a "ghost point" outside the computational domain as mentioned before. The time derivatives $(C_1)_t, (C_2)_t, (C_3)_t$ are re-calculated for implementation of the Giles boundary conditions by applying the pressure derivative correction

as follows:

$$\Delta\left(\frac{\partial C_1}{\partial t}\right) = 0 \tag{3.13}$$

$$\Delta\left(\frac{\partial C_2}{\partial t}\right) = -\overline{c}\Delta\left(\frac{\partial p'}{\partial y}\right) \tag{3.14}$$

$$\Delta\left(\frac{\partial C_3}{\partial t}\right) = -\overline{v}\Delta\left(\frac{\partial p'}{\partial y}\right) \tag{3.15}$$

3.2 Giles Outflow-Wall Corner Condition

Recall Eq. (3.2),

$$\left.\frac{\partial}{\partial t}\left(\overline{\rho}\overline{c}v'\right)\right|_{\text{corner}} = 0 = \left.\frac{\partial C_2}{\partial t}\right|_{\text{corner}}$$

At the outflow boundary, C_2 is an outgoing characteristic and therefore cannot be modified. Recall that the present analysis assumes that the inflow/outflow boundary is orthogonal to the wall boundary at the corner. Hence, this approach to developing the compatibility conditions cannot be used to derive wall corner conditions for the Giles outflow boundary condition when the outflow is orthogonal to the wall boundary at the corners. For a non-orthogonal boundary intersection, this approach results in a valid wall corner condition as shown in the next section.

3.3 Wall Corner Conditions for the Chain-rule Form of Giles Boundary Conditions

Since the BASS code solves governing equations in the non-conservative chain rule form of Euler equations, the above wall condition is also derived for the chain-rule form of Giles boundary conditions.

Define :

Unit vectors tangent and normal to the non-reflecting boundary

$$\overrightarrow{m} = m_x\hat{i} + m_y\hat{j} \tag{3.16}$$

$$\overrightarrow{n} = n_x\hat{i} + n_y\hat{j} \tag{3.17}$$

Unit vectors tangent and normal to the wall boundary

$$\overrightarrow{M_w} = M_{wx}\hat{i} + M_{wy}\hat{j} \tag{3.18}$$

$$\overrightarrow{N_w} = N_{wx}\hat{i} + N_{wy}\hat{j} \tag{3.19}$$

and

$$\overrightarrow{\overline{V}} = \overline{u}\hat{i} + \overline{v}\hat{j}$$

$$\overrightarrow{V'} = u'\hat{i} + v'\hat{j}$$

$$\overline{V}_m = \overrightarrow{\overline{V}} \bullet \overrightarrow{m}, \quad \overline{V}_n = \overrightarrow{\overline{V}} \bullet \overrightarrow{n}$$

$$V'_m = \overrightarrow{V'} \bullet \overrightarrow{m}, \quad V'_n = \overrightarrow{V'} \bullet \overrightarrow{n}$$

$$\xi_m = \frac{\partial \xi}{\partial m}, \quad \eta_m = \frac{\partial \eta}{\partial m}$$

The one-dimensional characteristic variables for 2D Euler equations can be written as

$$C_1 = p' - \overline{c}^2 \rho' \qquad \text{(incoming if } \overline{\mathrm{V}}_\mathrm{n} < 0) \tag{3.20}$$

$$C_2 = \overline{\rho c}\,(V_m') \qquad \text{(incoming if } \overline{\mathrm{V}}_\mathrm{n} < 0) \tag{3.21}$$

$$C_3 = p' - \overline{\rho c}\,(V_n') \qquad \text{(incoming if } \overline{\mathrm{V}}_\mathrm{n} - \overline{\mathrm{c}} < 0) \tag{3.22}$$

$$C_4 = p' + \overline{\rho c}\,(V_n') \qquad \text{(incoming if } \overline{\mathrm{V}}_\mathrm{n} + \overline{\mathrm{c}} < 0) \tag{3.23}$$

Re-writing the two-dimensional Giles boundary conditions using the chain-rule formulation in Curvilinear co-ordinates:

Inflow:

$$\left.\frac{\partial C}{\partial t}\right|_{NoWallBC} = [A]\,\frac{\partial C}{\partial \xi} + [B]\,\frac{\partial C}{\partial \eta} \tag{3.24}$$

where

$$C = \begin{pmatrix} C_1 \\ C_2 \\ C_3 \end{pmatrix},$$

$$A = \begin{pmatrix} 0 & 0 & 0 & 0 \\ 0 & -\xi_m \overline{V}_m & -\frac{1}{2}\xi_m(\overline{c} - \overline{V}_n) & -\frac{1}{2}\xi_m(\overline{c} + \overline{V}_n) \\ 0 & -\frac{1}{2}\xi_m(\overline{c} + \overline{V}_n) & -\xi_m \overline{V}_m & 0 \end{pmatrix},$$

$$B = \begin{pmatrix} 0 & 0 & 0 & 0 \\ 0 & -\eta_m \overline{V}_m & -\frac{1}{2}\eta_m(\overline{c} - \overline{V}_n) & -\frac{1}{2}\eta_m(\overline{c} + \overline{V}_n) \\ 0 & -\frac{1}{2}\eta_m(\overline{c} + \overline{V}_n) & -\eta_m \overline{V}_m & 0 \end{pmatrix}$$

Outflow:

$$\frac{\partial C_4}{\partial t} + \xi_m \overline{V_n} \frac{\partial C_2}{\partial \xi} + \xi_m \overline{V_m} \frac{\partial C_3}{\partial \xi} + \eta_m \overline{V_n} \frac{\partial C_2}{\partial \eta} + \eta_m \overline{V_m} \frac{\partial C_3}{\partial \eta} = 0 \tag{3.25}$$

3.3.1 Giles Inflow-Wall Corner Condition

For an unsteady flow, not only is the flow through the wall in the normal direction zero, but also its time derivative.

$$\overrightarrow{V'} \bullet \overrightarrow{N_w} = 0, \qquad \frac{\partial}{\partial t}\left(\overrightarrow{V'} \bullet \overrightarrow{N_w}\right) = 0 \tag{3.26}$$

Flow through the wall $\dfrac{\partial}{\partial t}\left(\overrightarrow{V'} \bullet \overrightarrow{N_w}\right)$ can be written as a function of C_2, C_3, and C_4:

$$\overline{\rho c}\, \frac{\partial}{\partial t}\left(\overrightarrow{V'} \bullet \overrightarrow{N_w}\right)\Big|_{NoWallBC} = \left(\overrightarrow{m} \bullet \overrightarrow{N_w}\right) \frac{\partial C_2}{\partial t}\Big|_{NoWallBC} + \frac{1}{2}\left(\overrightarrow{n} \bullet \overrightarrow{N_w}\right) \frac{\partial (C_4 - C_3)}{\partial t}\Big|_{NoWallBC} \tag{3.27}$$

And,

$$\overline{\rho c}\,\frac{\partial}{\partial t}\left(\overrightarrow{V'}\bullet\overrightarrow{N_w}\right)\Big|_{WallBC} = \left(\overrightarrow{m}\bullet\overrightarrow{N_w}\right)\,\frac{\partial C_2}{\partial t}\Big|_{WallBC} + \frac{1}{2}\left(\overrightarrow{n}\bullet\overrightarrow{N_w}\right)\,\frac{\partial(C_4-C_3)}{\partial t}\Big|_{WallBC} = 0 \tag{3.28}$$

$$\Delta\left[\overline{\rho c}\frac{\partial}{\partial t}\left(\overrightarrow{V'}\bullet\overrightarrow{N_w}\right)\right] = \overline{\rho c}\,\frac{\partial}{\partial t}\left(\overrightarrow{V'}\bullet\overrightarrow{N_w}\right)\Big|_{WallBC} - \overline{\rho c}\,\frac{\partial}{\partial t}\left(\overrightarrow{V'}\bullet\overrightarrow{N_w}\right)\Big|_{NoWallBC} \tag{3.29}$$

$$\Longrightarrow \Delta\left[\overline{\rho c}\frac{\partial}{\partial t}\left(\overrightarrow{V'}\bullet\overrightarrow{N_w}\right)\right] = \left(\overrightarrow{m}\bullet\overrightarrow{N_w}\right)\Delta\left[\frac{\partial C_2}{\partial t}\right] + \frac{1}{2}\left(\overrightarrow{n}\bullet\overrightarrow{N_w}\right)\Delta\left[\frac{\partial(C_4-C_3)}{\partial t}\right] \tag{3.30}$$

where

$$\Delta\left[\frac{\partial C}{\partial t}\right] = \frac{\partial C}{\partial t}\Big|_{WallBC} - \frac{\partial C}{\partial t}\Big|_{NoWallBC} \tag{3.31}$$

Each one of $\frac{\partial C_2}{\partial t}$, $\frac{\partial C_3}{\partial t}$, and $\frac{\partial C_4}{\partial t}$ are in turn functions of $\frac{\partial C_2}{\partial \eta}$, $\frac{\partial C_3}{\partial \eta}$, and $\frac{\partial C_4}{\partial \eta}$ which are again functions of $\frac{\partial u'}{\partial \eta}$, $\frac{\partial v'}{\partial \eta}$, and $\frac{\partial p'}{\partial \eta}$. Therefore, the change in time derivatives of the characteristic variables due to the wall boundary condition can be expressed in terms of η-derivatives of the primitive variables. The time derivative of C_4 cannot be changed because it is outgoing acoustic wave at the inflow boundary.

$$\Longrightarrow \qquad \Delta\left[\frac{\partial C_4}{\partial t}\right]_{\text{corner}} = 0 \tag{3.32}$$

We do not want to change the η-derivatives of u' and v'.

$$\Longrightarrow \qquad \Delta\,\frac{\partial u'}{\partial \eta}\Big|_{\text{corner}} = 0, \qquad \Delta\,\frac{\partial v'}{\partial \eta}\Big|_{\text{corner}} = 0 \tag{3.33}$$

Correction to the η-derivatives of characteristic variables is given by

$$\Delta\left[\frac{\partial C_1}{\partial \eta}\right] = \Delta\left[\frac{\partial p'}{\partial \eta}\right] \tag{3.34}$$

$$\Delta\left[\frac{\partial C_2}{\partial \eta}\right] = 0 \tag{3.35}$$

$$\Delta\left[\frac{\partial C_3}{\partial \eta}\right] = \Delta\left[\frac{\partial p'}{\partial \eta}\right] \tag{3.36}$$

$$\Delta\left[\frac{\partial C_4}{\partial \eta}\right] = \Delta\left[\frac{\partial p'}{\partial \eta}\right] \tag{3.37}$$

Therefore, the correction to the time derivatives of the characteristic variables is given by

$$\Delta\left[\frac{\partial C_1}{\partial t}\right] = 0 \tag{3.38}$$

$$\Delta\left[\frac{\partial C_2}{\partial t}\right] = -\eta_m \overline{c}\,\Delta\left[\frac{\partial p'}{\partial \eta}\right] \tag{3.39}$$

$$\Delta\left[\frac{\partial C_3}{\partial t}\right] = -\eta_m \overline{V}_m \Delta\left[\frac{\partial p'}{\partial \eta}\right] \tag{3.40}$$

$$\Delta\left[\frac{\partial C_4}{\partial t}\right] = 0 \tag{3.41}$$

The central idea of this approach is to correct the pressure normal derivative at the wall corner point $\Delta\left[\frac{\partial p'}{\partial \eta}\right]$ such that the flow normal to the wall, $\frac{\partial}{\partial t}\left(\overrightarrow{V'} \bullet \overrightarrow{N_w}\right) = 0$. So we need to express $\Delta\left[\frac{\partial p'}{\partial \eta}\right]$ in terms of the flow normal to the wall $\frac{\partial}{\partial t}\left(\overrightarrow{V'} \bullet \overrightarrow{N_w}\right)$. This is achieved by substituting $\Delta\left(\frac{\partial C_2}{\partial t}\right)$, $\Delta\left(\frac{\partial C_3}{\partial t}\right)$, and $\Delta\left(\frac{\partial C_4}{\partial t}\right)$ from the above equations into Eq. (4.99).

$$\Longrightarrow \qquad \Delta\left[\frac{\partial p'}{\partial \eta}\right]_{\text{corner}} = \frac{\overline{\rho c}\,\frac{\partial}{\partial t}\left(\overrightarrow{V'} \bullet \overrightarrow{N_w}\right)\Big|_{NoWallBC}}{\eta_m\left(\left(\overrightarrow{m} \bullet \overrightarrow{N_w}\right)\overline{c} + \frac{1}{2}\left(\overrightarrow{n} \bullet \overrightarrow{N_w}\right)\overline{V}_m\right)} \tag{3.42}$$

The above correction for normal derivative of pressure reduces to the expression obtained for the pressure derivative correction for the Cartesian form of Giles boundary conditions when the inflow and wall boundaries are orthogonal to each other at the corners.

Corrections to $\frac{\partial C}{\partial t}$ are then calculated using Eqs. (4.107) to (4.110). Finally, the time derivatives of the characteristics are corrected:

$$\left.\frac{\partial C}{\partial t}\right|_{\text{WallBC}} = \left.\frac{\partial C}{\partial t}\right|_{\text{NoWallBC}} + \Delta\left[\frac{\partial C}{\partial t}\right] \tag{3.43}$$

The time derivatives of primitive variables are then computed from $\left.\frac{\partial C}{\partial t}\right|_{\text{WallBC}}$.

3.3.2 Giles Outflow-Wall Corner Condition

The outflow wall corner boundary condition is obtained by following the same procedure adopted for the inflow boundary. At the outflow boundary C_1, C_2, and C_3 are outgoing characteristics and C_4 is the only incoming characteristic. Hence,

$$\Delta\left[\frac{\partial C_1}{\partial t}\right]_{\text{corner}} = \Delta\left[\frac{\partial C_2}{\partial t}\right]_{\text{corner}} = \Delta\left[\frac{\partial C_3}{\partial t}\right]_{\text{corner}} = 0 \tag{3.44}$$

As mentioned earlier,

$$\Delta\left[\frac{\partial C_4}{\partial t}\right] = -\eta_m \overline{V}_m \Delta\left[\frac{\partial p'}{\partial \eta}\right]$$

The pressure derivative correction at the outflow wall corner will then be (using

Eq. (4.99))

$$\Delta \left[\frac{\partial p'}{\partial \eta}\right]_{\text{corner}} = \frac{\overline{\rho c}\,\frac{\partial}{\partial t}\left(\overrightarrow{V'} \bullet \overrightarrow{N_w}\right)\Big|_{NoWallBC}}{\frac{1}{2}\eta_m \left(\overrightarrow{n} \bullet \overrightarrow{N_w}\right)\overline{V}_m} \tag{3.45}$$

One limitation of this method is that whenever the wall boundary is orthogonal to the outflow boundary at the corners, the denominator of $\Delta \left[\frac{\partial p'}{\partial \eta}\right]_{\text{corner}}$ goes to zero and hence the method cannot be applied at the outflow boundary in such cases.

Once the pressure derivative correction is obtained, it is propagated into the interior domain and the values of $\left.\frac{\partial C}{\partial t}\right|_{\text{WallBC}}$ are calculated as described in the previous section.

Chapter 4

Giles Boundary Conditions for 2D Euler Equations in Curvilinear Co-ordinates

The theoretical framework for the extension of one and two-dimensional Giles boundary conditions (in Cartesian co-ordinates) to boundary conditions in a Curvilinear co-ordinate system is presented in this chapter. The general theory and its application to Euler equations and well-posedness analysis presented in chapter(4) is closely followed to derive the boundary conditions in Curvilinear co-ordinates.

4.1 Non-dimensional 2D Linearized Euler Equations in Curvilinear Co-ordinates

The 2D Cartesian conservative form of unsteady, compressible, Euler equations in Eq. (2.51) can be written in a vector form as:

$$\frac{\partial Q}{\partial t} + \frac{\partial E}{\partial x} + \frac{\partial F}{\partial y} = 0 \tag{4.1}$$

For the present analysis, these equations are re-written in a generalized Curvilinear co-ordinate system with no grid motion whose Curvilinear co-ordinates are:

$$\begin{aligned} \tau &= t \\ \xi &= \xi(x, y) \\ \eta &= \eta(x, y) \end{aligned} \tag{4.2}$$

Using the chain-rule formulation, these equations are written in Curvilinear co-ordinate system as:

$$\frac{\partial Q}{\partial t} + \frac{\partial \xi}{\partial x}\frac{\partial E}{\partial \xi} + \frac{\partial \eta}{\partial x}\frac{\partial E}{\partial \eta} + \frac{\partial \xi}{\partial x}\frac{\partial F}{\partial \xi} + \frac{\partial \eta}{\partial x}\frac{\partial F}{\partial \eta} = 0 \tag{4.3}$$

where,

$$Q = \begin{pmatrix} \rho \\ \rho u \\ \rho v \\ E_{total} \end{pmatrix} \tag{4.4}$$

The above equations are linearized about an assumed uniform mean flow ($\overline{\rho},\ \overline{u},\ \overline{v},\ \overline{p}$) to give

$$\frac{\partial U}{\partial t} + \begin{pmatrix} \overline{U} & \xi_x\overline{\rho} & \xi_y\overline{\rho} & 0 \\ 0 & \overline{U} & 0 & \frac{\xi_x}{\overline{\rho}} \\ 0 & 0 & \overline{U} & \frac{\xi_y}{\overline{\rho}} \\ 0 & \xi_x\gamma\overline{p} & \xi_y\gamma\overline{p} & \overline{U} \end{pmatrix} \frac{\partial U}{\partial \xi} + \begin{pmatrix} \overline{V} & \eta_x\overline{\rho} & \eta_y\overline{\rho} & 0 \\ 0 & \overline{V} & 0 & \frac{\eta_x}{\overline{\rho}} \\ 0 & 0 & \overline{V} & \frac{\eta_y}{\overline{\rho}} \\ 0 & \eta_x\gamma\overline{p} & \eta_y\gamma\overline{p} & \overline{V} \end{pmatrix} \frac{\partial U}{\partial \eta} = 0 \qquad (4.5)$$

where U is the vector of perturbation variables, $U = \begin{pmatrix} \rho' \\ u' \\ v' \\ p' \end{pmatrix}$,

The Contravariant mean velocities are given by:

$$\overline{U} = \xi_x\overline{u} + \xi_y\overline{v} \qquad (4.6)$$

$$\overline{V} = \eta_x\overline{u} + \eta_y\overline{v} \qquad (4.7)$$

The linearized equations are non-dimensionalized using the steady density $\overline{\rho}$ and speed of sound $\overline{c}$. This gives the equations in the form required for Fourier analysis:

$$\frac{\partial U}{\partial t} + [A]\frac{\partial U}{\partial \xi} + [B]\frac{\partial U}{\partial \eta} = 0 \qquad (4.8)$$

where

$$A = \begin{pmatrix} \overline{U} & \xi_x & \xi_y & 0 \\ 0 & \overline{U} & 0 & \xi_x \\ 0 & 0 & \overline{U} & \xi_y \\ 0 & \xi_x & \xi_y & \overline{U} \end{pmatrix}, \qquad B = \begin{pmatrix} \overline{V} & \eta_x & \eta_y & 0 \\ 0 & \overline{V} & 0 & \eta_x \\ 0 & 0 & \overline{V} & \eta_y \\ 0 & \eta_x & \eta_y & \overline{V} \end{pmatrix} \tag{4.9}$$

It should be noted that in addition to the approximation errors due to the steady state perturbations and non-uniformities in the mean flow, and the non-uniformities in grid metrics also contribute to the overall error.

4.2 Fourier Analysis

A wave-like solution to the Euler equations in Eq. (4.8) of the form

$$U(\xi, \eta, t) = ue^{i(k\xi + l\eta - \omega t)} \tag{4.10}$$

is considered for the Fourier analysis. Before beginning the analysis, the following terms are defined for convenience of displaying lengthy equations:

$$\Psi = \sqrt{\xi_x^2 + \xi_y^2}, \qquad \Phi = \sqrt{\eta_x^2 + \eta_y^2}$$

$$\mu = \xi_x \eta_x + \xi_y \eta_y, \qquad \nu = \xi_x \eta_y - \xi_y \eta_x$$

Following the theory described in chapter 3, the dispersion relation is first obtained.

$$
\begin{aligned}
det\left(-\omega I + kA + lB\right) &= det\begin{bmatrix} \overline{U}k + \overline{V}l - \omega & \xi_x k + \eta_x l & \xi_y k + \eta_y l & 0 \\ 0 & \overline{U}k + \overline{V}l - \omega & 0 & \xi_x k + \eta_x l \\ 0 & 0 & \overline{U}k + \overline{V}l - \omega & \xi_y k + \eta_y l \\ 0 & \xi_x k + \eta_x l & \xi_y k + \eta_y l & \overline{U}k + \overline{V}l - \omega \end{bmatrix} \\
&= \left(\overline{U}k + \overline{V}l - \omega\right)^2 \left[\left(\overline{U}k + \overline{V}l - \omega\right)^2 - \left(\xi_x k + \eta_x l\right)^2 - \left(\xi_y k + \eta_y l\right)^2\right] \\
&= 0 \qquad (4.11)
\end{aligned}
$$

The first two roots of the dispersion relation are identical.

$$k_{1,2} = \frac{\omega - \overline{V}l}{\overline{U}} \qquad (4.12)$$

The other two roots are given by

$$\left(\overline{U}k + \overline{V}l - \omega\right)^2 - \left(\xi_x k + \eta_x l\right)^2 - \left(\xi_y k + \eta_y l\right)^2 = 0 \qquad (4.13)$$

$$k_{3,4} = \frac{\overline{U}\left(\overline{V}l - \omega\right) - \mu l}{\Psi^2 - \overline{U}^2} \pm \frac{\left[\left(\overline{U}\left(\overline{V}l - \omega\right) - \mu l\right)^2 + \left(\Psi^2 - \overline{U}^2\right)\left(\left(\overline{V}l - \omega\right)^2 - l^2\Phi^2\right)\right]^{1/2}}{\Psi^2 - \overline{U}^2} \qquad (4.14)$$

Hence the third and fourth roots are:

$$k_3 = \frac{\left(\omega - \overline{V}l\right)\left(-\overline{U} + S_1\right)}{\Psi^2 - \overline{U}^2} \tag{4.15}$$

$$k_4 = \frac{\left(\omega - \overline{V}l\right)\left(-\overline{U} - S_2\right)}{\Psi^2 - \overline{U}^2} \tag{4.16}$$

where

$$S_1 = -\frac{\mu l}{\omega - \overline{V}l} + \sqrt{\Psi^2 - \frac{\left(\nu^2 - \Phi^2\overline{U}^2\right)l^2}{\left(\omega - \overline{V}l\right)^2} + \frac{2\mu\overline{U}l}{\left(\omega - \overline{V}l\right)}} \tag{4.17}$$

$$S_2 = \frac{\mu l}{\omega - \overline{V}l} + \sqrt{\Psi^2 - \frac{\left(\nu^2 - \Phi^2\overline{U}^2\right)l^2}{\left(\omega - \overline{V}l\right)^2} + \frac{2\mu\overline{U}l}{\left(\omega - \overline{V}l\right)}} \tag{4.18}$$

4.3 Eigenvectors

4.3.1 Root 1: Entropy Wave

$$k_1 = \frac{\omega - \overline{V}l}{\overline{U}}, \qquad \omega = \overline{U}k_1 + \overline{V}l \tag{4.19}$$

Substituting for ω gives

$$(-\omega I + k_1 A + lB) = \begin{pmatrix} 0 & (\xi_x k_1 + \eta_x l) & (\xi_y k_1 + \eta_y l) & 0 \\ 0 & 0 & 0 & (\xi_x k_1 + \eta_x l) \\ 0 & 0 & 0 & (\xi_y k_1 + \eta_y l) \\ 0 & (\xi_x k_1 + \eta_x l) & (\xi_y k_1 + \eta_y l) & 0 \end{pmatrix} \tag{4.20}$$

Right eigenvector is chosen as

$$u_1^R = \begin{pmatrix} -\xi_x \\ 0 \\ 0 \\ 0 \end{pmatrix} \tag{4.21}$$

and a corresponding left eigenvector is

$$u_1^L = \begin{pmatrix} -\xi_x & 0 & 0 & \xi_x \end{pmatrix} \tag{4.22}$$

The vector v_1^L, which is needed to construct the non-reflecting boundary condi-

tions, is calculated following the procedure given in the theory section.

$$\begin{aligned} v_1^L &= \frac{1}{\overline{U}} u_1^L A \\ &= \begin{pmatrix} -\xi_x & 0 & 0 & \xi_x \end{pmatrix} \end{aligned} \tag{4.23}$$

This choice of eigenvectors corresponds to the entropy wave traveling downstream at a speed $\overline{U} > 0$. This can be verified by noting that the only non-zero term in the right eigenvector is the density, so that the wave has varying entropy, no vorticity and constant pressure. Also, the left eigenvector 'measures' entropy in the sense that $u_1^L U$ is equal to the linearized entropy, $\xi_x(p' - \rho')$ (remembering that $c = 1$ because of the non-dimensionalization).

These eigenvectors are obtained by multiplying with an arbitrary factor. They may be multiplied by an arbitrary constant or a function of λ and they would still be eigenvectors. In the present work, corresponding to all the four roots of the dispersion relation, the arbitrary factors were chosen to give the simplest form for the eigenvectors subject to the one restriction that at $\lambda = 0$, $u^L u^R = 1$. This restriction gives the orthonormal form for the vectors w which was assumed in the theory section, Eq. (2.21).

4.3.2 Root 2: Vorticity Wave

$$k_2 = \frac{\omega - \overline{V}l}{\overline{U}}, \qquad \omega = \overline{U}k_2 + \overline{V}l \tag{4.24}$$

The second set of eigenvectors for the multiple root is given by

Right eigenvector:

$$u_2^R = \frac{1}{\Psi^2}\begin{pmatrix} 0 \\ -\xi_y\left(1-\overline{V}\lambda\right) - \eta_y\overline{U}\lambda \\ \xi_x\left(1-\overline{V}\lambda\right) + \eta_x\overline{U}\lambda \\ 0 \end{pmatrix} \tag{4.25}$$

Left eigenvector:

$$u_2^L = \begin{pmatrix} 0 & \left(-\xi_y\left(1-\overline{V}\lambda\right) - \eta_y\overline{U}\lambda\right) & \left(\xi_x\left(1-\overline{V}\lambda\right) + \eta_x\overline{U}\lambda\right) & 0 \end{pmatrix} \tag{4.26}$$

The vector v_2^L, which is needed to construct the non-reflecting boundary conditions, is calculated following the procedure given in the theory section.

$$\begin{aligned} v_2^L &= \frac{1}{\overline{U}}u_2^L A \\ &= \begin{pmatrix} 0 & \left(-\xi_y\left(1-\overline{V}\lambda\right) - \eta_y\overline{U}\lambda\right) & \left(\xi_x\left(1-\overline{V}\lambda\right) + \eta_x\overline{U}\lambda\right) & -\lambda \end{pmatrix} \end{aligned} \tag{4.27}$$

This root corresponds to the vorticity wave traveling downstream at a speed $\overline{U} > 0$, which can be verified by noting that the right eigenvector gives a wave with vorticity, but uniform entropy and pressure. Since the first two roots are a multiple root, it must be verified that the chosen right and left eigenvectors satisfy the necessary

orthogonality relations.

$$v_1^L u_2^R = 0 \tag{4.28}$$

$$v_2^L u_1^R = 0 \tag{4.29}$$

It is easily verified that these relations are satisfied.

The above choice of eigenvectors for the first and second roots is not unique. Any linear combinations of the eigenvectors is itself an eigenvector, and the only constraint is the required orthogonality conditions. The motivation for this particular choice is a knowledge of the distinct behavior of the entropy and vorticity variables in fluid dynamics, which subsequently simplified the algebra at later stages of this analysis.

4.3.3 Root 3: Downstream Running Pressure Wave

$$k_3 = \frac{\left(\omega - \overline{V}l\right)\left(S_1 - \overline{U}\right)}{\Psi^2 - \overline{U}^2}, \quad \omega = \left(\overline{U}k_3 + \overline{V}l\right) + \sqrt{\left(\xi_x k_3 + \eta_x l\right)^2 + \left(\xi_y k_3 + \eta_y l\right)^2} \tag{4.30}$$

Substituting for ω gives

$$(-\omega I + k_3 A + lB) = \begin{pmatrix} \overline{U}k_3 + \overline{V}l - \omega & \xi_x k_3 + \eta_x l & \xi_y k_3 + \eta_y l & 0 \\ 0 & \overline{U}k_3 + \overline{V}l - \omega & 0 & \xi_x k_3 + \eta_x l \\ 0 & 0 & \overline{U}k_3 + \overline{V}l - \omega & \xi_y k_3 + \eta_y l \\ 0 & \xi_x k_3 + \eta_x l & \xi_y k_3 + \eta_y l & \overline{U}k_3 + \overline{V}l - \omega \end{pmatrix} \tag{4.31}$$

Right eigenvector:

$$u_3^R = \frac{1}{2\left(\Psi - \overline{U}\right)\Psi^2} \begin{pmatrix} \left(1 - \overline{V}\lambda\right)\left(\Psi^2 - \overline{U}S_1\right) \\ \xi_x\left(1 - \overline{V}\lambda\right)\left(S_1 - \overline{U}\right) + \eta_x\left(\Psi^2 - \overline{U}^2\right)\lambda \\ \xi_y\left(1 - \overline{V}\lambda\right)\left(S_1 - \overline{U}\right) + \eta_y\left(\Psi^2 - \overline{U}^2\right)\lambda \\ \left(1 - \overline{V}\lambda\right)\left(\Psi^2 - \overline{U}S_1\right) \end{pmatrix} \tag{4.32}$$

Left eigenvector:

$$u_3^L = \frac{1}{\left(\Psi - \overline{U}\right)} \begin{pmatrix} u_{31} & u_{32} & u_{33} & u_{34} \end{pmatrix} \tag{4.33}$$

where

$$u_{31} = \left(1 - \overline{V}\lambda\right)\left(\Psi^2 - \overline{U}S_1\right)$$

$$u_{32} = \xi_x \left(1 - \overline{V}\lambda\right)\left(S_1 - \overline{U}\right) + \eta_x \left(\Psi^2 - \overline{U}^2\right)\lambda$$

$$u_{33} = \xi_y \left(1 - \overline{V}\lambda\right)\left(S_1 - \overline{U}\right) + \eta_y \left(\Psi^2 - \overline{U}^2\right)\lambda$$

$$u_{34} = \left(1 - \overline{V}\lambda\right)\left(\Psi^2 - \overline{U}S_1\right)$$

The vector v_3^L, which is needed to construct the non-reflecting boundary conditions, is calculated following the procedure given in the theory section.

$$\begin{aligned} v_3^L &= \frac{1}{\Psi + \overline{U}}\, u_3^L A \\ &= \begin{pmatrix} v_{31} & v_{32} & v_{33} & v_{34} \end{pmatrix} \end{aligned} \tag{4.34}$$

where

$$v_{31} = 0$$

$$v_{32} = \xi_x \left(1 - \overline{V}\lambda\right) + \eta_x \overline{U}\lambda$$

$$v_{33} = \xi_y \left(1 - \overline{V}\lambda\right) + \eta_y \overline{U}\lambda$$

$$v_{34} = \left(1 - \overline{V}\lambda\right) S_1 + \mu\lambda$$

This wave corresponds to an isentropic, irrotational pressure wave, traveling downstream at a speed $\overline{U} + 1$ provided $\overline{U} > -1$.

4.3.4 Root 4: Upstream Running Pressure Wave

$$k_4 = -\frac{\left(\omega - \overline{V}l\right)\left(S_2 + \overline{U}\right)}{\Psi^2 - \overline{U}^2}, \quad \omega = \left(\overline{U}k_4 + \overline{V}l\right) - \sqrt{\left(\xi_x k_4 + \eta_x l\right)^2 + \left(\xi_y k_4 + \eta_y l\right)^2} \tag{4.35}$$

Substituting for ω gives

$$(-\omega I + k_4 A + lB) = \begin{pmatrix} \overline{U}k_4 + \overline{V}l - \omega & \xi_x k_4 + \eta_x l & \xi_y k_4 + \eta_y l & 0 \\ 0 & \overline{U}k_4 + \overline{V}l - \omega & 0 & \xi_x k_4 + \eta_x l \\ 0 & 0 & \overline{U}k_4 + \overline{V}l - \omega & \xi_y k_4 + \eta_y l \\ 0 & \xi_x k_4 + \eta_x l & \xi_y k_4 + \eta_y l & \overline{U}k_4 + \overline{V}l - \omega \end{pmatrix} \tag{4.36}$$

Right eigenvector:

$$u_4^R = \frac{1}{2\left(\Psi + \overline{U}\right)\Psi^2} \begin{pmatrix} \left(1 - \overline{V}\lambda\right)\left(\Psi^2 + \overline{U}S_2\right) \\ -\xi_x\left(1 - \overline{V}\lambda\right)\left(S_2 + \overline{U}\right) + \eta_x\left(\Psi^2 - \overline{U}^2\right)\lambda \\ -\xi_y\left(1 - \overline{V}\lambda\right)\left(S_2 + \overline{U}\right) + \eta_y\left(\Psi^2 - \overline{U}^2\right)\lambda \\ \left(1 - \overline{V}\lambda\right)\left(\Psi^2 + \overline{U}S_2\right) \end{pmatrix} \tag{4.37}$$

Left eigenvector :

$$u_4^L = \frac{1}{\left(\Psi + \overline{U}\right)} \begin{pmatrix} u_{41} & u_{42} & u_{43} & u_{44} \end{pmatrix} \tag{4.38}$$

where

$$u_{41} = 0$$

$$u_{42} = -\xi_x \left(1 - \overline{V}\lambda\right) \left(S_2 + \overline{U}\right) + \eta_x \left(\Psi^2 - \overline{U}^2\right) \lambda$$

$$u_{43} = -\xi_y \left(1 - \overline{V}\lambda\right) \left(S_2 + \overline{U}\right) + \eta_y \left(\Psi^2 - \overline{U}^2\right) \lambda$$

$$u_{44} = \left(1 - \overline{V}\lambda\right) \left(\Psi^2 + \overline{U} S_2\right)$$

The vector v_4^L, which is needed to construct the non-reflecting boundary conditions, is calculated following the procedure given in the theory section.

$$\begin{aligned} v_4^L &= -\frac{1}{\Psi - \overline{U}}\, u_4^L A \qquad (4.39) \\ &= \begin{pmatrix} 0 & -\xi_x \left(1 - \overline{V}\lambda\right) - \eta_x \overline{U}\lambda & -\xi_y \left(1 - \overline{V}\lambda\right) - \eta_y \overline{U}\lambda & \left(1 - \overline{V}\lambda\right) S_2 - \mu\lambda \end{pmatrix} \end{aligned}$$

This wave corresponds to an isentropic, irrotational pressure wave, traveling upstream at a speed $\overline{U} - 1$ provided $\overline{U} < 1$.

4.4 One-dimensional, Unsteady Boundary Conditions in Curvilinear Co-ordinates

If the computational domain is $0 < x < 1$, and $0 < \overline{U} < 1$, then the boundary at $x = 0$ is an inflow boundary with incoming waves corresponding to the first three roots, and the boundary at $x = 1$ is an outflow boundary with just one incoming wave due to the fourth root.

When $\lambda = 0$, $S_1 = S_2 = \Psi$, and so the right eigenvectors w^R are

$$w_1^R = \begin{pmatrix} -\xi_x \\ 0 \\ 0 \\ 0 \end{pmatrix}, \quad w_2^R = \begin{pmatrix} 0 \\ -\xi_y/\Psi^2 \\ \xi_x/\Psi^2 \\ 0 \end{pmatrix}, \quad w_3^R = \begin{pmatrix} 1/2\Psi \\ \xi_x/2\Psi^2 \\ \xi_y/2\Psi^2 \\ 1/2\Psi \end{pmatrix}, \quad w_4^R = \begin{pmatrix} 1/2\Psi \\ -\xi_x/2\Psi^2 \\ -\xi_y/2\Psi^2 \\ 1/2\Psi \end{pmatrix} \tag{4.40}$$

and the left eigenvectors w^L are

$$\begin{aligned} w_1^L &= \begin{pmatrix} -\xi_x & 0 & 0 & \xi_x \end{pmatrix} \\ w_2^L &= \begin{pmatrix} 0 & -\xi_y & \xi_x & 1 \end{pmatrix} \\ w_3^L &= \begin{pmatrix} 0 & \xi_x & \xi_y & \Psi \end{pmatrix} \\ w_4^L &= \begin{pmatrix} 0 & -\xi_x & -\xi_y & \Psi \end{pmatrix} \end{aligned} \tag{4.41}$$

Hence the transformation to, and from, 1-D characteristic variables is given by

the following two matrix equations.

$$\begin{pmatrix} C_1 \\ C_2 \\ C_3 \\ C_4 \end{pmatrix} = \begin{pmatrix} -\xi_x & 0 & 0 & \xi_x \\ 0 & -\xi_y & \xi_x & 0 \\ 0 & \xi_x & \xi_y & \Psi \\ 0 & -\xi_x & -\xi_y & \Psi \end{pmatrix} \begin{pmatrix} \rho' \\ u' \\ v' \\ p' \end{pmatrix} \tag{4.42}$$

$$\begin{pmatrix} \rho' \\ u' \\ v' \\ p' \end{pmatrix} = \begin{pmatrix} -\frac{1}{\xi_x} & 0 & \frac{1}{2\Psi} & \frac{1}{2\Psi} \\ 0 & -\frac{\xi_y}{\Psi^2} & \frac{\xi_x}{2\Psi^2} & -\frac{\xi_x}{2\Psi^2} \\ 0 & \frac{\xi_x}{\Psi^2} & \frac{\xi_y}{2\Psi^2} & -\frac{\xi_y}{2\Psi^2} \\ 0 & 0 & \frac{1}{2\Psi} & \frac{1}{2\Psi} \end{pmatrix} \begin{pmatrix} C_1 \\ C_2 \\ C_3 \\ C_4 \end{pmatrix} \tag{4.43}$$

ρ', u', v', and p' are the perturbations from the uniform flow about which the Euler equations were linearized, and C_1, C_1, C_3, and C_4 are the amplitudes of the four characteristic waves. It can be seen the above transformations reduce to their corresponding Cartesian form of characteristics for an orthogonal grid.

At the inflow boundary the correct unsteady, non-reflecting, boundary conditions are

$$\begin{pmatrix} C_1 \\ C_2 \\ C_3 \end{pmatrix} = 0 \tag{4.44}$$

while at the outflow boundary the correct non-reflecting boundary condition is

$$C_4 = 0 \tag{4.45}$$

4.5 Approximate, 2D, Unsteady Boundary Conditions in Curvilinear Co-ordinates

Following the theory presented earlier, the second order non-reflecting boundary conditions are obtained by taking the second-order approximation to the left eigenvectors v^L in the limit $\lambda \approx 0$. In this limit, $S_1 = S_2 \approx \Psi$ and so one obtains the following approximate eigenvectors.

$$\overline{v_1}^L = \begin{pmatrix} -\xi_x & 0 & 0 & \xi_x \end{pmatrix}$$

$$\overline{v_2}^L = \begin{pmatrix} 0 & -\xi_y\left(1-\overline{V}\lambda\right) - \eta_y\overline{U}\lambda & \xi_x\left(1-\overline{V}\lambda\right) + \eta_x\overline{U}\lambda & -\nu\lambda \end{pmatrix}$$

$$\overline{v_3}^L = \begin{pmatrix} 0 & \xi_x\left(1-\overline{V}\lambda\right) + \eta_x\overline{U}\lambda & \xi_y\left(1-\overline{V}\lambda\right) + \eta_y\overline{U}\lambda & \Psi\left(1-\overline{V}\lambda\right) + \mu\lambda \end{pmatrix}$$

$$\overline{v_4}^L = \begin{pmatrix} 0 & -\xi_x\left(1-\overline{V}\lambda\right) - \eta_x\overline{U}\lambda & -\xi_y\left(1-\overline{V}\lambda\right) - \eta_y\overline{U}\lambda & \Psi\left(1-\overline{V}\lambda\right) - \mu\lambda \end{pmatrix} \tag{4.46}$$

Actually, the first two eigenvectors are exact since the only approximation which has been made is $S \approx \Psi$ in the third and fourth eigenvectors. Consequently, the inflow boundary conditions will be perfectly non-reflecting for both of the incoming entropy and vorticity characteristics.

The second step is to multiply by ω and replace ω by $-\dfrac{\partial}{\partial t}$ and l by $\dfrac{\partial}{\partial y}$. This

gives the inflow boundary condition

$$\begin{pmatrix} -\xi_x & 0 & 0 & \xi_x \\ 0 & -\xi_y & \xi_x & 0 \\ 0 & \xi_x & \xi_y & \Psi \end{pmatrix} \frac{\partial U}{\partial t} + \begin{pmatrix} 0 & 0 & 0 & 0 \\ 0 & -\xi_y\overline{V} + \eta_y\overline{U} & \xi_x\overline{V} - \eta_x\overline{U} & \nu \\ 0 & \xi_x\overline{V} - \eta_x\overline{U} & \xi_y\overline{V} - \eta_y\overline{U} & \Psi\overline{V} - \mu \end{pmatrix} \frac{\partial U}{\partial \eta} = 0 \tag{4.47}$$

and the outflow boundary condition

$$\begin{pmatrix} 0 & -\xi_x & -\xi_y & \Psi \end{pmatrix} \frac{\partial U}{\partial t} + \begin{pmatrix} 0 & -\xi_x\overline{V} + \eta_x\overline{U} & -\xi_y\overline{V} + \eta_y\overline{U} & \Psi\overline{V} + \mu \end{pmatrix} \frac{\partial U}{\partial \eta} = 0 \tag{4.48}$$

For implementation purposes it is preferable to rewrite these equations using the one-dimensional characteristics.

$$\frac{\partial}{\partial t} \begin{pmatrix} C_1 \\ C_2 \\ C_3 \end{pmatrix} + \begin{pmatrix} 0 & 0 & 0 & 0 \\ 0 & \overline{V} - \frac{\mu\overline{U}}{\Psi^2} & \frac{\nu}{2\Psi^2}\left(\Psi + \overline{U}\right) & \frac{\nu}{2\Psi^2}\left(\Psi - \overline{U}\right) \\ 0 & \frac{-\nu\overline{U}}{\Psi^2} & \overline{V} - \frac{\mu}{2\Psi^2}\left(\Psi + \overline{U}\right) & -\frac{\mu}{2\Psi^2}\left(\Psi - \overline{U}\right) \end{pmatrix} \frac{\partial}{\partial \eta} \begin{pmatrix} C_1 \\ C_2 \\ C_3 \\ C_4 \end{pmatrix} = 0 \tag{4.49}$$

$$\frac{\partial C_4}{\partial t} + \begin{pmatrix} 0 & \frac{\nu\overline{U}}{\Psi^2} & \frac{\mu}{2\Psi^2}\left(\Psi + \overline{U}\right) & \overline{V} + \frac{\mu}{2\Psi^2}\left(\Psi - \overline{U}\right) \end{pmatrix} \frac{\partial}{\partial \eta} \begin{pmatrix} C_1 \\ C_2 \\ C_3 \\ C_4 \end{pmatrix} = 0 \tag{4.50}$$

Before using these conditions it must be verified that they form a well-posed IBVP. If they do not, then no matter how they are implemented they will produce a divergent solution on a sufficiently fine grid.

4.6 Analysis of Well-posedness

4.6.1 Inflow Boundary Conditions

The well-posedness of the second approximation non-reflecting boundary conditions can be analyzed using the theory discussed earlier. To simplify the analysis we shift to a frame of reference which is moving with speed $\overline{V}$ in a direction normal to the ξ grid line. The transformed equations of motion and boundary conditions then correspond to $\overline{V} = 0$ which simplifies the algebra, and well-posedness in this frame of reference is clearly both necessary and sufficient for well-posedness in the original frame of reference.

At the inflow boundary there are three incoming waves and the generalized incoming mode is

$$U(\xi, \eta, t) = \left[\sum_{n=1}^{3} a_n u_n^R e^{ik_n \xi} \right] e^{i(l\eta - \omega t)} \tag{4.51}$$

with $Im(\omega) \geq 0$. Using the assumption that $\overline{V} = 0$ the wave numbers are given by

$$k_1 = k_2 = \frac{\omega}{\overline{U}} \tag{4.52}$$

$$k_3 = \frac{\omega \left(S_1 - \overline{U} \right)}{\Psi^2 - \overline{U}^2} \tag{4.53}$$

where

$$S_1 = -\mu\lambda + \sqrt{\Psi^2 - \left(\nu^2 - \Psi^2 \overline{U}^2 \right) \lambda^2 + 2\mu\overline{U}\lambda} \tag{4.54}$$

with the correct square root being taken in the definition of S to ensure that if ω and S are both real then S is positive, and if ω or S is complex then $Im(k_3) > 0$.

Following the procedure presented in the theory section, the elements of the critical matrix C are obtained from $C_{mn} = \overline{v}_m^L u_n^R$.

$$C = \begin{pmatrix} 1 & 0 & 0 \\ 0 & \dfrac{\left(\xi_x + \eta_x \overline{U}\lambda\right)^2 + \left(\xi_y + \eta_y \overline{U}\lambda\right)^2}{\Psi^2} & 0 \\ 0 & 0 & \dfrac{S_1 - \overline{U}}{2\left(\Psi - \overline{U}\right)\Psi^2}\left[\left(\xi_x + \eta_x \overline{U}\lambda\right)^2 + \left(\xi_y + \eta_y \overline{U}\lambda\right)^2\right] \end{pmatrix} \tag{4.55}$$

If $\omega = (-\mu + i\nu)\left(\dfrac{\overline{U}}{\Psi^2}\right)|l|$ (satisfying the condition that $Im(\omega) \geq 0$), then

$$\lambda = \frac{-\mu - i\nu}{\Phi \overline{U}} \quad \text{and} \quad S_1 = \frac{\Psi^2}{\overline{U}}$$

(with the correct branch of the square root being taken to ensure that $Im(k_3) \geq 0$). Hence, for this value of ω,

$$C = \begin{pmatrix} 1 & 0 & 0 \\ 0 & 0 & 0 \\ 0 & 0 & 0 \end{pmatrix}$$

so there is clearly a non-trivial incoming mode, $U(\xi, \eta, t) = a_2 u_2^R e^{i(k_2\xi + l\eta - \omega t)}$, and the inflow boundary conditions are ill-posed.

It may appear that there is a second incoming mode, $U(\xi, \eta, t) = a_3 u_3^R e^{i(k_3\xi + l\eta - \omega t)}$, but it is actually a multiple of the first, because when $\omega = (-\mu + i\nu)\left(\dfrac{\overline{U}}{\Psi^2}\right)|l|$, $k_3 = k_2$ and u_3^R is a multiple of u_2^R. This degenerate situation was discussed in the theory section and hence the initial-boundary-value problem is ill-posed with just one ill-posed mode.

4.6.2 Outflow Boundary Conditions

At the outflow the generalized incoming mode is

$$U(\xi, \eta, t) = u_4^R e^{ik_4\xi} e^{i(l\eta - \omega t)} \tag{4.56}$$

with $Im(\omega) \geq 0$. Since $\overline{V} = 0$ the wave number is given by

$$k_4 = -\frac{\omega\left(S_2 + \overline{U}\right)}{\Psi^2 - \overline{U}^2} \tag{4.57}$$

where

$$S_2 = \mu\lambda + \sqrt{\Psi^2 - \left(\nu^2 - \Psi^2\overline{U}^2\right)\lambda^2 + 2\mu\overline{U}\lambda} \tag{4.58}$$

Again, the correct square root must be taken in the definition of S to ensure that if ω and S are both real then S is positive, and if ω or S is complex then $Im(k_4) < 0$. Since there is now only one incoming mode, the matrix C is simply a scalar.

$$C = \frac{1}{2\Psi^2}\left(\Psi S_2 + \Psi^2 - \Phi^2\overline{U}\left(\Psi - \overline{U}\right)\lambda^2\right) \tag{4.59}$$

The outflow conditions are ill-posed if there is a solution to

$$\Psi S_2 = -\Psi^2 + \Phi^2\overline{U}\left(\Psi - \overline{U}\right)\lambda^2 \tag{4.60}$$

Substituting for S_2 and solving for λ gives $\lambda = \dfrac{-\mu - i\nu}{\Phi\overline{U}}$. This implies that $\omega = (-\mu + i\nu)\left(\dfrac{\overline{U}}{\Psi^2}\right)|l|$ and $S_2 = \dfrac{\Psi^2}{\overline{U}}$, as with the inflow analysis. However, assuming an

orthogonal grid, when these values are substituted back into Eq. (4.60) we obtain

$$\frac{\Psi^3}{\overline{U}} = -\frac{\Psi^3}{\overline{U}} \tag{4.61}$$

This inconsistent equation contradicts the supposition that there is an incoming mode which satisfies the boundary conditions, and so we conclude that the outflow boundary condition is well-posed for orthogonal grids at domain boundaries. The proof for well-posedness of non-orthogonal grids is not provided here.

4.7 Modified Boundary Conditions

To overcome the ill-posedness of the inflow boundary conditions the third inflow boundary condition is modified. It must be noted that requiring v_3^L to be orthogonal to u_1^R and u_2^R is overly restrictive. Since the first two inflow boundary conditions already require that $a_1 = a_2 = 0$, it is only needed that v_3^L is orthogonal to u_4^R. Thus a new definition of $\overline{v}_3^L$ is proposed, which is equal to $(\overline{v}_3^L)_{old}$ plus λ times some multiple of the leading order term in $\overline{v}_2^L$.

$$\begin{aligned} \overline{v}_3^L &= \begin{bmatrix} 0 & \xi_x\left(1-\overline{V}\lambda\right)+\eta_x\overline{U}\lambda & \xi_y\left(1-\overline{V}\lambda\right)+\eta_y\overline{U}\lambda & \Psi\left(1-\overline{V}\lambda\right)+\mu\lambda \end{bmatrix} \\ &+ \lambda m \begin{bmatrix} 0 & -\xi_y & \xi_x & 0 \end{bmatrix} \end{aligned} \tag{4.62}$$

The variable m will be chosen to minimize $\overline{v}_3^L u_4^R$, which controls the magnitude of the reflection coefficient, and at the same time will produce a well-posed boundary condition. The motivation for this approach is that the second approximation to the scalar wave equation is well-posed and produces fourth order reflection [40]. Substituting definition gives

$$\overline{v}_3^L u_4^R = \frac{1}{2}\left(\frac{\Psi-\overline{U}}{\Psi+\overline{U}}\right)\left(-\Psi S_2+\Psi^2+2\mu\left(\Psi+\overline{U}\right)\lambda+\left(\nu m+\Phi^2\overline{U}^2\right)\left(\Psi+\overline{U}\right)\lambda^2\right) \tag{4.63}$$

The binomial series expansion for $S_2(\lambda)$ is given by

$$\begin{aligned} S_2 &= \mu\lambda+\Psi\left(1+\frac{\mu\overline{U}}{\Psi^2}\lambda-\frac{\nu^2-\Phi^2\overline{U}^2}{2\Psi^2}\lambda^2\right) \\ &+ \mu\left(O(\lambda)+O\left(\lambda^3\right)\right)+O\left(\lambda^4\right) \end{aligned} \tag{4.64}$$

Assuming orthogonality of the grid at the inflow boundary,

$$\overline{\xi} \,.\, \overline{\eta} = 0 \tag{4.65}$$

where,

$$\overline{\xi} = \frac{\xi_x}{|\xi|}\hat{i} + \frac{\xi_y}{|\xi|}\hat{j}, \qquad |\xi| = \sqrt{\xi_x^2 + \xi_y^2}$$

$$\overline{\eta} = \frac{\eta_x}{|\eta|}\hat{i} + \frac{\eta_y}{|\eta|}\hat{j}, \qquad |\eta| = \sqrt{\eta_x^2 + \eta_y^2}$$

$$\implies \quad \mu = \xi_x\xi_y + \eta_x\eta_y = 0 \qquad \text{(or)} \qquad X_\xi X_\eta + Y_\xi Y_\eta = 0$$

For orthogonal grid at the inflow boundary,

$$\overline{v}_3^L u_4^R = \frac{1}{2}\left(\frac{\Psi - \overline{U}}{\Psi + \overline{U}}\right)\left(-\Psi S_2 + \Psi^2 + \left(\nu m + \Phi^2\overline{U}^2\right)\left(\Psi + \overline{U}\right)\lambda^2\right) \tag{4.66}$$

and

$$S_2 = \Psi - \left(\frac{\nu^2 - \Phi^2\overline{U}^2}{2\Psi}\right)\lambda^2 + O\left(\lambda^4\right) \tag{4.67}$$

$$\implies \quad -\Psi S_2 + \Psi^2 = \left(\frac{\nu^2 - \Phi^2\overline{U}^2}{2}\right)\lambda^2 + O\left(\lambda^4\right) \tag{4.68}$$

From Eqns. (4.66) and (4.68), the reflection co-efficient is fourth order if m is chosen such that

$$\left(\nu m + \Phi^2\overline{U}^2\right)\left(\Psi + \overline{U}\right) = -\frac{1}{2}\left(\nu^2 - \Phi^2\overline{U}^2\right) \tag{4.69}$$

To obtain a simplified expression for m from the above equation requires the use of orthogonality condition at the grid boundary.

$$\implies \quad m = -\frac{\Phi^2}{2\nu}\left(\Psi + \overline{U}\right) \tag{4.70}$$

Thus the new form of $\overline{v}_3^L$ is

$$\overline{v}_3^L|_{\overline{V}=0} = \begin{pmatrix} 0 & \xi_x - \dfrac{\eta_x}{2}\left(\Psi - \overline{U}\right)\lambda & \xi_y - \dfrac{\eta_y}{2}\left(\Psi - \overline{U}\right)\lambda & \Psi \end{pmatrix} \tag{4.71}$$

To prove the well-posedness of the modified inflow boundary conditions, the critical matrix C is re-calculated.

$$C = \begin{pmatrix} 1 & 0 & 0 \\ 0 & \dfrac{\left(\xi_x + \eta_x\overline{U}\lambda\right)^2 + \left(\xi_y + \eta_y\overline{U}\lambda\right)^2}{\Psi^2} & 0 \\ 0 & 0 & \dfrac{1}{2\Psi^2}\left(\Psi S_1 + \Psi^2 - \dfrac{\lambda^2}{2}\Phi^2\left(\Psi^2 - \overline{U}^2\right)\right) \end{pmatrix} \tag{4.72}$$

Proof of well-posedness is provided only for an orthogonal grid at the boundary, for which $\mu = 0$. $\det(C)$ implies either

$$-\Psi S_1 = \Psi^2 - \frac{1}{2}\Phi^2\left(\Psi^2 - \overline{U}^2\right)\lambda^2 \tag{4.73}$$

or

$$\left(\xi_x + \eta_x\overline{U}\lambda\right)^2 + \left(\xi_y + \eta_y\overline{U}\lambda\right)^2 = 0 \tag{4.74}$$

Only the first possibility is examined here:

We have,

$$S_1|_{\mu=0,\overline{V}=0} = \sqrt{\Psi^2 - \left(\nu^2 - \Phi^2\overline{U}^2\right)\lambda^2}$$

Substituting S_1 into Eq. (5.69) and squaring both sides we obtain,

$$\Psi^2 - \Psi^2\left(\nu^2 - \Phi^2\overline{U}^2\right)\lambda^2 = \Psi^2 - \Psi^2\Phi^2\left(\Psi^2 - \overline{U}^2\right)\lambda^2 + \frac{1}{4}\Phi^2\left(\Psi^2 - \overline{U}^2\right)^2\lambda^4 \quad (4.75)$$

We can write,

$$\Psi^2\Phi^2 = \mu^2 + \nu^2 \quad (4.76)$$

which for an orthogonal grid becomes $\Psi^2\Phi^2 = \nu^2$.

Using the above relation it is obvious that the co-efficients of the λ^2 terms on both sides are equal; thus the condition for ill-posedness reduces to

$$\frac{1}{4}\Phi^2\left(\Psi^2 - \overline{U}^2\right)^2\lambda^4 = 0 \quad \Longrightarrow \quad \lambda = 0 \quad (4.77)$$

For $\mu = 0$, $\lambda = 0$, and $\overline{V} = 0$, we get $S_1 = \Psi$. Substituting these values of λ and S_1 back into Eq. (4.73), we get:

$$-\Psi^2 = \Psi^2$$

which is clearly inconsistent. Hence the first possibility does not lead to an ill-posed mode.

Recall that the $\overline{v}_3^L$ obtained above is in a reference frame moving with a speed $\overline{V}$.

In the original reference frame where $\overline{V} \neq 0$,

$$\overline{v}_3^L = \begin{pmatrix} 0 & \xi_x - \left(\xi_x \overline{V} + \frac{\eta_x}{2}\left(\Psi - \overline{U}\right)\right)\lambda & \xi_y - \left(\xi_y \overline{V} + \frac{\eta_y}{2}\left(\Psi - \overline{U}\right)\right)\lambda & \Psi\overline{V} \end{pmatrix} \tag{4.78}$$

Therefore, the modified non-dimensional inflow boundary conditions in terms of primitive flow variables are,

$$\begin{pmatrix} -\xi_x & 0 & 0 & \xi_x \\ 0 & -\xi_y & \xi_x & 0 \\ 0 & \xi_x & \xi_y & \Psi \end{pmatrix} \frac{\partial U}{\partial t} + \begin{pmatrix} 0 & 0 & 0 & 0 \\ 0 & -\xi_y \overline{V} + \eta_y \overline{U} & \xi_x \overline{V} - \eta_x \overline{U} & \nu \\ 0 & \xi_x \overline{V} + \frac{\eta_x}{2}\left(\Psi - \overline{U}\right) & \xi_y \overline{V} + \frac{\eta_y}{2}\left(\Psi - \overline{U}\right) & \Psi\overline{V} - \mu \end{pmatrix} \frac{\partial U}{\partial \eta} = 0 \tag{4.79}$$

A corresponding modified outflow boundary condition derived using a similar procedure is:

$$\begin{pmatrix} 0 & -\xi_x & -\xi_y & \Psi \end{pmatrix} \frac{\partial U}{\partial t} + \begin{pmatrix} 0 & -\xi_x \overline{V} + \frac{\eta_x}{2}\left(\Psi + \overline{U}\right) & -\xi_y \overline{V} + \frac{\eta_y}{2}\left(\Psi + \overline{U}\right) & \Psi\overline{V} + \mu \end{pmatrix} \frac{\partial U}{\partial \eta} = 0 \tag{4.80}$$

The modified, well-posed, non-dimensional, 2D Curvilinear boundary conditions written in terms of the characteristic variables are:

Inflow:

$$\frac{\partial}{\partial t}\begin{pmatrix} C_1 \\ C_2 \\ C_3 \end{pmatrix} + \begin{pmatrix} 0 & 0 & 0 & 0 \\ 0 & \overline{V} - \dfrac{\mu\overline{U}}{\Psi^2} & \dfrac{\nu\left(\Psi+\overline{U}\right)}{2\Psi^2} & \dfrac{\nu\left(\Psi-\overline{U}\right)}{2\Psi^2} \\ 0 & \dfrac{\nu\left(\Psi-\overline{U}\right)}{2\Psi^2} & \overline{V} + \dfrac{\mu\left(\Psi-\overline{U}\right)}{4\Psi^2} & -\dfrac{\mu\left(\Psi-\overline{U}\right)}{4\Psi^2} \end{pmatrix} \frac{\partial}{\partial \eta}\begin{pmatrix} C_1 \\ C_2 \\ C_3 \\ C_4 \end{pmatrix} = 0 \tag{4.81}$$

Outflow:

$$\frac{\partial C_4}{\partial t} + \begin{pmatrix} 0 & \dfrac{\nu\left(\Psi+\overline{U}\right)}{2\Psi^2} & \dfrac{\mu\left(\Psi+\overline{U}\right)}{4\Psi^2} & \overline{V} + \dfrac{\mu\left(\Psi-\overline{U}\right)}{4\Psi^2} \end{pmatrix} \frac{\partial}{\partial \eta}\begin{pmatrix} C_1 \\ C_2 \\ C_3 \\ C_4 \end{pmatrix} = 0 \tag{4.82}$$

4.8 Giles Boundary Conditions for 2D Euler Equations in Curvilinear Co-ordinates

A summary of the dimensional boundary conditions derived in this chapter for the 2D Euler equations in Curvilinear co-ordinates is presented in this section.

a) **Transformation to, and from, one-dimensional characteristic variables**

$$\begin{pmatrix} C_1 \\ C_2 \\ C_3 \\ C_4 \end{pmatrix} = \begin{pmatrix} -\overline{c}^2\xi_x & 0 & 0 & \xi_x \\ 0 & -\overline{\rho c}\xi_y & \overline{\rho c}\xi_x & 0 \\ 0 & \overline{\rho c}\xi_x & \overline{\rho c}\xi_y & \Psi \\ 0 & -\overline{\rho c}\xi_x & -\overline{\rho c}\xi_y & \Psi \end{pmatrix} \begin{pmatrix} \rho' \\ u' \\ v' \\ p' \end{pmatrix} \tag{4.83}$$

$$\begin{pmatrix} \rho' \\ u' \\ v' \\ p' \end{pmatrix} = \begin{pmatrix} -\frac{1}{\overline{c}^2\xi_x} & 0 & \frac{1}{2\overline{c}^2\Psi} & \frac{1}{2\overline{c}^2\Psi} \\ 0 & -\frac{\xi_y}{\overline{\rho c}\Psi^2} & \frac{\xi_x}{2\overline{\rho c}\Psi^2} & -\frac{\xi_x}{2\overline{\rho c}\Psi^2} \\ 0 & \frac{\xi_x}{\overline{\rho c}\Psi^2} & \frac{\xi_y}{2\overline{\rho c}\Psi^2} & -\frac{\xi_y}{2\overline{\rho c}\Psi^2} \\ 0 & 0 & \frac{1}{2\Psi} & \frac{1}{2\Psi} \end{pmatrix} \begin{pmatrix} C_1 \\ C_2 \\ C_3 \\ C_4 \end{pmatrix} \tag{4.84}$$

b) **One-dimensional Unsteady Boundary Conditions.**

Inflow:

$$\begin{pmatrix} C_1 \\ C_2 \\ C_3 \end{pmatrix} = 0 \tag{4.85}$$

Outflow:

$$C_4 = 0 \tag{4.86}$$

c) **Two-dimensional, Unsteady Inflow Boundary Conditions.**

$$\frac{\partial}{\partial t}\begin{pmatrix} C_1 \\ C_2 \\ C_3 \end{pmatrix} + \begin{pmatrix} 0 & 0 & 0 & 0 \\ 0 & \overline{V} - \dfrac{\mu\overline{U}}{\Psi^2} & \dfrac{\nu\left(\Psi\overline{c} + \overline{U}\right)}{2\Psi^2} & \dfrac{\nu\left(\Psi\overline{c} - \overline{U}\right)}{2\Psi^2} \\ 0 & \dfrac{\nu\left(\Psi\overline{c} - \overline{U}\right)}{2\Psi^2} & \overline{V} + \dfrac{\mu\left(\Psi\overline{c} - \overline{U}\right)}{4\Psi^2} & -\dfrac{\mu\left(\Psi\overline{c} - \overline{U}\right)}{4\Psi^2} \end{pmatrix} \frac{\partial}{\partial \eta}\begin{pmatrix} C_1 \\ C_2 \\ C_3 \\ C_4 \end{pmatrix} = 0 \tag{4.87}$$

d) **Two-dimensional, Unsteady Outflow Boundary Conditions.**

$$\frac{\partial C_4}{\partial t} + \begin{pmatrix} 0 & \dfrac{\nu\overline{U}}{\Psi^2} & \dfrac{\mu}{2\Psi^2}\left(\Psi\overline{c} + \overline{U}\right) & \overline{V} + \dfrac{\mu}{2\Psi^2}\left(\Psi\overline{c} - \overline{U}\right) \end{pmatrix} \frac{\partial}{\partial \eta}\begin{pmatrix} C_1 \\ C_2 \\ C_3 \\ C_4 \end{pmatrix} = 0 \tag{4.88}$$

e) **Modified, Two-dimensional, Unsteady Outflow Boundary Conditions.**

$$\frac{\partial C_4}{\partial t} + \begin{pmatrix} 0 & \dfrac{\nu}{2\Psi^2}\left(\Psi\overline{c} + \overline{U}\right) & \dfrac{\mu}{4\Psi^2}\left(\Psi\overline{c} + \overline{U}\right) & \overline{V} + \dfrac{\mu}{4\Psi^2}\left(\Psi\overline{c} - \overline{U}\right) \end{pmatrix} \frac{\partial}{\partial \eta}\begin{pmatrix} C_1 \\ C_2 \\ C_3 \\ C_4 \end{pmatrix} = 0 \tag{4.89}$$

where,

$$\Psi = \sqrt{\xi_x^2 + \xi_y^2}, \qquad \Phi = \sqrt{\eta_x^2 + \eta_y^2}$$

$$\mu = \xi_x\eta_x + \xi_y\eta_y, \qquad \nu = \xi_x\eta_y - \xi_y\eta_x$$

It is to be noted that the Curvilinear Giles boundary conditions derived from

the Curvilinear form of Euler equations have extra terms containing the factor $\mu = \xi_x\eta_x + \xi_y\eta_y$ which are not present in the chain rule form of the Giles boundary conditions derived from the Cartesian form of Euler equations. The significance of these additional terms will be discussed in subsequent chapters.

4.9 Wall Corner Compatibility Conditions for 2D Curvilinear Giles Boundary Conditions

In this section, wall corner conditions are derived for the extended two-dimensional Curvilinear Giles boundary conditions.

Define :

Unit vectors tangent and normal to the non-reflecting boundary

$$\overrightarrow{m} = \frac{-\xi_y}{\sqrt{\xi_x^2+\xi_y^2}}\hat{i} + \frac{\xi_x}{\sqrt{\xi_x^2+\xi_y^2}}\hat{j} \tag{4.90}$$

$$\overrightarrow{n} = \frac{\xi_x}{\sqrt{\xi_x^2+\xi_y^2}}\hat{i} + \frac{\xi_y}{\sqrt{\xi_x^2+\xi_y^2}}\hat{j} \tag{4.91}$$

$$\tag{4.92}$$

Unit vectors tangent and normal to the wall boundary

$$\overrightarrow{M_w} = M_{wx}\hat{i} + M_{wy}\hat{j} \tag{4.93}$$

$$\overrightarrow{N_w} = N_{wx}\hat{i} + N_{wy}\hat{j} \tag{4.94}$$

and

$$\overrightarrow{\overline{V}} = \overline{u}\hat{i} + \overline{v}\hat{j}$$

$$\overrightarrow{V'} = u'\hat{i} + v'\hat{j}$$

4.9.1 Giles Inflow-Wall Corner Condition

For an unsteady flow, not only is the flow through the wall in the normal direction zero, but also its time derivative.

$$\overrightarrow{V'}\bullet\overrightarrow{N_w} = 0, \qquad \frac{\partial}{\partial t}\left(\overrightarrow{V'}\bullet\overrightarrow{N_w}\right) = 0 \tag{4.95}$$

Flow through the wall $\frac{\partial}{\partial t}\left(\overrightarrow{V'}\bullet\overrightarrow{N_w}\right)$ can be written as a function of C_2, C_3, and C_4:

$$\overline{\rho c}\,\frac{\partial}{\partial t}\left(\overrightarrow{V'}\bullet\overrightarrow{N_w}\right)\Big|_{\text{NoWallBC}} = \left(\overrightarrow{m}\bullet\overrightarrow{N_w}\right)\frac{\partial C_2}{\partial t}\Big|_{\text{NoWallBC}} + \frac{1}{2}\left(\overrightarrow{n}\bullet\overrightarrow{N_w}\right)\frac{\partial(C_3-C_4)}{\partial t}\Big|_{\text{NoWallBC}} \tag{4.96}$$

And,

$$\overline{\rho c}\,\frac{\partial}{\partial t}\left(\overrightarrow{V'}\bullet\overrightarrow{N_w}\right)\Big|_{\text{WallBC}} = \left(\overrightarrow{m}\bullet\overrightarrow{N_w}\right)\frac{\partial C_2}{\partial t}\Big|_{\text{WallBC}} + \frac{1}{2}\left(\overrightarrow{n}\bullet\overrightarrow{N_w}\right)\frac{\partial(C_3-C_4)}{\partial t}\Big|_{\text{WallBC}} = 0 \tag{4.97}$$

$$\Delta\left[\overline{\rho c}\frac{\partial}{\partial t}\left(\overrightarrow{V'}\bullet\overrightarrow{N_w}\right)\right] = \overline{\rho c}\,\frac{\partial}{\partial t}\left(\overrightarrow{V'}\bullet\overrightarrow{N_w}\right)\Big|_{\text{WallBC}} - \overline{\rho c}\,\frac{\partial}{\partial t}\left(\overrightarrow{V'}\bullet\overrightarrow{N_w}\right)\Big|_{\text{NoWallBC}} \tag{4.98}$$

$$\Longrightarrow \Delta\left[\overline{\rho c}\frac{\partial}{\partial t}\left(\overrightarrow{V'}\bullet\overrightarrow{N_w}\right)\right] = \left(\overrightarrow{m}\bullet\overrightarrow{N_w}\right)\Delta\left[\frac{\partial C_2}{\partial t}\right] + \frac{1}{2}\left(\overrightarrow{n}\bullet\overrightarrow{N_w}\right)\Delta\left[\frac{\partial(C_3-C_4)}{\partial t}\right] \tag{4.99}$$

where

$$\Delta\left[\frac{\partial C}{\partial t}\right] = \frac{\partial C}{\partial t}\Big|_{\text{WallBC}} - \frac{\partial C}{\partial t}\Big|_{\text{NoWallBC}} \tag{4.100}$$

Each one of $\frac{\partial C_2}{\partial t}$, $\frac{\partial C_3}{\partial t}$, and $\frac{\partial C_4}{\partial t}$ are in turn functions of $\frac{\partial C_2}{\partial \eta}$, $\frac{\partial C_3}{\partial \eta}$, and $\frac{\partial C_4}{\partial \eta}$ which are again functions of $\frac{\partial u'}{\partial \eta}$, $\frac{\partial v'}{\partial \eta}$, and $\frac{\partial p'}{\partial \eta}$. Therefore, the change in time derivatives

of the characteristic variables due to the wall boundary condition can be expressed in terms of η-derivatives of the primitive variables. The time derivative of C_4 cannot be changed because it is outgoing acoustic wave at the inflow boundary.

$$\Longrightarrow \qquad \Delta \left[\frac{\partial C_4}{\partial t}\right]_{\text{corner}} = 0 \tag{4.101}$$

We do not want to change the η-derivatives of u' and v'.

$$\Longrightarrow \qquad \left.\frac{\partial u'}{\partial \eta}\right|_{\text{corner}} = 0, \qquad \left.\frac{\partial v'}{\partial \eta}\right|_{\text{corner}} = 0 \tag{4.102}$$

Correction to the η-derivatives of characteristic variables is given by

$$\Delta \left[\frac{\partial C_1}{\partial \eta}\right] = \xi_x \, \Delta \left[\frac{\partial p'}{\partial \eta}\right] \tag{4.103}$$

$$\Delta \left[\frac{\partial C_2}{\partial \eta}\right] = 0 \tag{4.104}$$

$$\Delta \left[\frac{\partial C_3}{\partial \eta}\right] = \sqrt{\xi_x^2 + \xi_y^2} \, \Delta \left[\frac{\partial p'}{\partial \eta}\right] \tag{4.105}$$

$$\Delta \left[\frac{\partial C_4}{\partial \eta}\right] = \sqrt{\xi_x^2 + \xi_y^2} \, \Delta \left[\frac{\partial p'}{\partial \eta}\right] \tag{4.106}$$

Therefore, the correction to the time derivatives of the characteristic variables is

given by

$$\Delta\left[\frac{\partial C_1}{\partial t}\right] = 0 \tag{4.107}$$

$$\Delta\left[\frac{\partial C_2}{\partial t}\right] = -\nu\overline{c}\Delta\left[\frac{\partial p'}{\partial \eta}\right] \tag{4.108}$$

$$\Delta\left[\frac{\partial C_3}{\partial t}\right] = -\Psi\overline{V}\Delta\left[\frac{\partial p'}{\partial \eta}\right] \tag{4.109}$$

$$\Delta\left[\frac{\partial C_4}{\partial t}\right] = 0 \tag{4.110}$$

The central idea of this approach is to correct the pressure normal derivative at the wall corner point $\Delta\left[\frac{\partial p'}{\partial \eta}\right]$ such that the flow normal to the wall, $\frac{\partial}{\partial t}\left(\overrightarrow{V'}\bullet\overrightarrow{N_w}\right) = 0$. So we need to express $\Delta\left[\frac{\partial p'}{\partial \eta}\right]$ in terms of the flow normal to the wall $\frac{\partial}{\partial t}\left(\overrightarrow{V'}\bullet\overrightarrow{N_w}\right)$. This is achieved by substituting $\Delta\left(\frac{\partial C_2}{\partial t}\right)$, $\Delta\left(\frac{\partial C_3}{\partial t}\right)$, and $\Delta\left(\frac{\partial C_4}{\partial t}\right)$ from the above equations into Eq. (4.99).

$$\Longrightarrow \qquad \Delta\left[\frac{\partial p'}{\partial \eta}\right]_{\text{corner}} = \frac{\overline{\rho c}\,\frac{\partial}{\partial t}\left(\overrightarrow{V'}\bullet\overrightarrow{N_w}\right)\Big|_{\text{NoWallBC}}}{\nu\left(\overrightarrow{m}\bullet\overrightarrow{N_w}\right)\overline{c} + \frac{1}{2}\Psi\left(\overrightarrow{n}\bullet\overrightarrow{N_w}\right)\overline{V}} \tag{4.111}$$

After the pressure derivative correction at the corner point is obtained, its effect is propagated a few points into (depending on the spatial discretization scheme being used) the interior of the computational domain. This method of derivative correction propagation was proposed by Hixon [77]

Corrections to $\frac{\partial C}{\partial t}$ are then calculated using Eqs. (4.107) to (4.110). Finally, the time derivatives of the characteristics are corrected:

$$\left.\frac{\partial C}{\partial t}\right|_{\text{WallBC}} = \left.\frac{\partial C}{\partial t}\right|_{\text{NoWallBC}} + \Delta\left[\frac{\partial C}{\partial t}\right] \tag{4.112}$$

The time derivatives of primitive variables are then computed from $\left.\frac{\partial C}{\partial t}\right|_{\text{WallBC}}$.

4.9.2 Giles Outflow-Wall Corner Condition

The outflow wall corner boundary condition is obtained by following the same procedure adopted for the inflow boundary. At the outflow boundary C_1, C_2, and C_3 are outgoing characteristics and C_4 is the only incoming characteristic. Hence,

$$\Delta\left[\frac{\partial C_1}{\partial t}\right]_{\text{corner}} = \Delta\left[\frac{\partial C_2}{\partial t}\right]_{\text{corner}} = \Delta\left[\frac{\partial C_3}{\partial t}\right]_{\text{corner}} = 0 \tag{4.113}$$

$$\Delta\left[\frac{\partial C_4}{\partial t}\right] = -\left[\Psi\overline{V} + \mu\overline{c}\right]\Delta\left[\frac{\partial p'}{\partial \eta}\right] \tag{4.114}$$

The pressure derivative correction at the outflow wall corner will then be (using Eq. (4.99))

$$\Delta\left[\frac{\partial p'}{\partial \eta}\right]_{\text{corner}} = -\frac{\overline{\rho c}\,\dfrac{\partial}{\partial t}\left(\overrightarrow{V'}\bullet\overrightarrow{N_w}\right)\Big|_{\text{NoWallBC}}}{\dfrac{1}{2}\left(\overrightarrow{n}\bullet\overrightarrow{N_w}\right)\left[\Psi\overline{V} + \mu\overline{c}\right]} \tag{4.115}$$

For the modified outflow boundary condition:

$$\Delta\left[\frac{\partial C_1}{\partial t}\right]_{\text{corner}} = \Delta\left[\frac{\partial C_2}{\partial t}\right]_{\text{corner}} = \Delta\left[\frac{\partial C_3}{\partial t}\right]_{\text{corner}} = 0 \tag{4.116}$$

$$\Delta\left[\frac{\partial C_4}{\partial t}\right] = -\left[\Psi\overline{V} + \frac{\mu\overline{c}}{2}\right]\Delta\left[\frac{\partial p'}{\partial \eta}\right] \tag{4.117}$$

The pressure derivative correction at the outflow wall corner will then be (using

Eq. (4.99))

$$\Delta\left[\frac{\partial p'}{\partial \eta}\right]_{\text{corner}} = -\frac{\overline{\rho c}\,\dfrac{\partial}{\partial t}\left(\overrightarrow{V'}\bullet\overrightarrow{N_w}\right)\Big|_{\text{NoWallBC}}}{\dfrac{1}{2}\left(\overrightarrow{n}\bullet\overrightarrow{N_w}\right)\left[\Psi\overline{V}+\dfrac{\mu\bar{c}}{2}\right]} \tag{4.118}$$

As is the case with the wall conditions for the chain-rule form of Giles outflow wall condition, the Curvilinear Giles outflow wall condition also cannot be applied whenever the wall boundary is orthogonal to the outflow boundary, since $\overrightarrow{n}\bullet\overrightarrow{N_w}=0$, causing the denominator of $\Delta\left[\dfrac{\partial p'}{\partial \eta}\right]_{\text{corner}}$ to be zero.

Once the pressure derivative correction is obtained, it is propagated into the interior domain and the values of $\left.\dfrac{\partial C}{\partial t}\right|_{\text{WallBC}}$ are calculated as described in the previous section.

Chapter 5

Giles Boundary Conditions for 3D Euler Equations in Cartesian Co-ordinates

A straight forward extension of the two-dimensional Cartesian Giles boundary conditions to 3D linearized Euler equations is presented in this chapter.

5.1 Non-dimensional 3D Linearized Euler Equations in Cartesian Co-ordinates

The 3D Euler equations written in conservative form are:

$$\frac{\partial}{\partial t}\begin{pmatrix} \rho \\ \rho u \\ \rho v \\ \rho w \\ E_{total} \end{pmatrix} + \begin{pmatrix} \rho u \\ \rho u^2 + p \\ \rho uv \\ \rho uw \\ u\,(E+p) \end{pmatrix} + \begin{pmatrix} \rho v \\ \rho uv \\ \rho v^2 + p \\ \rho vw \\ v\,(E+p) \end{pmatrix} + \begin{pmatrix} \rho v \\ \rho uw \\ \rho vw \\ \rho w^2 + p \\ w\,(E+p) \end{pmatrix} = 0 \qquad (5.1)$$

The above equations are linearized about an assumed uniform mean flow ($\overline{\rho},\ \overline{u},\ \overline{v},\ \overline{w},\ \overline{p}$) to give

$$\frac{\partial Q}{\partial t} + \begin{pmatrix} \overline{u} & \overline{\rho} & 0 & 0 & 0 \\ 0 & \overline{u} & 0 & 0 & \frac{1}{\overline{\rho}} \\ 0 & 0 & \overline{u} & 0 & 0 \\ 0 & 0 & 0 & \overline{u} & 0 \\ 0 & \gamma\overline{p} & 0 & 0 & \overline{u} \end{pmatrix} \frac{\partial Q}{\partial x} + \begin{pmatrix} \overline{v} & 0 & \overline{\rho} & 0 & 0 \\ 0 & \overline{v} & 0 & 0 & 0 \\ 0 & 0 & \overline{v} & 0 & \frac{1}{\overline{\rho}} \\ 0 & 0 & 0 & \overline{v} & 0 \\ 0 & 0 & \gamma\overline{p} & 0 & \overline{v} \end{pmatrix} \frac{\partial Q}{\partial y} + \begin{pmatrix} \overline{w} & 0 & 0 & \overline{\rho} & 0 \\ 0 & \overline{w} & 0 & 0 & 0 \\ 0 & 0 & \overline{w} & 0 & 0 \\ 0 & 0 & 0 & \overline{w} & \frac{1}{\overline{\rho}} \\ 0 & 0 & 0 & \gamma\overline{p} & \overline{w} \end{pmatrix} \frac{\partial Q}{\partial z} = 0 \qquad (5.2)$$

where Q is the vector of perturbation variables, $Q = \begin{pmatrix} \rho' \\ u' \\ v' \\ w' \\ p' \end{pmatrix}$

The linearized equations are non-dimensionalized using the steady density $\overline{\rho}$ and speed of sound $\overline{c}$. The resulting equations are in the form required for Fourier analysis:

$$\frac{\partial Q}{\partial t} + [A]\frac{\partial Q}{\partial x} + [B]\frac{\partial Q}{\partial y} + [C]\frac{\partial Q}{\partial z} = 0 \tag{5.3}$$

where

$$A = \begin{pmatrix} \overline{u} & 1 & 0 & 0 & 0 \\ 0 & \overline{u} & 0 & 0 & 1 \\ 0 & 0 & \overline{u} & 0 & 0 \\ 0 & 0 & 0 & \overline{u} & 0 \\ 0 & 1 & 0 & 0 & \overline{u} \end{pmatrix}, \quad B = \begin{pmatrix} \overline{v} & 0 & 1 & 0 & 0 \\ 0 & \overline{v} & 0 & 0 & 0 \\ 0 & 0 & \overline{v} & 0 & 1 \\ 0 & 0 & 0 & \overline{v} & 0 \\ 0 & 0 & 1 & 0 & \overline{v} \end{pmatrix}, \quad C = \begin{pmatrix} \overline{w} & 0 & 0 & 1 & 0 \\ 0 & \overline{w} & 0 & 0 & 0 \\ 0 & 0 & \overline{w} & 0 & 0 \\ 0 & 0 & 0 & \overline{w} & 1 \\ 0 & 0 & 0 & 1 & \overline{w} \end{pmatrix} \tag{5.4}$$

5.2 Fourier Analysis

A wave-like solution to the Euler equations in Eq. (5.3)of the form

$$U(x,y,z,t) = ue^{i(kx+ly+mz-\omega t)} \tag{5.5}$$

is considered for the Fourier analysis.

Following the theory described in chapter 3, the dispersion relation is first obtained.

$det\left(-\omega I + kA + lB + mC\right) =$

$$det\begin{pmatrix} \overline{u}k+\overline{v}l+\overline{w}m-\omega & k & l & m & 0 \\ 0 & \overline{u}k+\overline{v}l+\overline{w}m-\omega & 0 & 0 & k \\ 0 & 0 & \overline{u}k+\overline{v}l+\overline{w}m-\omega & 0 & l \\ 0 & 0 & & \overline{u}k+\overline{v}l+\overline{w}m-\omega & m \\ 0 & k & l & m & \overline{u}k+\overline{v}l+\overline{w}m-\omega \end{pmatrix}$$

$$\begin{aligned} &= \left(\overline{u}k+\overline{u}l+\overline{w}m-\omega\right)^2\left[\left(\overline{u}k+\overline{u}l+\overline{w}m-\omega\right)^2 - k^2 + l^2 + m^2\right] \\ &= 0 \end{aligned} \tag{5.6}$$

For 3D Euler equations, the first three roots of the dispersion relation are identical.

$$k_{1,2,3} = \frac{\omega - \overline{v}l - \overline{w}m}{\overline{u}} \tag{5.7}$$

The fourth and the fifth roots are given by

$$\left(\overline{u}k + \overline{u}l + \overline{w}m - \omega\right)^2 - k^2 - l^2 - m^2 = 0 \tag{5.8}$$

$$k_{4,5} = \frac{\overline{u}\left(\overline{v}l + \overline{w}m - \omega\right)}{1 - \overline{u}^2} \pm \frac{\left(\left(\overline{u}\left(\overline{v}l + \overline{w}m - \omega\right)\right)^2 + \left(1 - \overline{u}^2\right)\left(\overline{v}l + \overline{w}m - \omega\right)^2\right)^{1/2}}{1 - \overline{u}^2} \tag{5.9}$$

Hence the fourth and fifth roots are:

$$k_4 = \frac{\left(\omega - \overline{v}l - \overline{w}m\right)\left(-\overline{u} + S\right)}{1 - \overline{u}^2} \tag{5.10}$$

$$k_5 = \frac{\left(\omega - \overline{v}l - \overline{w}m\right)\left(-\overline{u} - S\right)}{1 - \overline{u}^2} \tag{5.11}$$

where

$$S = \sqrt{1 - \frac{\left(1 - \overline{u}^2\right)\left(l^2 + m^2\right)}{\left(\omega - \overline{v}l - \overline{w}m\right)^2}} \tag{5.12}$$

Define:

$$\lambda_y = \frac{l}{\omega}, \quad \lambda_z = \frac{m}{\omega}$$

5.3 Eigenvectors

5.3.1 Root 1: Entropy Wave

$$k_1 = \frac{\omega - \overline{v}l - \overline{w}m}{\overline{v}}, \qquad \omega = \overline{u}k_1 + \overline{v}l + \overline{w}m \tag{5.13}$$

Substituting for ω gives

$$(-\omega I + k_1 A + lB + mC) = \begin{pmatrix} 0 & k_1 & l & m & 0 \\ 0 & 0 & 0 & 0 & k_1 \\ 0 & 0 & 0 & 0 & l \\ 0 & k_1 & l & m & 0 \end{pmatrix} \tag{5.14}$$

Right eigenvector is chosen as

$$u_1^R = \begin{pmatrix} -1 \\ 0 \\ 0 \\ 0 \\ 0 \end{pmatrix} \tag{5.15}$$

and a corresponding left eigenvector is

$$u_1^L = \begin{pmatrix} -1 & 0 & 0 & 0 & 1 \end{pmatrix} \tag{5.16}$$

The vector v_1^L, which is needed to construct the non-reflecting boundary conditions,

is calculated following the procedure given in the theory section.

$$\begin{aligned} v_1^L &= \frac{1}{\overline{u}} u_1^L A \\ &= \begin{pmatrix} -1 & 0 & 0 & 0 & 1 \end{pmatrix} \end{aligned} \tag{5.17}$$

This choice of eigenvectors corresponds to the entropy wave propagating downstream at a speed $\overline{u} > 0$. This can be verified by noting that the only non-zero term in the right eigenvector is the density, so that the wave has varying entropy, no vorticity and constant pressure. Also, the left eigenvector 'measures' entropy in the sense that $u_1^L U$ is equal to the linearized entropy, $p' - \rho'$ (remembering that $c = 1$ because of the non-dimensionalization).

5.3.2 Root 2: Vorticity Wave

$$k_2 = \frac{\omega - \overline{v}l - \overline{w}m}{\overline{v}}, \qquad \omega = \overline{u}k_2 + \overline{v}l + \overline{w}m \tag{5.18}$$

The second set of eigenvectors for the multiple root is given by

Right eigenvector:

$$u_2^R = \begin{pmatrix} 0 \\ -\overline{u}\lambda_y \\ 1 - \overline{v}\lambda_y - \overline{w}\lambda_z \\ 0 \\ 0 \end{pmatrix} \tag{5.19}$$

Left eigenvector:

$$u_2^L = \begin{pmatrix} 0 & -\overline{u}\lambda_y & 1 - \overline{v}\lambda_y - \overline{w}\lambda_z & 0 & 0 \end{pmatrix} \tag{5.20}$$

The vector v_2^L, which is needed to construct the non-reflecting boundary conditions, is calculated following the procedure given in the theory section.

$$\begin{aligned} v_2^L &= \frac{1}{\overline{u}} u_2^L A \\ &= \begin{pmatrix} 0 & -\overline{u}\lambda_y & 1 - \overline{v}\lambda_y - \overline{w}\lambda_z & 0 & -\lambda_y \end{pmatrix} \end{aligned} \tag{5.21}$$

This root corresponds to the vorticity wave propagating downstream at a speed $\overline{u} > 0$, which can be verified by noting that the right eigenvector gives a wave with vorticity, but uniform entropy and pressure.

5.3.3 Root 3: Vorticity Wave

$$k_3 = \frac{\omega - \overline{v}l - \overline{w}m}{\overline{v}}, \qquad \omega = \overline{u}k_3 + \overline{v}l + \overline{w}m \tag{5.22}$$

The third set of eigenvectors for the multiple root is given by

Right eigenvector:

$$u_3^R = \begin{pmatrix} 0 \\ -\overline{u}\lambda_z \\ 0 \\ 1 - \overline{v}\lambda_y - \overline{w}\lambda_z \\ 0 \end{pmatrix} \tag{5.23}$$

Left eigenvector:

$$u_3^L = \begin{pmatrix} 0 & -\overline{u}\lambda_z & 0 & 1 - \overline{v}\lambda_y - \overline{w}\lambda_z & 0 \end{pmatrix} \tag{5.24}$$

The vector v_3^L, which is needed to construct the non-reflecting boundary conditions, is calculated following the procedure given in the theory section.

$$\begin{aligned} v_3^L &= \frac{1}{\overline{u}} u_3^L A \\ &= \begin{pmatrix} 0 & -\overline{u}\lambda_z & 0 & 1 - \overline{v}\lambda_y - \overline{w}\lambda_z & -\lambda_z \end{pmatrix} \end{aligned} \tag{5.25}$$

This root also corresponds to a vorticity wave propagating downstream at a speed $\overline{u} > 0$, which can be verified by noting that the right eigenvector gives a wave with vorticity, but uniform entropy and pressure.

5.3.4 Root 4: Downstream Running Pressure Wave

$$k_4 = \frac{(\omega - \overline{v}l - \overline{w}m)(S - \overline{u})}{1 - \overline{u}^2}, \quad \omega = (\overline{u}k_4 + \overline{v}l + \overline{w}m) + \sqrt{k_4^2 + l^2 + m^2} \tag{5.26}$$

Substituting for ω gives

$(-\omega I + k_4 A + lB + mC) =$

$$\begin{pmatrix} -\sqrt{k_4^2 + l^2 + m^2} & k_4 & l & m & 0 \\ 0 & -\sqrt{k_4^2 + l^2 + m^2} & 0 & 0 & k_4 \\ 0 & 0 & -\sqrt{k_4^2 + l^2 + m^2} & 0 & l \\ 0 & 0 & 0 & -\sqrt{k_4^2 + l^2 + m^2} & m \\ 0 & k_4 & l & m & -\sqrt{k_4^2 + l^2 + m^2} \end{pmatrix} \tag{5.27}$$

Right eigenvector:

$$u_4^R = \frac{1}{2(1 - \overline{u})} \begin{pmatrix} (1 - \overline{v}\lambda_y - \overline{w}\lambda_z)(1 - \overline{u}S) \\ (1 - \overline{v}\lambda_y - \overline{w}\lambda_z)(S - \overline{u}) \\ (1 - \overline{u}^2)\lambda_y \\ (1 - \overline{u}^2)\lambda_z \\ (1 - \overline{v}\lambda_y - \overline{w}\lambda_z)(1 - \overline{u}S) \end{pmatrix} \tag{5.28}$$

Left eigenvector:

$$u_4^L = \frac{1}{(1-\overline{u})} \begin{pmatrix} 0 & (1-\overline{v}\lambda_y - \overline{w}\lambda_z)(S-\overline{u}) & (1-\overline{u}^2)\lambda_y & (1-\overline{u}^2)\lambda_z & (1-\overline{v}\lambda_y - \overline{w}\lambda_z)(1-\overline{u}S) \end{pmatrix} \tag{5.29}$$

The vector v_4^L, which is needed to construct the non-reflecting boundary conditions, is calculated following the procedure given in the theory section.

$$\begin{aligned} v_4^L &= \frac{1}{1+\overline{u}}\, u_4^L A \\ &= \begin{pmatrix} 0 & (1-\overline{v}\lambda_y - \overline{w}\lambda_z) & \overline{u}\lambda_y & \overline{u}\lambda_z & (1-\overline{v}\lambda_y - \overline{w}\lambda_z)\, S \end{pmatrix} \end{aligned} \tag{5.30}$$

This wave corresponds to an isentropic, irrotational pressure wave, traveling downstream at a speed $\overline{u}+1$ provided $\overline{u} > -1$.

5.3.5 Root 5: Upstream Running Pressure Wave

$$k_5 = -\frac{(\omega - \overline{v}l - \overline{w}m)(S + \overline{u})}{1 - \overline{u}^2}, \quad \omega = (\overline{u}k_5 + \overline{v}l + \overline{w}m) + \sqrt{k_5^2 + l^2 + m^2} \tag{5.31}$$

Substituting for ω gives

$(-\omega I + k_5 A + lB + mC) =$

$$\begin{pmatrix} -\sqrt{k_5^2 + l^2 + m^2} & k_5 & l & m & 0 \\ 0 & -\sqrt{k_5^2 + l^2 + m^2} & 0 & 0 & k_5 \\ 0 & 0 & -\sqrt{k_5^2 + l^2 + m^2} & 0 & l \\ 0 & 0 & 0 & -\sqrt{k_5^2 + l^2 + m^2} & m \\ 0 & k_5 & l & m & -\sqrt{k_5^2 + l^2 + m^2} \end{pmatrix} \tag{5.32}$$

Right eigenvector:

$$u_5^R = \frac{1}{2(1 + \overline{u})} \begin{pmatrix} (1 - \overline{v}\lambda_y - \overline{w}\lambda_z)(1 + \overline{u}S) \\ -(1 - \overline{v}\lambda_y - \overline{w}\lambda_z)(S + \overline{u}) \\ (1 - \overline{u}^2)\lambda_y \\ (1 - \overline{u}^2)\lambda_z \\ (1 - \overline{v}\lambda_y - \overline{w}\lambda_z)(1 + \overline{u}S) \end{pmatrix} \tag{5.33}$$

Left eigenvector:

$$u_5^L = \frac{1}{(1+\overline{u})} \begin{pmatrix} 0 & -(1-\overline{v}\lambda_y - \overline{w}\lambda_z)(S+\overline{u}) & (1-\overline{u}^2)\lambda_y & (1-\overline{u}^2)\lambda_z & (1-\overline{v}\lambda_y - \overline{w}\lambda_z)(1+\overline{u}S) \end{pmatrix} \tag{5.34}$$

The vector v_5^L, which is needed to construct the non-reflecting boundary conditions, is calculated following the procedure given in the theory section.

$$\begin{aligned} v_5^L &= -\frac{1}{1-\overline{u}}\, u_5^L A \\ &= \begin{pmatrix} 0 & -(1-\overline{v}\lambda_y - \overline{w}\lambda_z) & -\overline{u}\lambda_y & -\overline{u}\lambda_z & (1-\overline{v}\lambda_y - \overline{w}\lambda_z)\, S \end{pmatrix} \end{aligned} \tag{5.35}$$

This wave corresponds to an isentropic, irrotational pressure wave, traveling downstream at a speed $\overline{u} - 1$ provided $\overline{u} < 1$.

5.4 One-dimensional, Unsteady Boundary Conditions for 3D Euler Equations

If the computational domain is $0 < x < 1$, and $0 < \overline{u} < 1$, then the boundary at $x = 0$ is an inflow boundary with incoming waves corresponding to the first four roots, and the boundary at $x = 1$ is an outflow boundary with just one incoming wave due to the fifth root.

When $\lambda_y = \lambda_z = 0$, $S = 1$, and so the right eigenvectors w^R are

$$w_1^R = \begin{pmatrix} -1 \\ 0 \\ 0 \\ 0 \\ 0 \end{pmatrix}, \quad w_2^R = \begin{pmatrix} 0 \\ 0 \\ 1 \\ 0 \\ 0 \end{pmatrix}, \quad w_3^R = \begin{pmatrix} 0 \\ 0 \\ 0 \\ 1 \\ 0 \end{pmatrix}, \quad w_4^R = \begin{pmatrix} \frac{1}{2} \\ \frac{1}{2} \\ 0 \\ 0 \\ \frac{1}{2} \end{pmatrix}, \quad w_4^R = \begin{pmatrix} \frac{1}{2} \\ -\frac{1}{2} \\ 0 \\ 0 \\ \frac{1}{2} \end{pmatrix} \tag{5.36}$$

and the left eigenvectors w^L are

$$\begin{aligned} w_1^L &= \begin{pmatrix} -1 & 0 & 0 & 0 & 1 \end{pmatrix} \\ w_2^L &= \begin{pmatrix} 0 & 0 & 1 & 0 & 0 \end{pmatrix} \\ w_3^L &= \begin{pmatrix} 0 & 0 & 0 & 1 & 0 \end{pmatrix} \\ w_4^L &= \begin{pmatrix} 0 & 1 & 0 & 0 & 1 \end{pmatrix} \\ w_5^L &= \begin{pmatrix} 0 & -1 & 0 & 0 & 1 \end{pmatrix} \end{aligned} \tag{5.37}$$

Hence the transformation to, and from, 1-D characteristic variables is given by the following two matrix equations.

$$\begin{pmatrix} C_1 \\ C_2 \\ C_3 \\ C_4 \\ C_5 \end{pmatrix} = \begin{pmatrix} -1 & 0 & 0 & 0 & 1 \\ 0 & 0 & 1 & 0 & 0 \\ 0 & 0 & 0 & 1 & 0 \\ 0 & 1 & 0 & 0 & 1 \\ 0 & -1 & 0 & 0 & 1 \end{pmatrix} \begin{pmatrix} \rho' \\ u' \\ v' \\ w' \\ p' \end{pmatrix} \tag{5.38}$$

$$\begin{pmatrix} \rho' \\ u' \\ v' \\ w' \\ p' \end{pmatrix} = \begin{pmatrix} -1 & 0 & 0 & \frac{1}{2} & \frac{1}{2} \\ 0 & 0 & 0 & \frac{1}{2} & -\frac{1}{2} \\ 0 & 1 & 0 & 0 & 0 \\ 0 & 0 & 1 & 0 & 0 \\ 0 & 0 & 0 & \frac{1}{2} & \frac{1}{2} \end{pmatrix} \begin{pmatrix} C_1 \\ C_2 \\ C_3 \\ C_4 \\ C_5 \end{pmatrix} \tag{5.39}$$

ρ', u', v', w', and p' are the perturbations from the uniform flow about which the Euler equations were linearized, and C_1, C_1, C_3, C_4, and C_5 are the amplitudes of the four characteristic waves. At the inflow boundary the correct unsteady, non-reflecting, boundary conditions are

$$\begin{pmatrix} C_1 \\ C_2 \\ C_3 \\ C_4 \end{pmatrix} = 0 \tag{5.40}$$

while at the outflow boundary the correct non-reflecting boundary condition is

$$C_5 = 0 \tag{5.41}$$

5.5 Approximate, Quasi-3D, Unsteady Boundary Conditions for 3D Euler Equations

By dividing the dispersion relation by ω it is clear that k_n/ω, u_n^R, u_n^L, v_n^L are all functions of l/ω and m/ω. Thus a sequence of approximations can be obtained by expanding v_n^L in a Taylor series as a function of $\lambda_y = l/\omega$ and $\lambda_z = m/\omega$.

$$\begin{aligned} v_n^L(\lambda_y, \lambda_z) &= v_n^L\big|_{\lambda_y=\lambda_z=0} + \lambda_y \left.\frac{dv_n^L}{d\lambda_y}\right|_{\lambda_y=\lambda_z=0} + \lambda_z \left.\frac{dv_n^L}{d\lambda_z}\right|_{\lambda_y=\lambda_z=0} \\ &+ \frac{1}{2}\lambda_y^2 \left.\frac{d^2v_n^L}{d\lambda_y^2}\right|_{\lambda_y=\lambda_z=0} + \frac{1}{2}\lambda_y^2 \left.\frac{d^2v_n^L}{d\lambda_y^2}\right|_{\lambda_y=\lambda_z=0} + \ldots \end{aligned} \tag{5.42}$$

The first order approximation obtained by just keeping the leading term gives the one-dimensional boundary conditions which have already been discussed. The second order approximation is

$$\begin{aligned} \overline{v}_n^L(\lambda_y, \lambda_z) &= v_n^L\big|_{\lambda_y=\lambda_z=0} + \lambda_y \left.\frac{dv_n^L}{d\lambda_y}\right|_{\lambda_y=\lambda_z=0} + \lambda_z \left.\frac{dv_n^L}{d\lambda_z}\right|_{\lambda_y=\lambda_z=0} \\ &= u_n^L\big|_{\lambda_y=\lambda_z=0} + \frac{l}{\omega}\left[\frac{k_n}{\omega}\frac{du_n^L}{d\lambda_y}A\right]\Bigg|_{\lambda_y=\lambda_z=0} + \frac{m}{\omega}\left[\frac{k_n}{\omega}\frac{du_n^L}{d\lambda_z}A\right]\Bigg|_{\lambda_y=\lambda_z=0} \end{aligned} \tag{5.43}$$

The over bar denotes the fact that $\overline{v}$ is an approximation to v. This produces the boundary condition

$$\left(u_n^L\big|_{\lambda_y=\lambda_z=0} + \frac{l}{\omega}\left[\frac{k_n}{\omega}\frac{du_n^L}{d\lambda_y}A\right]\Bigg|_{\lambda_y=\lambda_z=0} + \frac{m}{\omega}\left[\frac{k_n}{\omega}\frac{du_n^L}{d\lambda_z}A\right]\Bigg|_{\lambda_y=\lambda_z=0}\right)U = 0 \tag{5.44}$$

Multiplying by ω, and replacing ω, l and m by $i\frac{\partial}{\partial t}$, $-i\frac{\partial}{\partial y}$ and $-i\frac{\partial}{\partial z}$ respectively gives,

$$u_n^L\big|_{\lambda_y=\lambda_z=0}\frac{\partial U}{\partial t} - \left[\frac{k_n}{\omega}\,\frac{du_n^L}{d\lambda_y}\,A\right]\Bigg|_{\lambda_y=\lambda_z=0}\frac{\partial U}{\partial y} - \left[\frac{k_n}{\omega}\,\frac{du_n^L}{d\lambda_z}\,A\right]\Bigg|_{\lambda_y=\lambda_z=0}\frac{\partial U}{\partial z} = 0 \quad (5.45)$$

Following the theory presented above, the second order non-reflecting boundary conditions are obtained by taking the second-order approximation to the left eigenvectors v^L in the limit $\lambda_y = \lambda_z \approx 0$. In this limit, $S \approx 1$ and so one obtains the following approximate eigenvectors.

$$\overline{v_1}^L = \begin{pmatrix} -1 & 0 & 0 & 0 & 1 \end{pmatrix}$$

$$\overline{v_2}^L = \begin{pmatrix} 0 & -\overline{u}\lambda_y & 1-\overline{v}\lambda_y-\overline{w}\lambda_z & 0 & -\lambda_y \end{pmatrix}$$

$$\overline{v_3}^L = \begin{pmatrix} 0 & -\overline{u}\lambda_z & 0 & 1-\overline{v}\lambda_y-\overline{w}\lambda_z & -\lambda_z \end{pmatrix}$$

$$\overline{v_4}^L = \begin{pmatrix} 0 & 1-\overline{v}\lambda_y-\overline{w}\lambda_z & \overline{u}\lambda_y & \overline{u}\lambda_z & 1-\overline{v}\lambda_y-\overline{w}\lambda_z \end{pmatrix}$$

$$\overline{v_5}^L = \begin{pmatrix} 0 & -(1-\overline{v}\lambda_y-\overline{w}\lambda_z) & -\overline{u}\lambda_y & -\overline{u}\lambda_z & 1-\overline{v}\lambda_y-\overline{w}\lambda_z \end{pmatrix} \quad (5.46)$$

Actually, the first three eigenvectors are exact since the only approximation which has been made is $S \approx 1$ in the fourth and five eigenvectors. Consequently, the inflow boundary conditions will be perfectly non-reflecting for both of the incoming entropy and vorticity characteristics.

The second step is to multiply by ω and replace ω by $-\frac{\partial}{\partial t}$, l by $\frac{\partial}{\partial y}$, and m by

$\frac{\partial}{\partial z}$. This gives the inflow boundary condition

$$\begin{pmatrix} -1 & 0 & 0 & 0 & 1 \\ 0 & 0 & 1 & 0 & 0 \\ 0 & 0 & 0 & 1 & 0 \\ 0 & 1 & 0 & 0 & 1 \end{pmatrix} \frac{\partial U}{\partial t} + \begin{pmatrix} 0 & 0 & 0 & 0 & \\ 0 & \overline{u} & \overline{v} & 0 & 1 \\ 0 & 0 & 0 & \overline{v} & 0 \\ 0 & \overline{v} & -\overline{u} & 0 & \overline{v} \end{pmatrix} \frac{\partial U}{\partial y} + \begin{pmatrix} 0 & 0 & 0 & 0 & \\ 0 & 0 & \overline{w} & 0 & 0 \\ 0 & \overline{u} & 0 & \overline{w} & 1 \\ 0 & \overline{w} & 0 & -\overline{u} & \overline{w} \end{pmatrix} \frac{\partial U}{\partial z} = 0 \tag{5.47}$$

and the outflow boundary condition

$$\begin{pmatrix} 0 & -1 & 0 & 0 & 1 \end{pmatrix} \frac{\partial U}{\partial t} + \begin{pmatrix} 0 & -\overline{v} & \overline{u} & 0 & \overline{v} \end{pmatrix} \frac{\partial U}{\partial y} + \begin{pmatrix} 0 & -\overline{w} & 0 & \overline{u} & \overline{w} \end{pmatrix} \frac{\partial U}{\partial z} = 0 \tag{5.48}$$

For implementation purposes it is preferable to rewrite these equations using the one-dimensional characteristics.

$$\frac{\partial}{\partial t}\begin{pmatrix} C_1 \\ C_2 \\ C_3 \\ C_4 \end{pmatrix} + \begin{pmatrix} 0 & 0 & 0 & 0 & 0 \\ 0 & \overline{v} & 0 & \frac{1}{2}(1+\overline{u}) & \frac{1}{2}(1-\overline{u}) \\ 0 & 0 & \overline{v} & 0 & 0 \\ 0 & -\overline{u} & 0 & \overline{v} & 0 \end{pmatrix} \frac{\partial}{\partial y}\begin{pmatrix} C_1 \\ C_2 \\ C_3 \\ C_4 \\ C_5 \end{pmatrix}$$

$$+ \begin{pmatrix} 0 & 0 & 0 & 0 & 0 \\ 0 & \overline{w} & 0 & 0 & 0 \\ 0 & 0 & \overline{w} & \frac{1}{2}(1+\overline{u}) & \frac{1}{2}(1-\overline{u}) \\ 0 & 0 & -\overline{u} & \overline{w} & 0 \end{pmatrix} \frac{\partial}{\partial z}\begin{pmatrix} C_1 \\ C_2 \\ C_3 \\ C_4 \\ C_5 \end{pmatrix} = 0 \quad (5.49)$$

$$\frac{\partial C_5}{\partial t} + \begin{pmatrix} 0 & \overline{u} & 0 & 0 & \overline{v} \end{pmatrix} \frac{\partial}{\partial y}\begin{pmatrix} C_1 \\ C_2 \\ C_3 \\ C_4 \\ C_5 \end{pmatrix} + \begin{pmatrix} 0 & 0 & \overline{u} & 0 & \overline{w} \end{pmatrix} \frac{\partial}{\partial z}\begin{pmatrix} C_1 \\ C_2 \\ C_3 \\ C_4 \\ C_5 \end{pmatrix} = 0 \quad (5.50)$$

Before using these conditions it must be verified that they form a well-posed IBVP. If they do not, then no matter how they are implemented they will produce a divergent solution on a sufficiently fine grid.

5.6 Analysis of Well-posedness

5.6.1 Inflow Boundary Conditions

The well-posedness of the second approximation non-reflecting boundary conditions can be analyzed using the theory discussed earlier. To simplify the analysis we shift to a frame of reference which is moving with speed $\overline{v}$ in y-direction and $\overline{w}$ in z-direction. The transformed equations of motion and boundary conditions then correspond to $\overline{v} = \overline{w} = 0$ which simplifies the algebra, and well-posedness in this frame of reference is clearly both necessary and sufficient for well-posedness in the original frame of reference.

At the inflow boundary there are three incoming waves and the generalized incoming mode is

$$U(x, y, z, t) = \left[\sum_{n=1}^{4} a_n u_n^R e^{ik_n x}\right] e^{i(ly+mz-\omega t)} \tag{5.51}$$

with $Im(\omega) \geq 0$. Using the assumption that $\overline{v} = \overline{w} = 0$ the wave numbers are given by

$$k_1 = k_2 = k_3 = \frac{\omega}{\overline{u}} \tag{5.52}$$

$$k_4 = \frac{\omega(S - \overline{u})}{1 - \overline{u}^2} \tag{5.53}$$

where

$$S = \sqrt{1 - \left(1 - \overline{u}^2\right)\left(\lambda_y^2 + \lambda_z^2\right)} \tag{5.54}$$

with the correct square root being taken in the definition of S to ensure that if ω and S are both real then S is positive, and if ω or S is complex then $Im(k_4) > 0$.

Following the procedure presented in the theory section, the elements of the critical matrix C are obtained from $C_{mn} = \overline{v}_m^L u_n^R$.

$$C = \begin{pmatrix} 1 & 0 & 0 & 0 \\ 0 & 1+\overline{u}^2\lambda_y^2 & \overline{u}^2\lambda_y\lambda_z & 0 \\ 0 & \overline{u}^2\lambda_y\lambda_z & 1+\overline{u}^2\lambda_z^2 & 0 \\ 0 & 0 & 0 & \frac{1}{2}\left[S+1+\overline{u}(1+\overline{u})\left(\lambda_y^2+\lambda_z^2\right)\right] \end{pmatrix} \tag{5.55}$$

If $\omega = +i\overline{u}\left|\sqrt{l^2+m^2}\right|$ (satisfying the condition that $Im\left(\omega\right) \geq 0$), then

$$\lambda_y^2 + \lambda_z^2 = -\frac{1}{\overline{u}^2} \quad \text{and} \quad S = \frac{1}{\overline{u}}$$

(with the correct branch of the square root being taken to ensure that $Im\left(k_4\right) \geq 0$). Hence, for this value of ω,

$$C = \begin{pmatrix} 1 & 0 & 0 & 0 \\ 0 & -\overline{u}^2\lambda_y\lambda_z^2 & \overline{u}^2\lambda_y^2\lambda_z & 0 \\ 0 & 0 & 0 & 0 \\ 0 & 0 & 0 & 0 \end{pmatrix}$$

so there is clearly a non-trivial incoming mode, $U\left(x,y,z,t\right) = a_3 u_3^R e^{i(k_3 x+ly+mz-\omega t)}$, and the inflow boundary conditions are ill-posed.

It may appear that there is a second incoming mode, $U\left(x,y,z,t\right) = a_4 u_4^R e^{i(k_4 x+ly+mz-\omega t)}$, but this is actually a multiple of the first, because when $\omega = i\overline{u}\left|\sqrt{l^2+m^2}\right|$, $k_4 = k_3$

and u_4^R is a multiple of u_3^R. This degenerate situation was discussed in the theory section, and hence the initial-boundary-value problem is ill-posed with two ill-posed modes.

5.6.2 Outflow Boundary Conditions

At the outflow the generalized incoming mode is

$$U(x,y,z,t) = u_5^R e^{ik_5 x} e^{i(ly+mz-\omega t)} \tag{5.56}$$

with $Im(\omega) \geq 0$. Since $\overline{v} = \overline{w} = 0$ the wave number is given by

$$k_5 = -\frac{\omega\left(S+\overline{u}\right)}{1-\overline{u}^2} \tag{5.57}$$

where

$$S = \sqrt{1-\left(1-\overline{u}^2\right)\left(\lambda_y^2+\lambda_z^2\right)} \tag{5.58}$$

Again, the correct square root must be taken in the definition of S to ensure that if ω and S are both real then S is positive, and if ω or S is complex then $Im(k_5) < 0$. Since there is now only one incoming mode, the matrix C is simply a scalar.

$$C = \frac{1}{2}\left[S+1-\overline{u}(1-\overline{u})\left(\lambda_y^2+\lambda_z^2\right)\right] \tag{5.59}$$

The outflow conditions are ill-posed if there is a solution to

$$S = -1+\overline{u}(1-\overline{u})\left(\lambda_y^2+\lambda_z^2\right) \tag{5.60}$$

Substituting the expression for S and squaring the above equation gives

$$1 - \left(1 - \overline{u}^2\right)\left(\lambda_y^2 + \lambda_z^2\right) = 1 - 2\overline{u}(1 - \overline{u})\left(\lambda_y^2 + \lambda_z^2\right) + \overline{u}^2(1 - \overline{u})^2\left(\lambda_y^2 + \lambda_z^2\right)^2 \quad (5.61)$$

This gives $\lambda_y^2 + \lambda_z^2 = -\frac{1}{\overline{u}^2}$. This implies that $\omega = +i\overline{u}\sqrt{l^2 + m^2}$ and $S = \frac{1}{\overline{u}}$, as with the inflow analysis. However, when these values are substituted back into Eq. (5.60) we obtain

$$\frac{1}{\overline{u}} = -\frac{1}{\overline{u}} \quad (5.62)$$

This inconsistent equation contradicts the supposition that there is an incoming mode which satisfies the boundary conditions, and so we conclude that the outflow boundary condition is well-posed.

5.7 Modified Boundary Conditions

To overcome the ill-posedness of the inflow boundary conditions the fourth inflow boundary condition is modified. It must be noted that requiring v_4^L to be orthogonal to u_1^R, u_2^R, and u_3^R is overly restrictive. Since the first three inflow boundary conditions already require that $a_1 = a_2 = a_3 = 0$, it is only needed that v_4^L is orthogonal to u_5^R. Thus a new definition of $\overline{v}_4^L$ is proposed, which is equal to $(\overline{v}_4^L)_{old}$ plus λ_y times some multiple of the leading order term in $\overline{v}_2^L$ and λ_z times some multiple of the leading order term in $\overline{v}_3^L$.

$$\begin{aligned} \overline{v}_4^L &= \begin{pmatrix} 0 & 1 & \overline{u}\lambda_y & \overline{u}\lambda_z & 1 \end{pmatrix} \\ &+ \lambda_y a \begin{pmatrix} 0 & 0 & 1 & 0 & 0 \end{pmatrix} \\ &+ \lambda_z b \begin{pmatrix} 0 & 0 & 0 & 1 & 0 \end{pmatrix} \end{aligned} \tag{5.63}$$

The variables a and b will be chosen to minimize $\overline{v}_4^L u_5^R$, which controls the magnitude of the reflection coefficient, and at the same time will produce a well-posed boundary condition. The motivation for this approach is that the second approximation to the scalar wave equation is well-posed and produces fourth order reflection [40]. Substituting definition gives

$$\overline{v}_4^L u_5^R = \frac{1}{2}\left(\frac{1-\overline{u}}{1+\overline{u}}\right)\left(-S + 1 + (1+\overline{u})\left((a+\overline{u})\,\lambda_y^2 + (b+\overline{u})\,\lambda_z^2\right)\right) \tag{5.64}$$

The binomial series expansion for $S(\lambda_y, \lambda_z)$ is given by

$$S = 1 - \frac{1}{2}\left(1 - \overline{u}^2\right)\left(\lambda_y^2 + \lambda_z^2\right) + O\left(\lambda_y^4, \lambda_z^4\right) \tag{5.65}$$

The reflection co-efficient is fourth order if a and b are chosen such that

$$a + \overline{u} = b + \overline{u} = -\frac{1}{2}(1 - \overline{u}) \tag{5.66}$$

Thus the new form of $\overline{v}_4^L$ is

$$\overline{v}_4^L\big|_{\overline{v}=\overline{w}=0} = \begin{pmatrix} 0 & 1 & -\frac{1}{2}(1-\overline{u})\lambda_y & -\frac{1}{2}(1-\overline{u})\lambda_y & 1 \end{pmatrix} \tag{5.67}$$

To prove the well-posedness of the modified inflow boundary conditions, the critical matrix C is re-calculated.

$$C = \begin{pmatrix} 1 & 0 & 0 & 0 \\ 0 & 1+\overline{u}^2\lambda_y^2 & \overline{u}^2\lambda_y\lambda_z & 0 \\ 0 & \overline{u}^2\lambda_y\lambda_z & 1+\overline{u}^2\lambda_z^2 & 0 \\ 0 & -\frac{1}{2}(1+\overline{u})\lambda_y & -\frac{1}{2}(1+\overline{u})\lambda_z & \frac{1}{2}\left(S+1-\frac{1}{2}\left(1-\overline{u}^2\right)\left(\lambda_y^2+\lambda_z^2\right)\right) \end{pmatrix} \tag{5.68}$$

$\det(C) = 0$ implies either

$$-S = 1 - \frac{1}{2}\left(1 - \overline{u}^2\right)\left(\lambda_y^2 + \lambda_z^2\right) \tag{5.69}$$

or

$$\lambda_y^2 + \lambda_z^2 = -\frac{1}{\overline{u}^2} \tag{5.70}$$

Examine the first possibility:

$$-S = 1 - \frac{1}{2}\left(1 - \overline{u}^2\right)\left(\lambda_y^2 + \lambda_z^2\right)$$

We have

$$S|_{\overline{v}=\overline{w}=0} = \sqrt{1 - \left(1 - \overline{u}^2\right)\left(\lambda_y^2 + \lambda_z^2\right)}$$

Substituting S, we get:

$$-\sqrt{1 - \left(1 - \overline{u}^2\right)\left(\lambda_y^2 + \lambda_z^2\right)} = 1 - \frac{1}{2}\left(1 - \overline{u}^2\right)\left(\lambda_y^2 + \lambda_z^2\right) \tag{5.71}$$

Squaring both sides we get:

$$1 - \left(1 - \overline{u}^2\right)\left(\lambda_y^2 + \lambda_z^2\right) = 1 - \left(1 - \overline{u}^2\right)\left(\lambda_y^2 + \lambda_z^2\right) + \frac{1}{4}\left(1 - \overline{u}^2\right)\left(\lambda_y^2 + \lambda_z^2\right)^2 \tag{5.72}$$

$$\implies \quad \lambda_y^2 + \lambda_z^2 = 0 \quad \implies S = 1 \tag{5.73}$$

Putting these values of $(\lambda_y^2 + \lambda_z^2)$ and S into Eq. (5.69) we have $-1 = 1$ which is clearly inconsistent. Hence, the first possibility given by Eq. (5.69) does not lead to ill-posed incoming modes.

In the original reference frame where $\overline{v} \neq 0$, and $\overline{w} \neq 0$,

$$\overline{v}_4^L = \begin{pmatrix} 0 & 1-\overline{v}\lambda_y - \overline{w}\lambda_z & -\frac{1}{2}(1-\overline{u})\lambda_y & -\frac{1}{2}(1-\overline{u})\lambda_z & 1-\overline{v}\lambda_y - \overline{w}\lambda_z \end{pmatrix} \quad (5.74)$$

Therefore, the modified non-dimensional inflow boundary conditions in terms of primitive flow variables are,

$$\begin{pmatrix} -1 & 0 & 0 & 0 & 1 \\ 0 & 0 & 1 & 0 & 0 \\ 0 & 0 & 0 & 1 & 0 \\ 0 & 1 & 0 & 0 & 1 \end{pmatrix} \frac{\partial U}{\partial t} + \begin{pmatrix} 0 & 0 & 0 & 0 & \\ 0 & \overline{u} & \overline{v} & 0 & 1 \\ 0 & 0 & 0 & \overline{v} & 0 \\ 0 & \overline{v} & \frac{1-\overline{u}}{2} & 0 & \overline{v} \end{pmatrix} \frac{\partial U}{\partial y} + \begin{pmatrix} 0 & 0 & 0 & 0 & \\ 0 & 0 & \overline{w} & 0 & 0 \\ 0 & \overline{u} & 0 & \overline{w} & 1 \\ 0 & \overline{w} & 0 & \frac{1-\overline{u}}{2} & \overline{w} \end{pmatrix} \frac{\partial U}{\partial z} = 0 \quad (5.75)$$

The well-posed, non-dimensional, 3D inflow boundary conditions in terms of characteristic variables are:

$$\frac{\partial}{\partial t}\begin{pmatrix} C_1 \\ C_2 \\ C_3 \\ C_4 \end{pmatrix} + \begin{pmatrix} 0 & 0 & 0 & 0 & 0 \\ 0 & \overline{v} & 0 & \frac{1}{2}(1+\overline{u}) & \frac{1}{2}(1-\overline{u}) \\ 0 & 0 & \overline{v} & 0 & 0 \\ 0 & \frac{1}{2}(1-\overline{u}) & 0 & \overline{v} & 0 \end{pmatrix} \frac{\partial}{\partial y}\begin{pmatrix} C_1 \\ C_2 \\ C_3 \\ C_4 \\ C_5 \end{pmatrix} + \begin{pmatrix} 0 & 0 & 0 & 0 & 0 \\ 0 & \overline{w} & 0 & 0 & 0 \\ 0 & 0 & \overline{w} & \frac{1}{2}(1+\overline{u}) & \frac{1}{2}(1-\overline{u}) \\ 0 & 0 & \frac{1}{2}(1-\overline{u}) & \overline{w} & 0 \end{pmatrix} \frac{\partial}{\partial z}\begin{pmatrix} C_1 \\ C_2 \\ C_3 \\ C_4 \\ C_5 \end{pmatrix} = 0 \tag{5.76}$$

A corresponding modified outflow BC can be derived following a similar procedure which gives the following condition at the outflow boundary:

$$\frac{\partial C_5}{\partial t} + \begin{pmatrix} 0 & \frac{1}{2}(1+\overline{u}) & 0 & 0 & \overline{v} \end{pmatrix} \frac{\partial}{\partial y}\begin{pmatrix} C_1 \\ C_2 \\ C_3 \\ C_4 \\ C_5 \end{pmatrix} + \begin{pmatrix} 0 & 0 & \frac{1}{2}(1+\overline{u}) & 0 & \overline{w} \end{pmatrix} \frac{\partial}{\partial z}\begin{pmatrix} C_1 \\ C_2 \\ C_3 \\ C_4 \\ C_5 \end{pmatrix} = 0 \tag{5.77}$$

5.8 Giles Boundary Conditions for 3D Euler Equations in Cartesian Co-ordinates

A summary of the boundary conditions derived for the linearized 3D Euler equations in chapter 5 is given in this section.

a) Transformation to, and from, One-dimensional Characteristic Variables

$$\begin{pmatrix} C_1 \\ C_2 \\ C_3 \\ C_4 \\ C_5 \end{pmatrix} = \begin{pmatrix} -\overline{c}^2 & 0 & 0 & 0 & 1 \\ 0 & 0 & \overline{\rho c} & 0 & 0 \\ 0 & 0 & 0 & \overline{\rho c} & 0 \\ 0 & \overline{\rho c} & 0 & 0 & 1 \\ 0 & -\overline{\rho c} & 0 & 0 & 1 \end{pmatrix} \begin{pmatrix} \rho' \\ u' \\ v' \\ w' \\ p' \end{pmatrix} \tag{5.78}$$

$$\begin{pmatrix} \rho' \\ u' \\ v' \\ w' \\ p' \end{pmatrix} = \begin{pmatrix} -\frac{1}{\overline{c}^2} & 0 & 0 & \frac{1}{2\overline{c}^2} & \frac{1}{2\overline{c}^2} \\ 0 & 0 & 0 & \frac{1}{2\overline{\rho c}} & -\frac{1}{2\overline{\rho c}} \\ 0 & \frac{1}{\overline{\rho c}} & 0 & 0 & 0 \\ 0 & 0 & \frac{1}{\overline{\rho c}} & 0 & 0 \\ 0 & 0 & 0 & \frac{1}{2} & \frac{1}{2} \end{pmatrix} \begin{pmatrix} C_1 \\ C_2 \\ C_3 \\ C_4 \\ C_5 \end{pmatrix} \tag{5.79}$$

b) One-dimensional, Unsteady, Boundary Conditions.

Inflow:

$$\begin{pmatrix} C_1 \\ C_2 \\ C_3 \\ C_4 \end{pmatrix} = 0 \tag{5.80}$$

Outflow:

$$C_5 = 0 \tag{5.81}$$

c) Unsteady, Quasi-3D, Inflow Boundary Conditions.

$$\frac{\partial}{\partial t}\begin{pmatrix} C_1 \\ C_2 \\ C_3 \\ C_4 \end{pmatrix} + \begin{pmatrix} 0 & 0 & 0 & 0 & 0 \\ 0 & \overline{v} & 0 & \frac{1}{2}(\overline{c}+\overline{u}) & \frac{1}{2}(\overline{c}-\overline{u}) \\ 0 & 0 & \overline{v} & 0 & 0 \\ 0 & \frac{1}{2}(\overline{c}-\overline{u}) & 0 & \overline{v} & 0 \end{pmatrix} \frac{\partial}{\partial y}\begin{pmatrix} C_1 \\ C_2 \\ C_3 \\ C_4 \\ C_5 \end{pmatrix}$$
$$+ \begin{pmatrix} 0 & 0 & 0 & 0 & 0 \\ 0 & \overline{w} & 0 & 0 & 0 \\ 0 & 0 & \overline{w} & \frac{1}{2}(\overline{c}+\overline{u}) & \frac{1}{2}(\overline{c}-\overline{u}) \\ 0 & 0 & \frac{1}{2}(\overline{c}-\overline{u}) & \overline{w} & 0 \end{pmatrix} \frac{\partial}{\partial z}\begin{pmatrix} C_1 \\ C_2 \\ C_3 \\ C_4 \\ C_5 \end{pmatrix} = 0 \tag{5.82}$$

d) Unsteady, Quasi-3D, Outflow Boundary Condition.

$$\frac{\partial C_5}{\partial t}+\begin{pmatrix} 0 & \overline{u} & 0 & 0 & \overline{v} \end{pmatrix}\frac{\partial}{\partial y}\begin{pmatrix} C_1 \\ C_2 \\ C_3 \\ C_4 \\ C_5 \end{pmatrix}+\begin{pmatrix} 0 & 0 & \overline{u} & 0 & \overline{w} \end{pmatrix}\frac{\partial}{\partial z}\begin{pmatrix} C_1 \\ C_2 \\ C_3 \\ C_4 \\ C_5 \end{pmatrix}=0 \quad (5.83)$$

e) Modified, Unsteady, Quasi-3D, Outflow Boundary Condition.

$$\frac{\partial C_5}{\partial t}+\begin{pmatrix} 0 & \frac{1}{2}(\overline{c}+\overline{u}) & 0 & 0 & \overline{v} \end{pmatrix}\frac{\partial}{\partial y}\begin{pmatrix} C_1 \\ C_2 \\ C_3 \\ C_4 \\ C_5 \end{pmatrix}+\begin{pmatrix} 0 & 0 & \frac{1}{2}(\overline{c}+\overline{u}) & 0 & \overline{w} \end{pmatrix}\frac{\partial}{\partial z}\begin{pmatrix} C_1 \\ C_2 \\ C_3 \\ C_4 \\ C_5 \end{pmatrix}=0 \quad (5.84)$$

Chapter 6

Ringleb Flow

To validate the Giles non-reflecting boundary conditions and the corresponding wall corner conditions, the Ringleb flow has been used as a test case. Ringleb flow provides for a very good test case due to the following reasons:

1. The analytical solution for the problem is available.
2. The flow is highly non-linear and is non-uniform at the Inflow and Outflow boundaries.
3. The flow bounded by wall geometry defined by a complex curve.
4. A wide range of geometries and flow configurations can be generated analytically for the test cases.

6.1 Equations for Ringleb Flow

Ringleb flow [66] is an exact solution of the Euler equations for an ideal gas obtained by using a hodograph transformation. Hodograph method is a technique for analyzing two-dimensional flow of an ideal fluid by regarding the position $X = (x, y)$ as a function of velocity $U = (u, v)$ and determining the partial differential equations satisfied by $X(U)$. This transformation to independent variables (u, v) and dependent variables (x, y) is a hodograph transformation [67].

The equations are transformed from the Cartesian (x, y) co-ordinate system to the (q, θ) hodograph plane where q is the velocity magnitude and θ is the angle the velocity vector makes with a reference axis. The momentum equations can be expressed in the stream function form as,

$$q^2 \frac{\partial^2 \psi}{\partial q^2} + q \left(1 + \frac{q^2}{c^2}\right) \frac{\partial \psi}{\partial q} + \left(1 - \frac{q^2}{c^2}\right) \frac{\partial^2 \psi}{\partial \theta^2} = 0 \tag{6.1}$$

where, ψ is the stream function defined such that the Cartesian velocity components are given by,

$$u = \frac{\rho_r}{\rho} \frac{\partial \psi}{\partial y}, \quad v = \frac{\rho_r}{\rho} \frac{\partial \psi}{\partial x} \tag{6.2}$$

where the subscript r indicates an arbitrary reference condition. This choice of stream function identically satisfies the continuity equation.

The particular solution representing Ringleb flow is given by,

$$\psi = \frac{1}{q} sin(\theta) \tag{6.3}$$

where the overbar indicates division by a reference quantity. The streamlines for this solution are given by,

$$x = \frac{1}{2\rho}\left(\frac{1}{\overline{q}^2} - \frac{2}{k^2}\right) + \frac{J}{2}, \quad y = \pm\frac{1}{k\overline{\rho}\overline{q}}\sqrt{1 - \left(\frac{\overline{q}}{k}\right)^2} \tag{6.4}$$

where

$$k = \frac{1}{\psi} \tag{6.5}$$

$$J = \frac{1}{\overline{c}} + \frac{1}{3\overline{c}^3} + \frac{1}{5\overline{c}^5} - \frac{1}{2}log\left(\frac{1+\overline{c}}{1-\overline{c}}\right) \tag{6.6}$$

$$\overline{c} = \sqrt{1 - \frac{\gamma-1}{2}\overline{q}^2} \tag{6.7}$$

$$\overline{\rho} = \overline{c}^{\frac{2}{\gamma-1}} \tag{6.8}$$

Pressure is given by,

$$p = \frac{\overline{\rho c}^2}{\gamma} \tag{6.9}$$

where γ is the ratio of specific heats.

The geometry of a particular test case is determined by choosing two streamlines to serve as solid walls along with lines of constant velocity as inflow and outflow boundaries [68]. A typical geometry for this flow is shown in Fig. (6-1), where the solid walls are formed by streamlines corresponding to $k = 0.8$ and $k = 1.6$, and the outflow boundary is given by $\overline{q} = 0.4$.

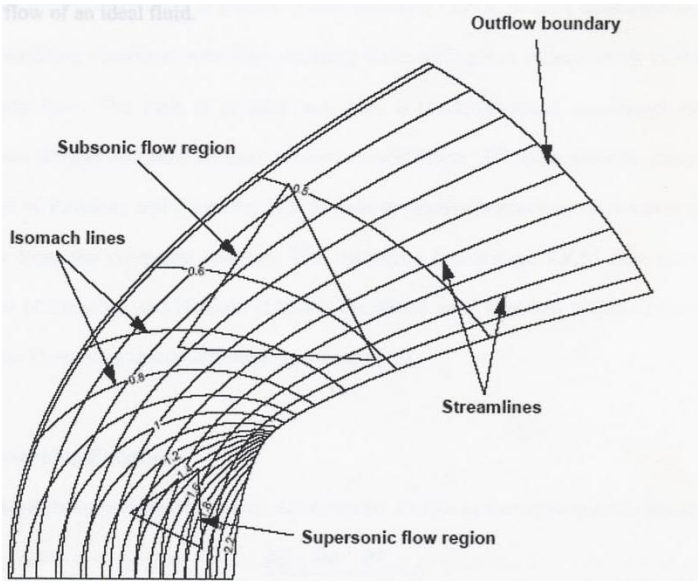

Figure 6-1: **A Typical Ringleb Flow Domain**

6.2 Characteristics of Ringleb Flow

The deceleration of a fluid through a sonic speed generally produces a shock, but this can be avoided if the boundary of the fluid has a special shape. Such shape is provided by a channel with walls at streamlines, assuming that the boundary layer effects may be neglected. The flow can occur according to the equations mentioned in the previous section, so that in the channel the speed of the fluid element increases from subsonic to supersonic and then decelerates back to subsonic without the occurrence of a shock. Thus Ringleb flow captures some physically important properties of exact solutions of the full nonlinear equations of high speed flow of an ideal fluid.

Chapter 7

Numerical Implementation

7.1 Flow Solver and Numerical Schemes

The extended Giles boundary conditions along with the wall corner conditions developed in the present work have been implemented in the NASA Glenn Research Center BASS (Broadband Acoustic Stator Simulator) code. The BASS Code is a high-accuracy Computational Aeroacoustics (CAA) code which solves the nonlinear Euler and Navier-Stokes equations in the non-conservative, chain rule form of the governing equations in order to solve flows with complex geometries. The lack of conservation is offset by the increased accuracy of the transformed equations ([73], [74]). It is a multi-block, parallel solver designed for structured grids. For spatial differences, four methods are available: explicit second-order central differencing, explicit sixth-order central differencing, Tam and Webb's optimized explicit fourth-order DRP (Dispersion-Relation-Preserving) central differencing [65], and Hixon's prefactored compact sixth-order central differencing [69].

For the present work, the RK 4L (fourth order, low-storage, Runge-Kutta) scheme is used for time marching along with the DRP scheme for spatial differencing. Kennedy and Carpernter's tenth-order artificial dissipation [71] is used to remove unresolved waves from the flow solution. The CFL number for all the simulations in this work was chosen as 1.1.

7.2 Mean Flow Boundary Condition

For the test cases in this work, in addition to the Giles non-reflecting boundary conditions, the BASS code implements the Mean Flow Boundary Condition developed by Hixon et. al [72]. The non-reflecting boundary conditions are designed to allow outgoing disturbances to exit the computational domain without generating spurious incoming disturbances. However, these boundary conditions do not maintain a desired mean flow when implemented in a nonlinear flow solver. In the initial transient phase, of a long-time unsteady flow calculation, large disturbances may propagate through the boundary and exit the domain. These disturbances affect the flow solution (such as flow angle at the inflow boundary) as they exit the boundary. To maintain the correct mean flow, the flow must be reset. One method to reset the flow at boundary is to impose an incoming disturbance originating at a source outside of the computational domain. the mean flow boundary condition sends waves into the computational domain in order to obtain the desired mean flow at the boundaries. In order to specify the correct mean flow boundary condition on an unsteady flow, the mean flow itself is calculated at the boundary.

7.3 Wall Boundary Condition

The wall boundary condition is designed to modify the flow solution to prohibit non-physical flow through the wall. The 'correction' implementation of Hixon [76], of the wall boundary condition developed by Tam and Dong [75] is used in BASS code.

At the wall, the time derivative of the normal momentum is set to zero:

$$\left(\rho\vec{V}\right)_t \bullet \vec{n} = 0 \tag{7.1}$$

The interior flow equations are solved using biased differencing at the wall, and an initial 'uncorrected' value for the time derivative of the conserved quantities is obtained at the wall. Using the chain rule form of the Euler equations, the uncorrected time derivative is:

$$Q_{t,uc} = -\left[\xi_x \{E\}_\xi + \eta_x \{E\}_\eta + \xi_y \{F\}_\xi + \eta_y \{F\}_\eta\right] \tag{7.2}$$

The wall boundary condition is used to determine the 'corrected' value of the time derivative at the wall:

$$\{Q\}_{\text{t,corrected}} = \{Q\}_{\text{t,uncorrected}} + \{\Delta Q\}_t \tag{7.3}$$

At the wall boundary, only the normal flux derivatives can be changed by the boundary condition. This change to the normal flux derivative at the wall has an effect on the time derivative at the wall. Assuming that the wall normal direction lies in the η

co-ordinate direction:

$$\{\Delta Q\}_t = -\left(\eta_x \{\Delta E\}_\eta + \eta_y \{\Delta F\}_\eta\right) \tag{7.4}$$

The normal flux derivatives are 'corrected' by modifying the value of the normal fluxes at a ghost point outside the flow domain. Depending on the size of the finite-differencing stencil used, the ghost point may affect the value of the normal derivative at grid points in the interior of the computational domain. This ghost point correction method is described fully in Ref. [77], and the wall boundary condition implementation for the chain rule form of the governing equations is also given.

Chapter 8

Results and Discussion

The Curvilinear Giles boundary conditions along with the wall corner conditions have been validated for the following Ringleb flow test cases:

1. $k = 0.50$ for the inner wall and 0.20 for the outer wall. $\overline{q} = 0.10$ for the inflow and outflow boundaries. The inflow Mach number is 0.10 and the maximum Mach number is 0.52 at the center of the inner wall.

2. $k = 0.60$ for the inner wall and 0.20 for the outer wall. $\overline{q} = 0.10$ for the inflow and outflow boundaries. The inflow Mach number is 0.10 and the maximum Mach number is 0.64 at the center of the inner wall.

3. $k = 0.70$ for the inner wall and 0.25 for the outer wall. $\overline{q} = 0.15$ for the inflow and outflow boundaries. The inflow Mach number is 0.14 and the maximum Mach number is 0.74 at the center of the inner wall.

4. $k = 0.80$ for the inner wall and 0.30 for the outer wall. $\overline{q} = 0.20$ for the inflow and outflow boundaries. The inflow Mach number is 0.20 and the maximum

Mach number is 0.86 at the center of the inner wall.

5. $k = 0.95$ for the inner wall and 0.45 for the outer wall. $\overline{q} = 0.25$ for the inflow and outflow boundaries. The inflow Mach number is 0.25 and the maximum Mach number is 1.05 at the center of the inner wall.

6. $k = 1.05$ for the inner wall and 0.55 for the outer wall. $\overline{q} = 0.35$ for the inflow and outflow boundaries. The inflow Mach number is 0.35 and the maximum Mach number is 1.20 at the center of the inner wall.

Each of the above test cases was run on the following grid sizes: 21x11, 31x16, 41x21 and 61x31.

Fig. (8-1) shows a 61x31 grid of two Ringleb flow geometries, with maximum velocities of 0.80 on the left and 1.05 on the right. The inflow and outflow boundaries are curved and the grid at the boundaries is non-orthogonal for all the test cases.

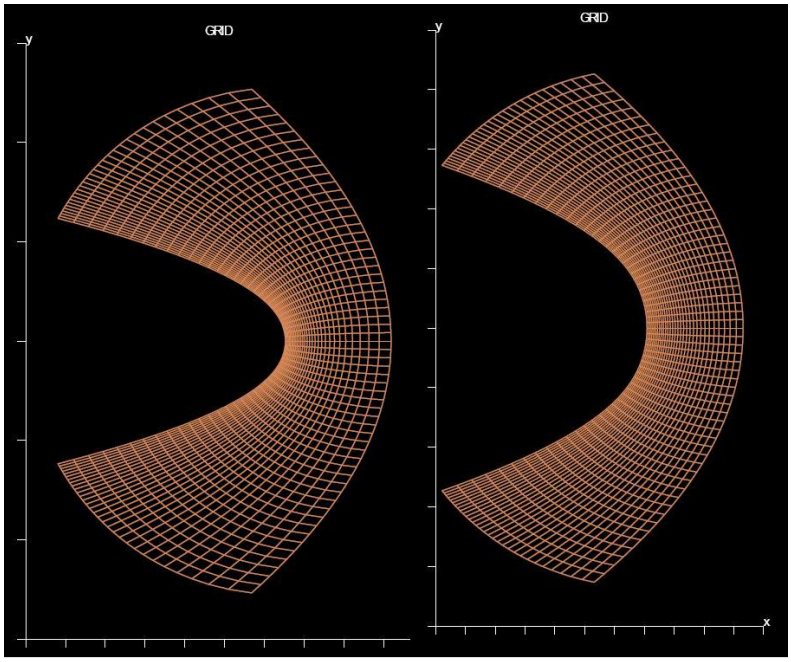

Figure 8-1: **A 61x31 Grid for kmax = 0.80, kmin = 0.30, $\overline{q}$ = 0.10 (left) and kmax = 1.05, kmin = 0.55, $\overline{q}$ = 0.35 (right)**

8.1 Wall Corner Condition

Fig. (8-2) shows a typical wall-corner flow vectors of Ringleb flow solution ($kmax = 0.70, kmin = 0.25, \overline{q} = 0.15$) computed using the Cartesian Giles boundary conditions without the wall condition. The wall condition for the 2D Cartesian Giles boundary conditions was tested on the Ringleb flow test cases and flow through the wall at the corner vanished. However, the correct flow solution at the corners could still not be computed when the wall condition was applied to the chain-rule form of Cartesian Giles and eventually caused the numerical solution to diverge as seen in Fig (8-3).

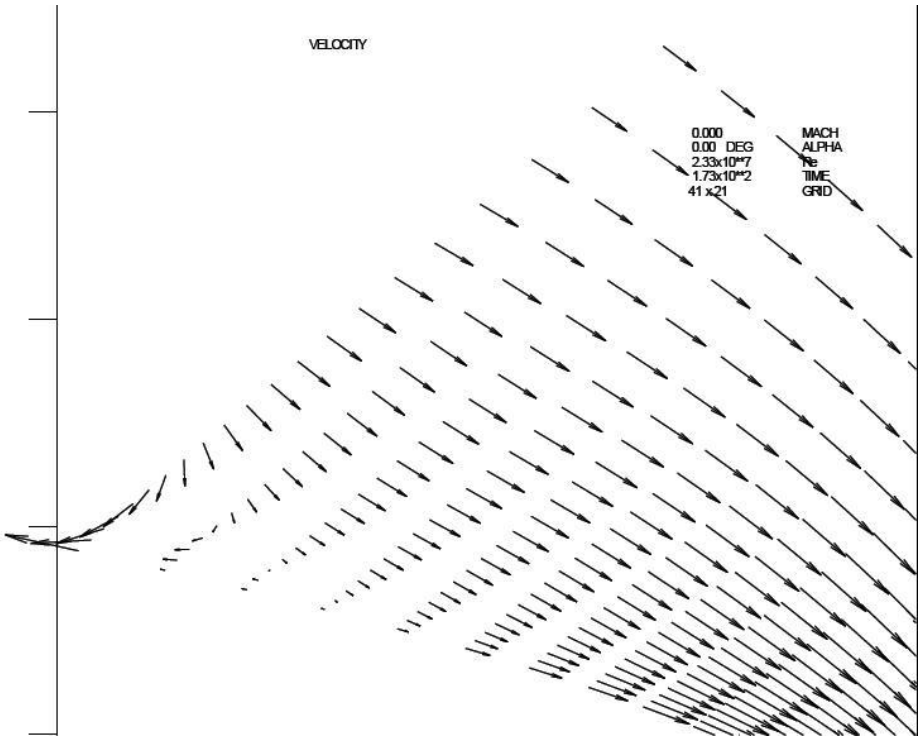

Figure 8-2: **Cartesian Giles Boundary Conditions without the Wall Condition**

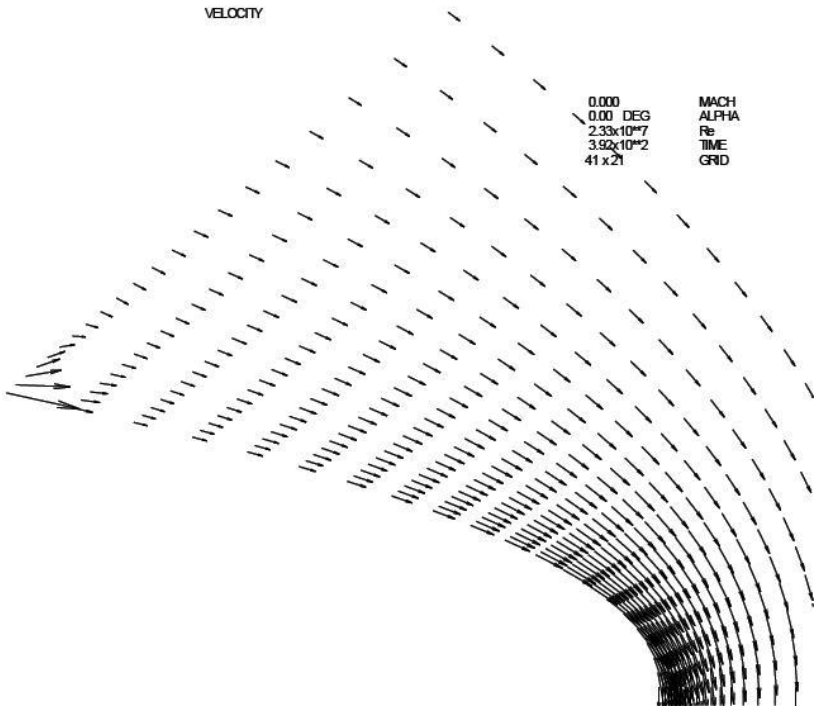

Figure 8-3: **Cartesian Giles Boundary Conditions with the Wall Condition**

As pointed out earlier, the Giles boundary conditions were derived from the Cartesian form of Euler equations and then transformed into Curvilinear co-ordinates using the chain rule formulation. The 2D Curvilinear boundary conditions in chapter 4 were derived starting with the Curvilinear form of Euler equations which resulted in new terms containing the factor $(\xi_x\eta_x + \xi_y\eta_y)$ that vanishes when the grid is orthogonal at the boundaries. These orthogonal terms were lost when deriving the boundary conditions from the Cartesian form of the governing equations.

When the Curvilinear boundary conditions were implemented without the additional terms, the solution at the corner showed similar behavior to that obtained from Cartesian Giles boundary conditions. Figs (8-4) and (8-5) show the velocity vectors of flow solution obtained using Curvilinear Giles boundary conditions without the extra terms. It is clearly seen that without the additional orthogonal terms, the corner problem is not eliminated in spite of the application of the wall condition.

Only the Curvilinear boundary conditions with the additional terms and with the wall corner condition solved the corner problem completely and obtained a converged solution as seen in Fig. (8-6).

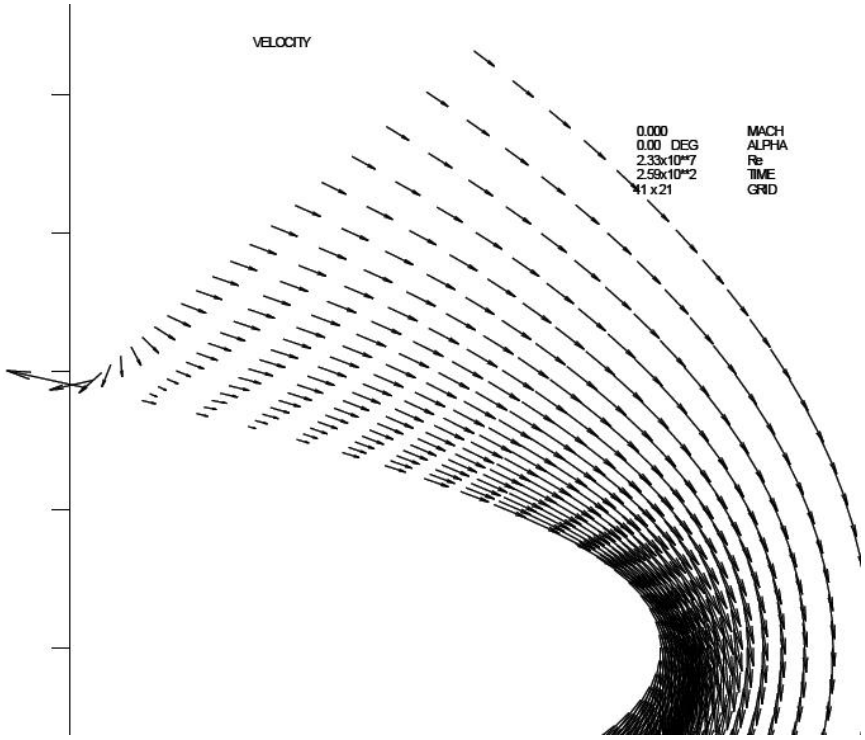

Figure 8-4: **Curvilinear Giles Boundary Conditions without Additional Terms and without the Wall Condition**

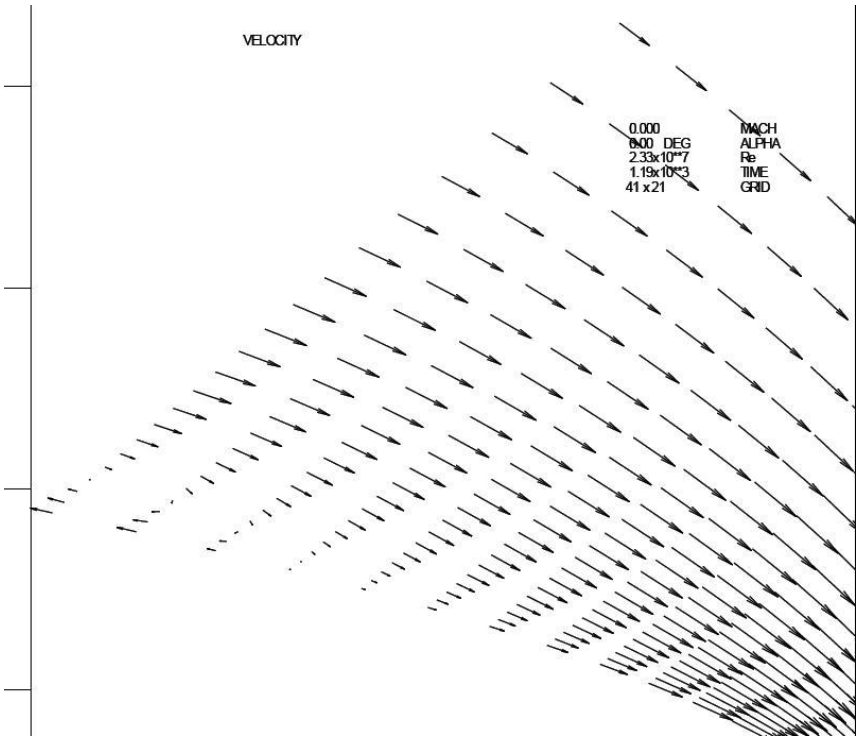

Figure 8-5: **Curvilinear Giles Boundary Conditions without Additional Terms and with the Wall Condition**

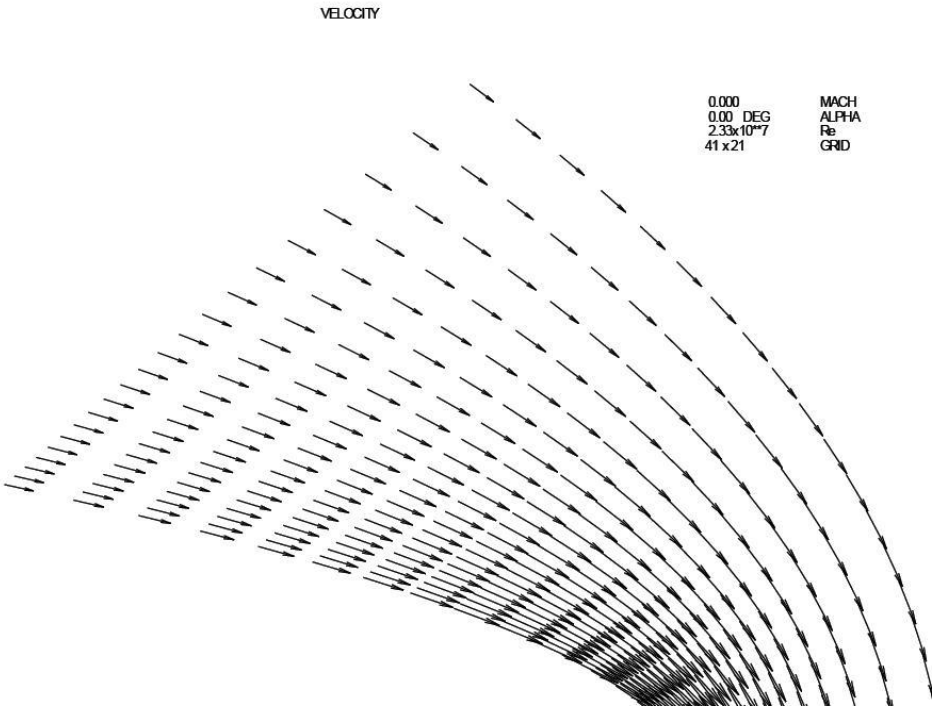

Figure 8-6: **Curvilinear Giles Boundary Conditions with Additional Terms and with the Wall Condition**

8.2 Long-term Instability

The Curvilinear boundary conditions have been tested on various ringleb flow geometries and grid densities. For a given Mach number, as the number of grid points were increased, the solution displayed instability waves running through the domain that eventually caused the solution to diverge. Figs. (8-7) - (8-12) shows the history of L2 errors of density for the entire computational domain for all the test cases. The long-term instability can be seen in each of the ringleb flow geometries beyond a certain number of grid points. Spurious wave reflections caused due to various reasons such as inaccuracy of the boundary conditions, type of spatial discretization scheme, interior and boundary stencils, have created a non-physical feedback loop from the downstream resulting in a long-term instability of flow solution. Change of the time marching scheme from RK4L to RK56 and RK67 did not solve the long-term instability problem.

Sufficient stretching of the grid towards the inflow and outflow boundaries eliminated the long-term instability in flow solution. Stretching the grid towards the boundaries breaks the feedback loop and damps the unresolved frequencies propagating through the domain. For 21x11 and 31x16 grids, stretching was not necessary for any of the test cases. Grid stretching was not required for a 41x21 grid, for the cases with a maximum velocity of 0.60 and 1.05. The L2-norm errors in Density for the test cases with grid stretching are listed in Tables (8.1) - (8.6). For a given number of grid points, as the grid stretching factor increases, the L2-norm error increases. The L2-norm error is calculated using the analytical solution of Ringleb flow.

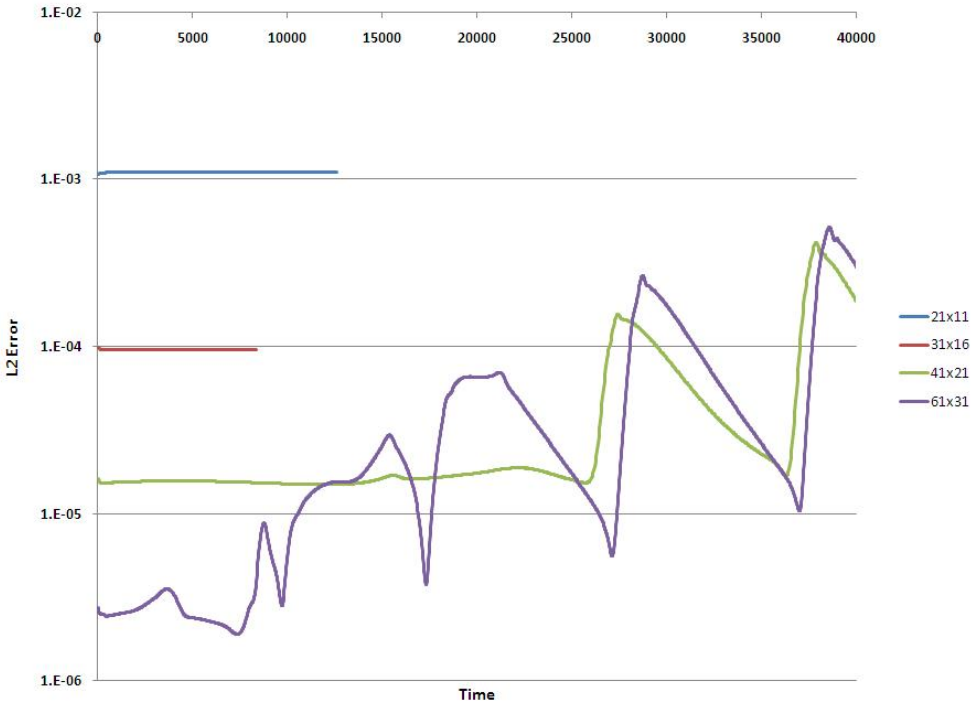

Figure 8-7: **L2 Error in Density for a Maximum Velocity of 0.50**

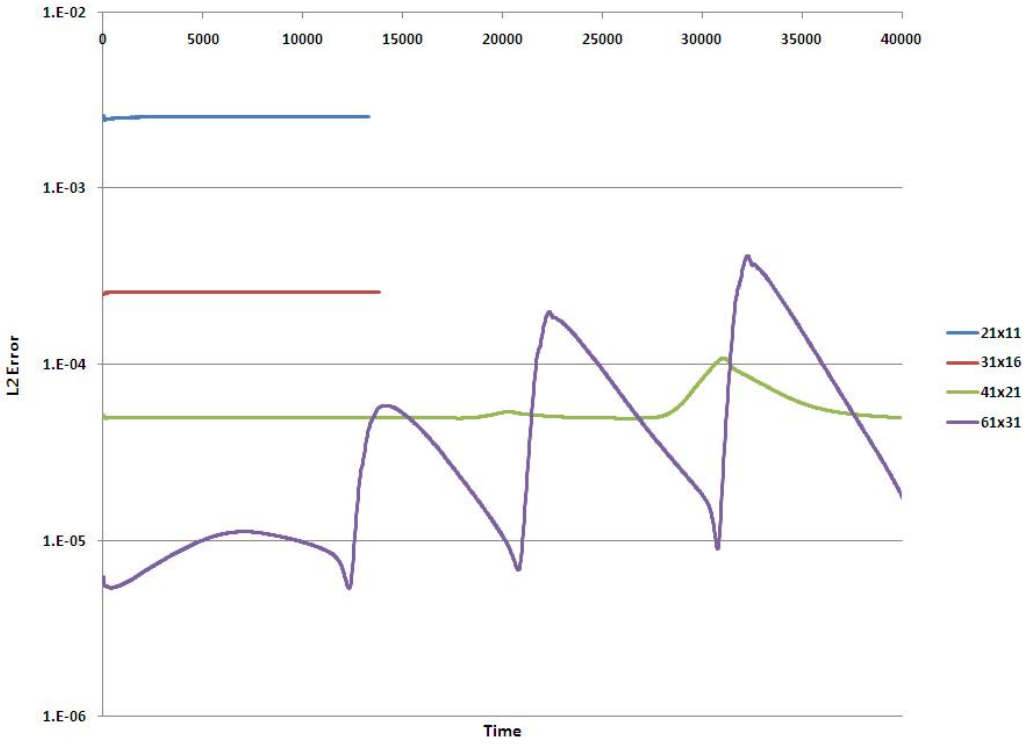

Figure 8-8: **L2 Error in Density for a Maximum Velocity of 0.60**

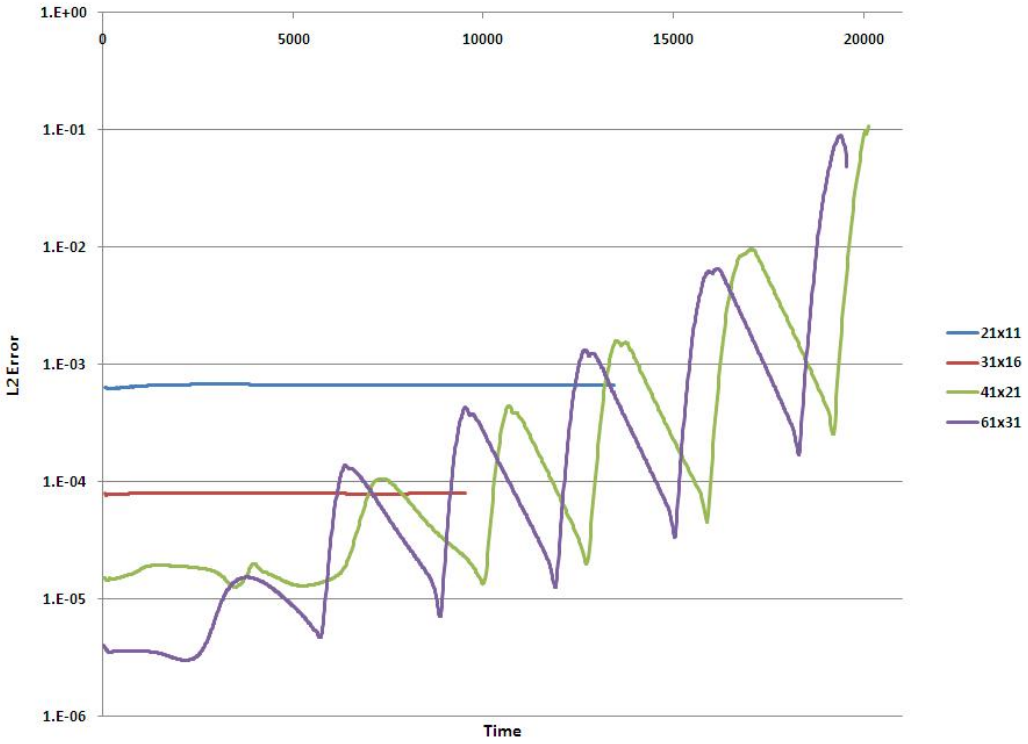

Figure 8-9: **L2 Error in Density for a Maximum Velocity of 0.70**

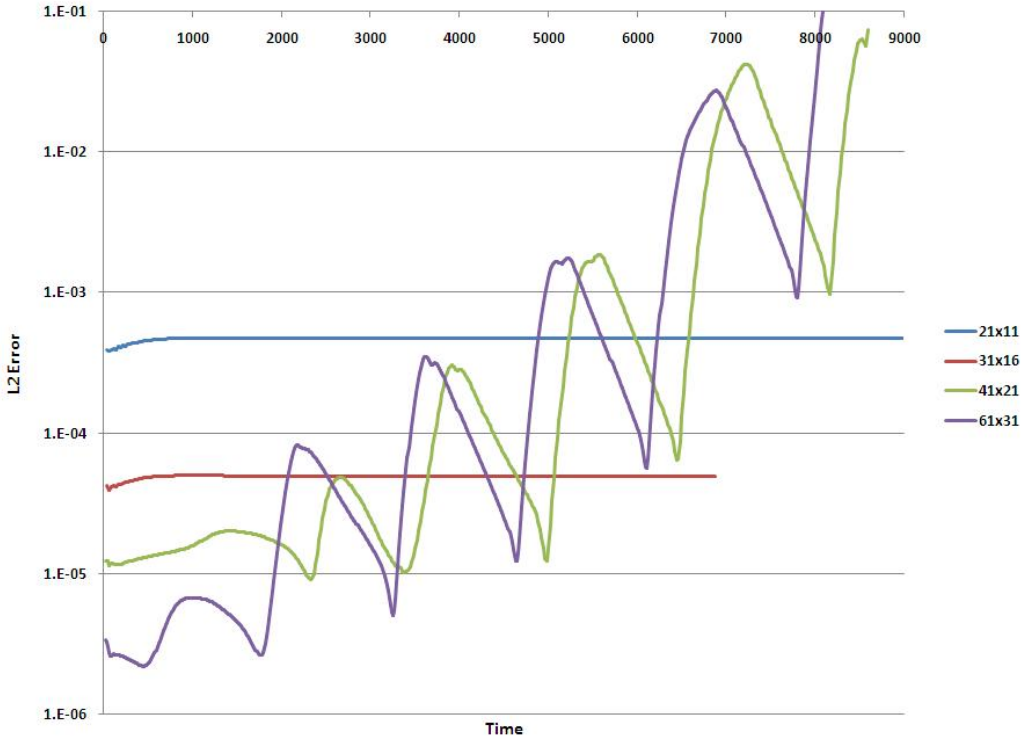

Figure 8-10: **L2 Error in Density for a Maximum Velocity of 0.80**

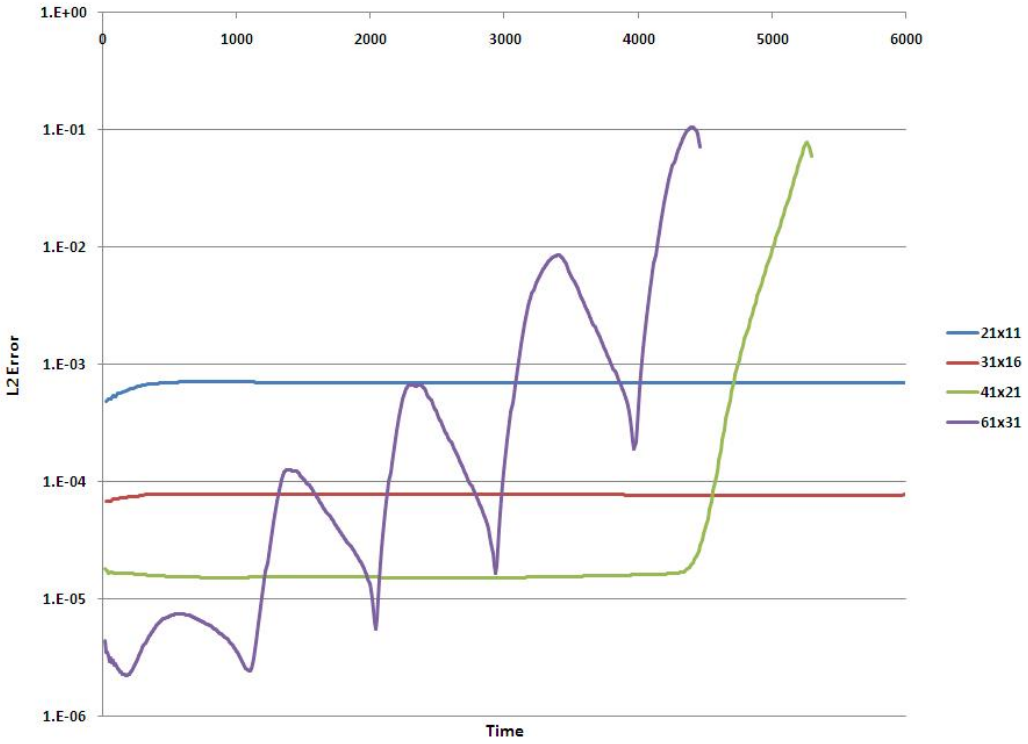

Figure 8-11: **L2 Error in Density for a Maximum Velocity of 0.95**

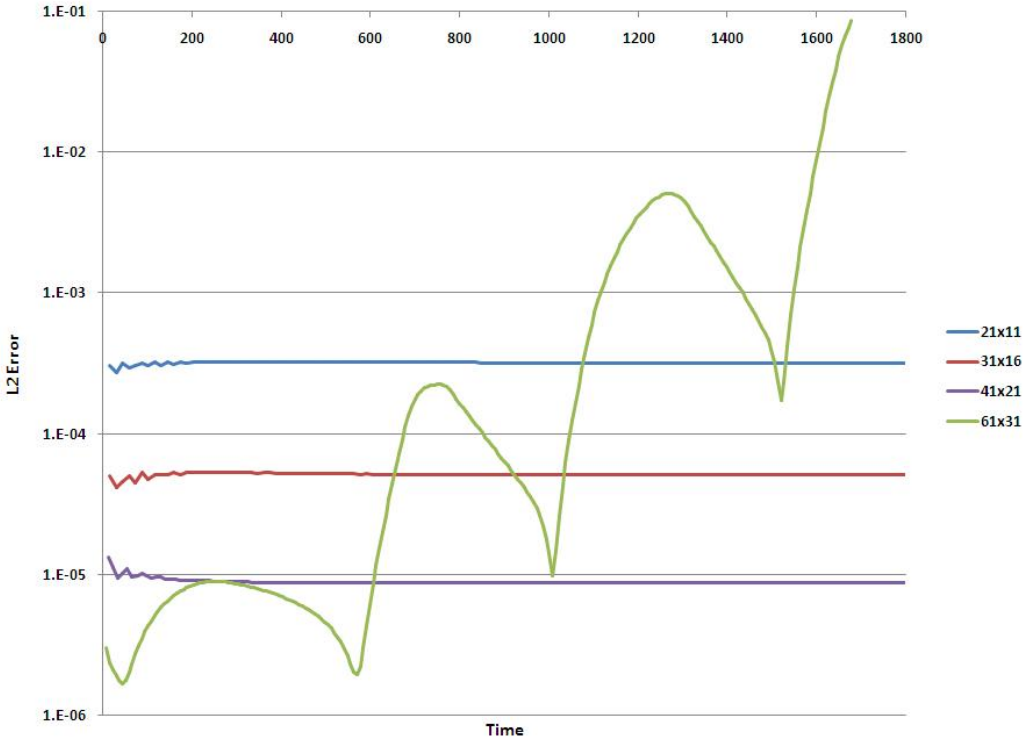

Figure 8-12: **L2 Error in Density for a Maximum Velocity of 1.05**

Table 8.1: **L2 Errors with Grid Stretching for a Maximum Velocity of 0.50**

Grid Size	Stretch Factor	rho	rhou	rhov	E
21x11	1.00	1.10E-03	5.98E-04	5.69E-03	2.13E-03
31x16	1.00	9.64E-05	3.48E-05	4.79E-05	1.83E-04
41x21	1.01	1.12E-05	1.68E-05	1.65E-05	2.11E-05
	1.02	1.19E-05	1.66E-05	1.08E-05	2.27E-05
61x31	1.05	4.10E-06	9.87E-06	8.24E-06	6.96E-06

Table 8.2: **L2 Errors with Grid Stretching for a Maximum Velocity of 0.60**

Grid Size	Stretch Factor	rho	rhou	rhov	E
21x11	1.00	2.57E-03	2.10E-03	1.32E-03	4.87E-03
31x16	1.00	2.59E-04	1.27E-04	1.35E-04	4.94E-04
41x21	1.00	4.95E-05	2.08E-05	2.01E-05	9.43E-05
61x31	1.02	8.37E-06	1.64E-05	1.77E-05	1.29E-05

Table 8.3: **L2 Errors with Grid Stretching for a Maximum Velocity of 0.70**

Grid Size	Stretch Factor	rho	rhou	rhov	E
21x11	1.00	6.74E-04	4.30E-04	7.37E-04	1.22E-03
31x16	1.00	7.86E-05	3.32E-05	4.00E-05	1.48E-04
41x21	1.01	1.63E-05	2.04E-05	1.40E-05	2.94E-05
	1.02	1.55E-05	1.63E-05	1.37E-05	2.81E-05
61x31	1.06	4.87E-06	7.86E-06	3.60E-06	8.43E-06
	1.08	4.22E-06	1.18E-05	6.45E-06	7.63E-06

Table 8.4: **L2 Errors with Grid Stretching for a Maximum Velocity of 0.80**

Grid Size	Stretch Factor	rho	rhou	rhov	E
21x11	1.00	4.73E-04	3.68E-04	4.36E-04	8.44E-04
31x16	1.00	4.78E-05	2.29E-05	3.97E-05	8.62E-05
41x21	1.01	1.20E-05	9.87E-06	1.44E-05	2.18E-05
	1.02	1.34E-05	1.37E-05	1.42E-05	2.39E-05
	1.03	1.53E-05	1.69E-05	1.42E-05	2.69E-05
61x31	1.06	6.41E-06	6.86E-06	3.67E-06	1.08E-05

Table 8.5: **L2 Errors with Grid Stretching for a Maximum Velocity of 0.95**

Grid Size	Stretch Factor	rho	rhou	rhov	E
21x11	1.00	7.01E-04	3.75E-04	3.83E-04	1.21E-03
31x16	1.00	7.75E-05	2.36E-05	3.43E-05	1.40E-04
41x21	1.01	1.46E-05	8.02E-06	9.65E-06	2.65E-05
61x31	1.05	1.32E-05	6.94E-06	3.52E-06	2.21E-05

Table 8.6: **L2 Errors with Grid Stretching for a Maximum Velocity of 1.05**

Grid Size	Stretch Factor	rho	rhou	rhov	E
21x11	1.00	3.19E-04	1.22E-04	1.66E-04	5.83E-04
31x16	1.00	5.21E-05	1.40E-05	2.31E-05	9.23E-05
41x21	1.00	8.73E-06	3.63E-06	6.69E-06	1.55E-05
	1.01	2.03E-05	7.45E-06	7.34E-06	3.46E-05
	1.02	3.75E-05	1.22E-05	9.82E-06	6.37E-05
61x31	1.06	1.00E-05	5.79E-06	3.65E-06	1.73E-05

8.3 Errors on Inflow and Outflow Boundaries

Figs. (8-13) - (8-24) show the plots of L2 errors of density on the inflow and outflow boundaries of the Ringleb flow test cases. For all the mach numbers tested, it can be seen that as the number of grid points is increased, the L2 error on the inflow and outflow boundaries decreased. However, the errors are higher for a higher grid stretching factor. In most cases, the errors at the wall corners are higher than the errors at the interior nodes.

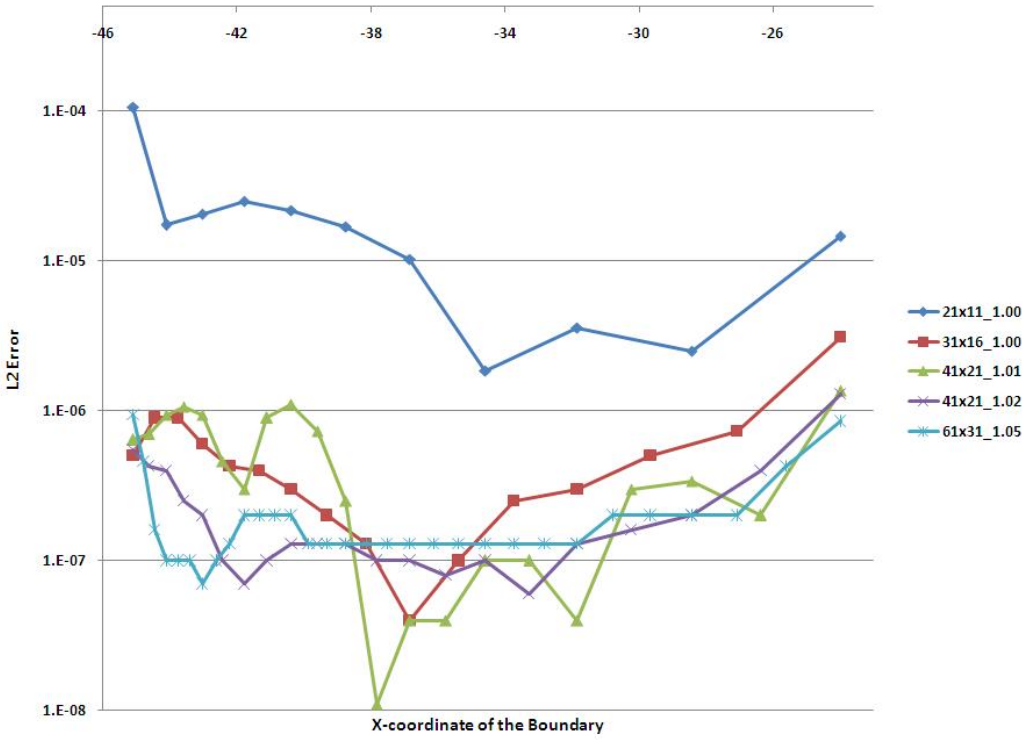

Figure 8-13: **Inflow Boundary L2 Error in Density for a Maximum Velocity of 0.50**

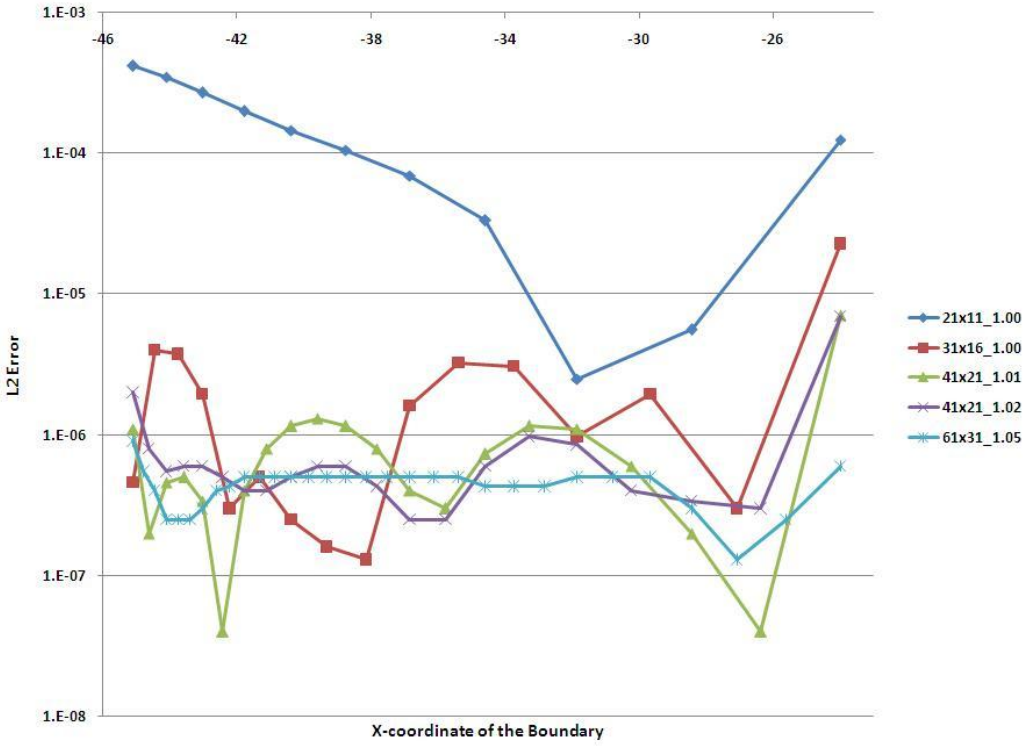

Figure 8-14: **Outflow Boundary L2 Error in Density for a Maximum Velocity of 0.50**

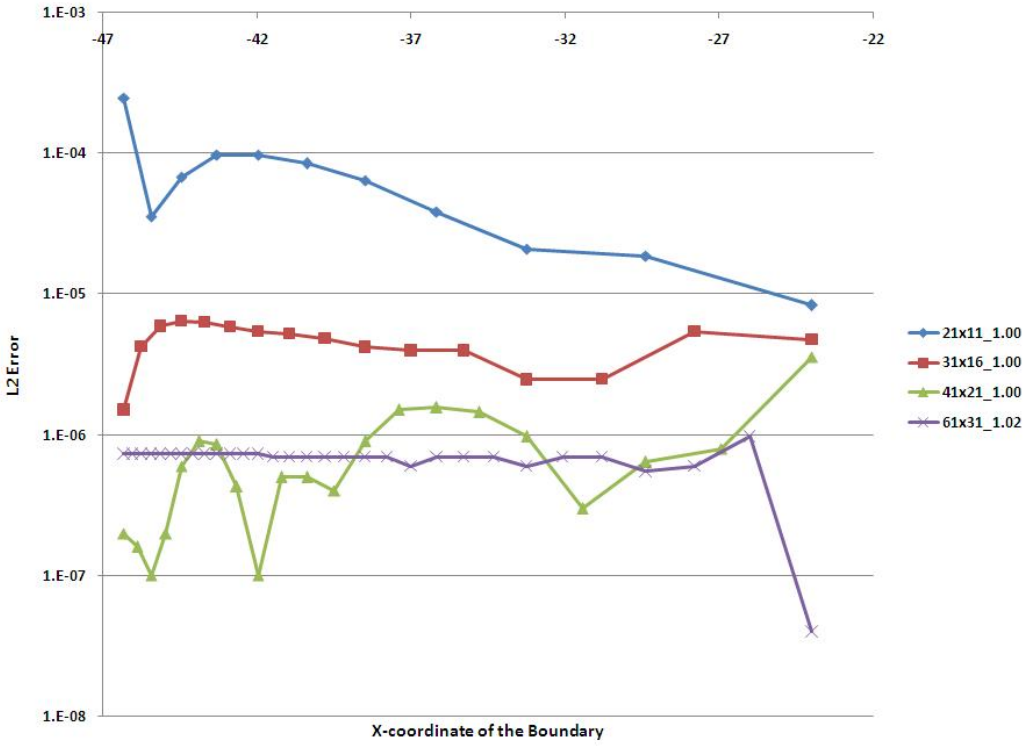

Figure 8-15: **Inflow Boundary L2 Error in Density for a Maximum Velocity of 0.60**

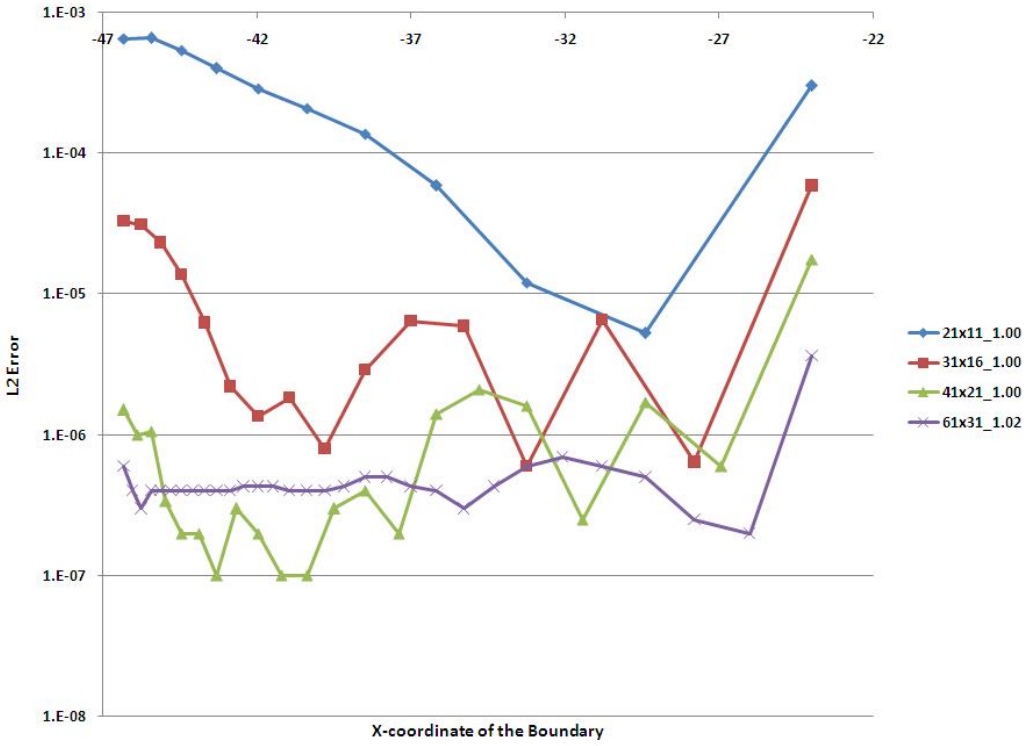

Figure 8-16: **Outflow Boundary L2 Error in Density for a Maximum Velocity of 0.60**

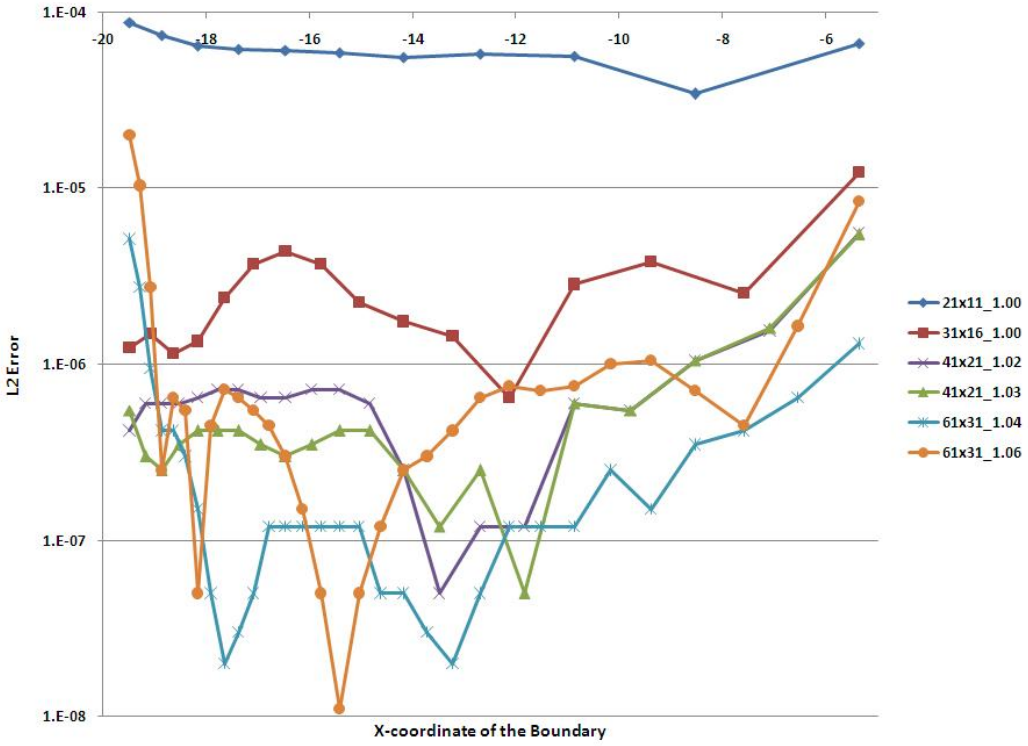

Figure 8-17: **Inflow Boundary L2 Error in Density for a Maximum Velocity of 0.70**

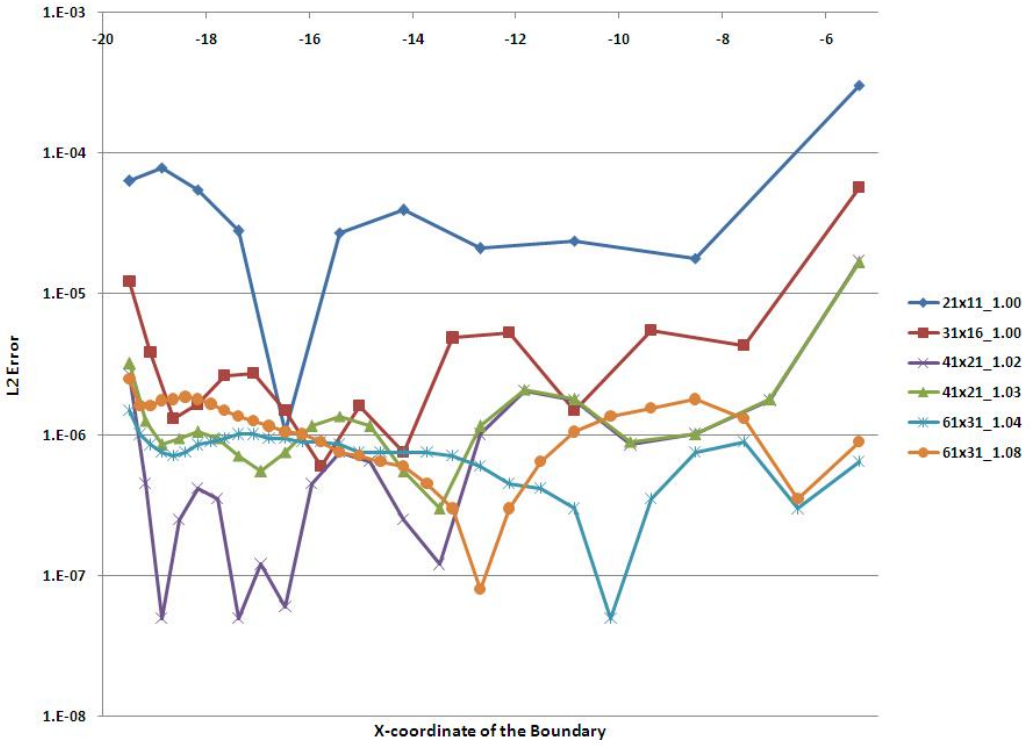

Figure 8-18: **Outflow Boundary L2 Error in Density for a Maximum Velocity of 0.70**

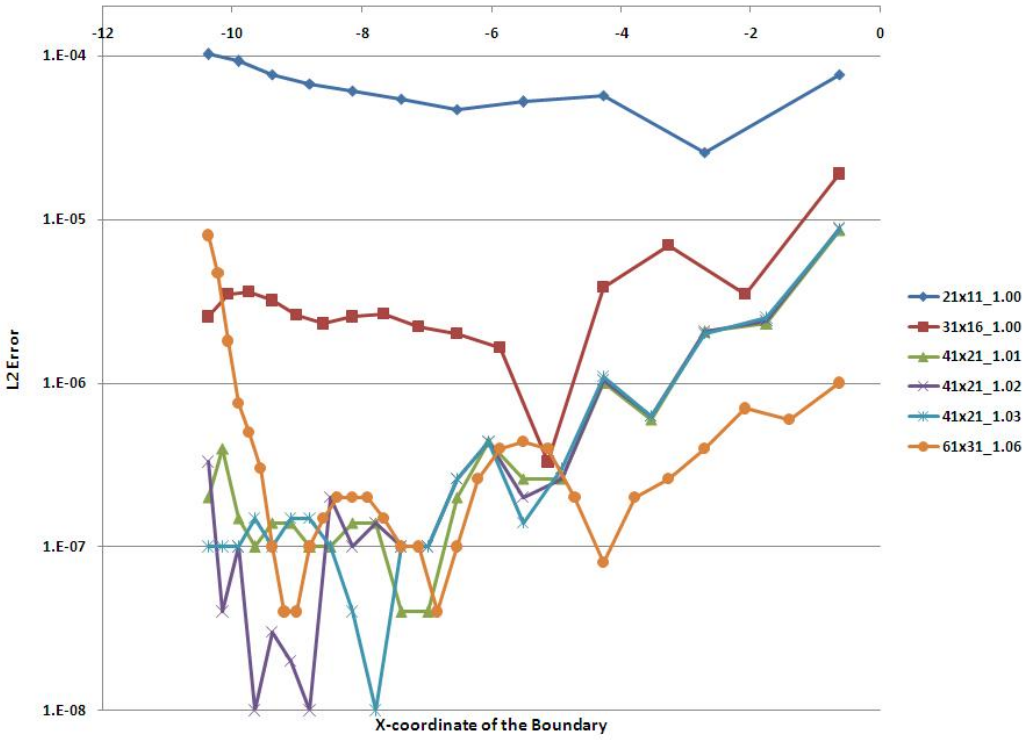

Figure 8-19: **Inflow Boundary L2 Error in Density for a Maximum Velocity of 0.80**

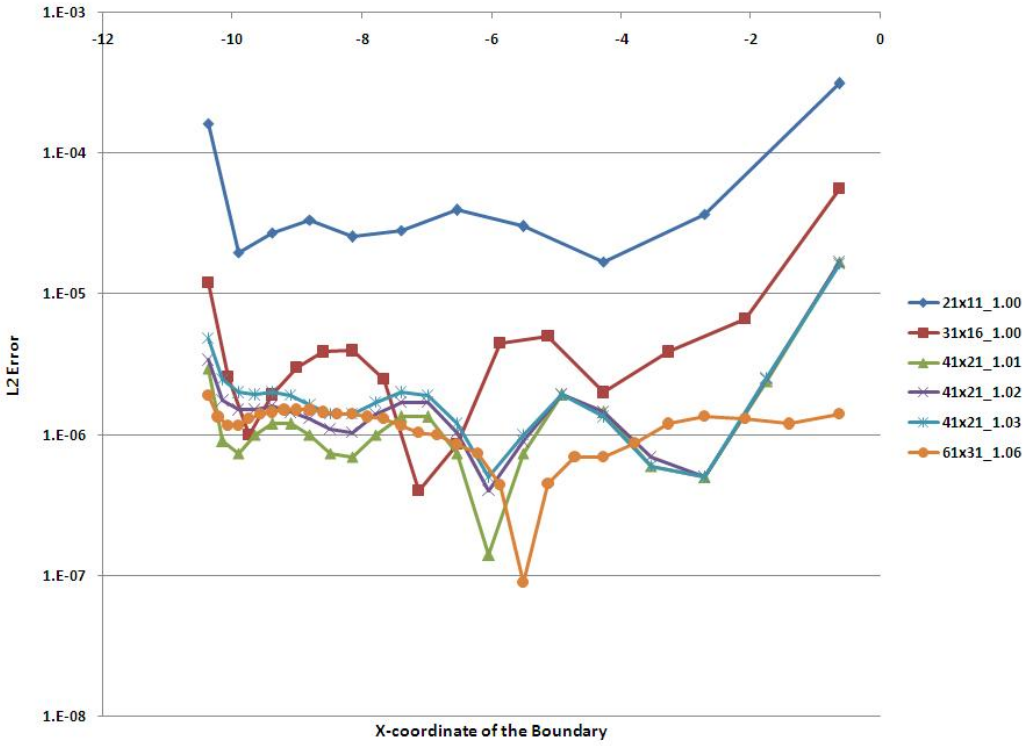

Figure 8-20: **Outflow Boundary L2 Error in Density for a Maximum Velocity of 0.80**

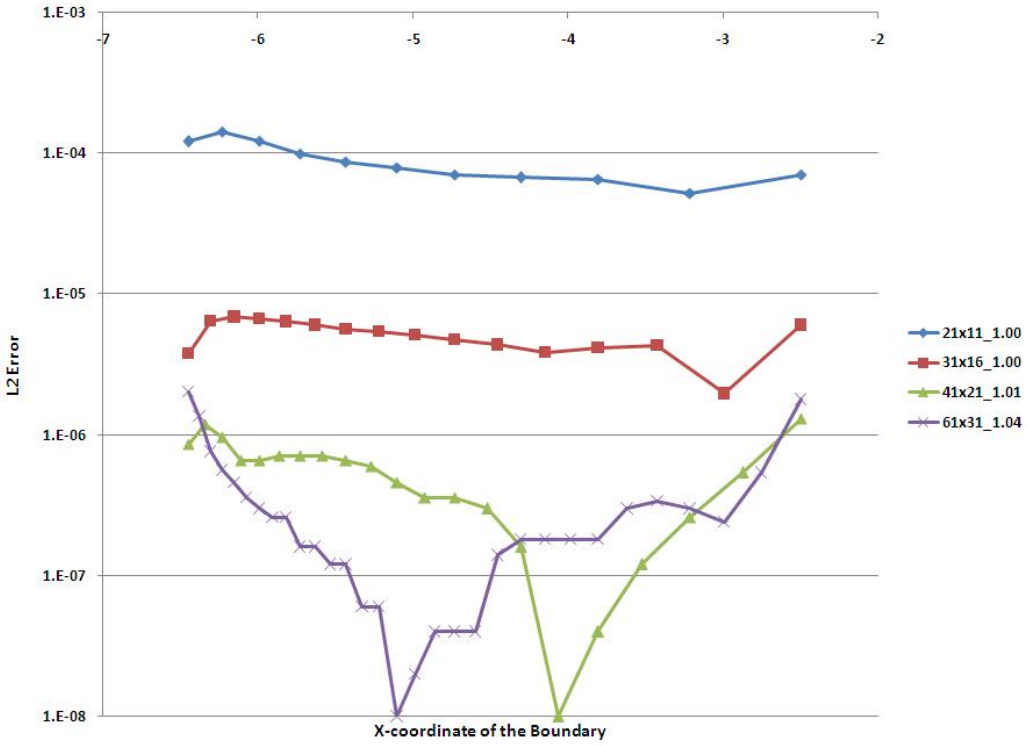

Figure 8-21: **Inflow Boundary L2 Error in Density for a Maximum Velocity of 0.95**

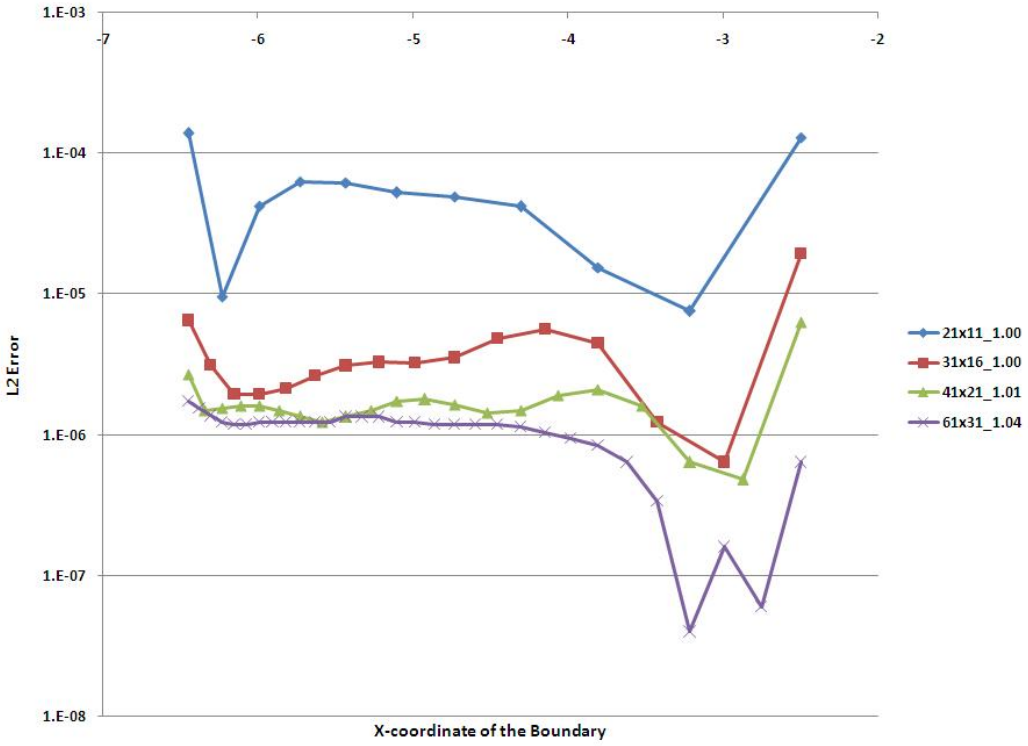

Figure 8-22: **Outflow Boundary L2 Error in Density for a Maximum Velocity of 0.95**

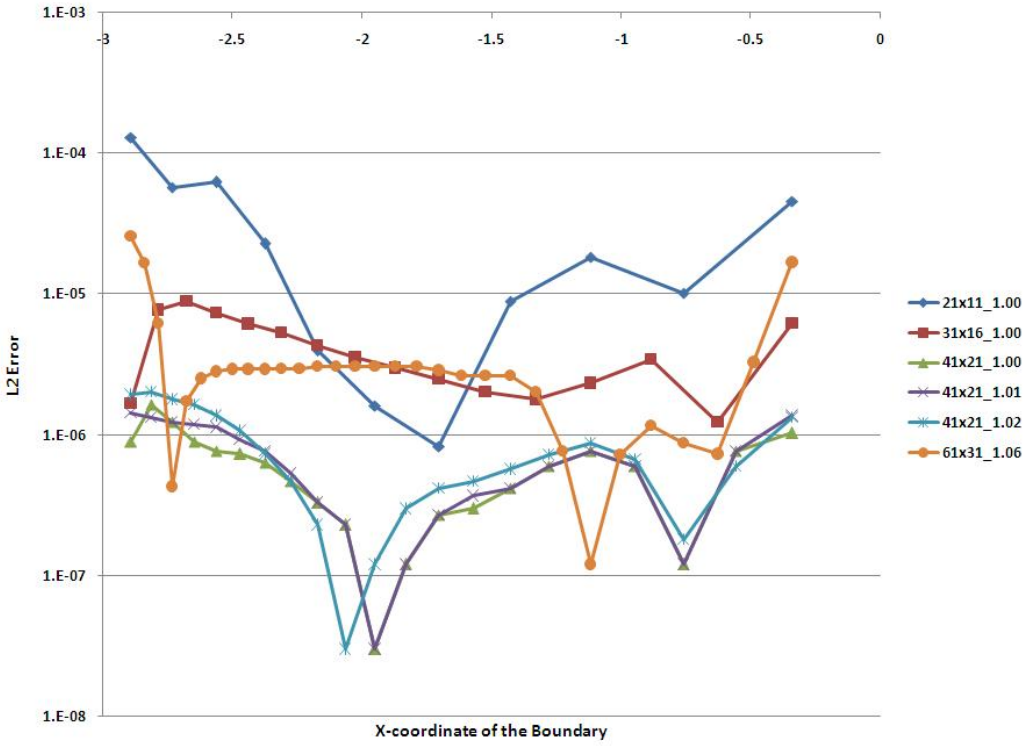

Figure 8-23: **Inflow Boundary L2 Error in Density for a Maximum Velocity of 1.05**

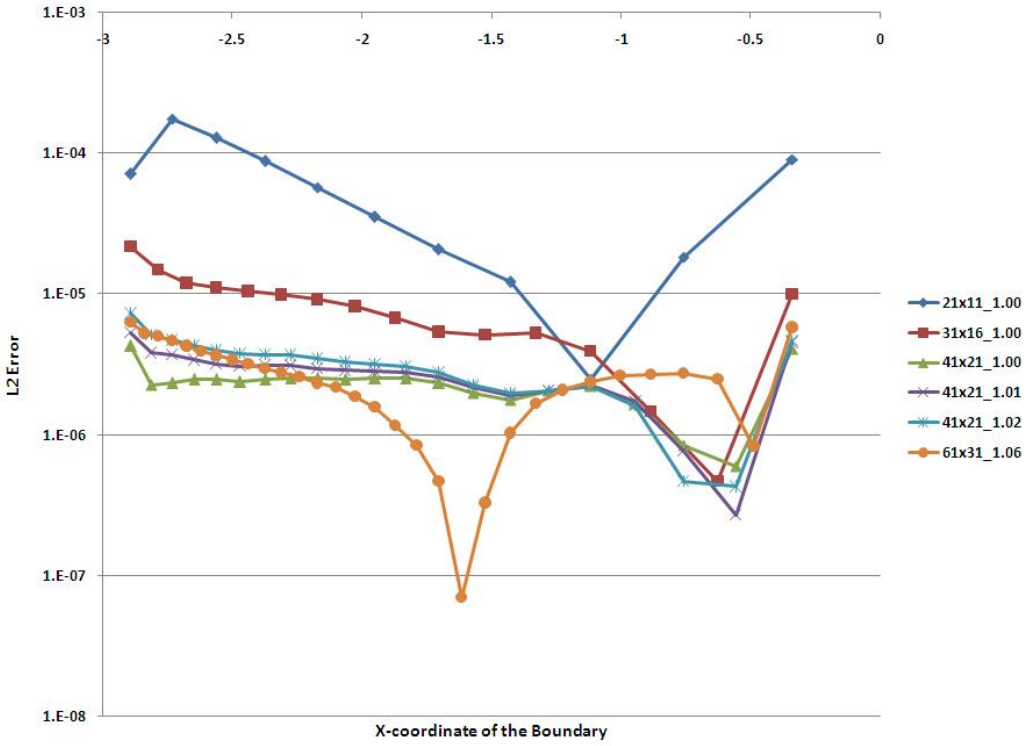

Figure 8-24: **Outflow Boundary L2 Error in Density for a Maximum Velocity of 1.05**

8.4 Errors on Inside and Outside Wall Boundaries

The L2-norm errors of density on the inside and outside walls for all the test cases have been plotted in Figs. (8-25) - (8-36). The x-coordinate of the plots runs from the inflow-wall corner to the outflow-wall corner. It is seen that the errors on the outside wall are lower than the errors on the inside wall. For the test case with maximum velocity of 0.50, it can be seen that the errors on the walls for the 41x21 grid and the 61x31 grid are similar. This is because the advantage of increase in grid points is offset by a large stretch factor. A similar trend in the L2 error is observed for cases with a maximum velocity of 0.60, 0.95, and 1.05.

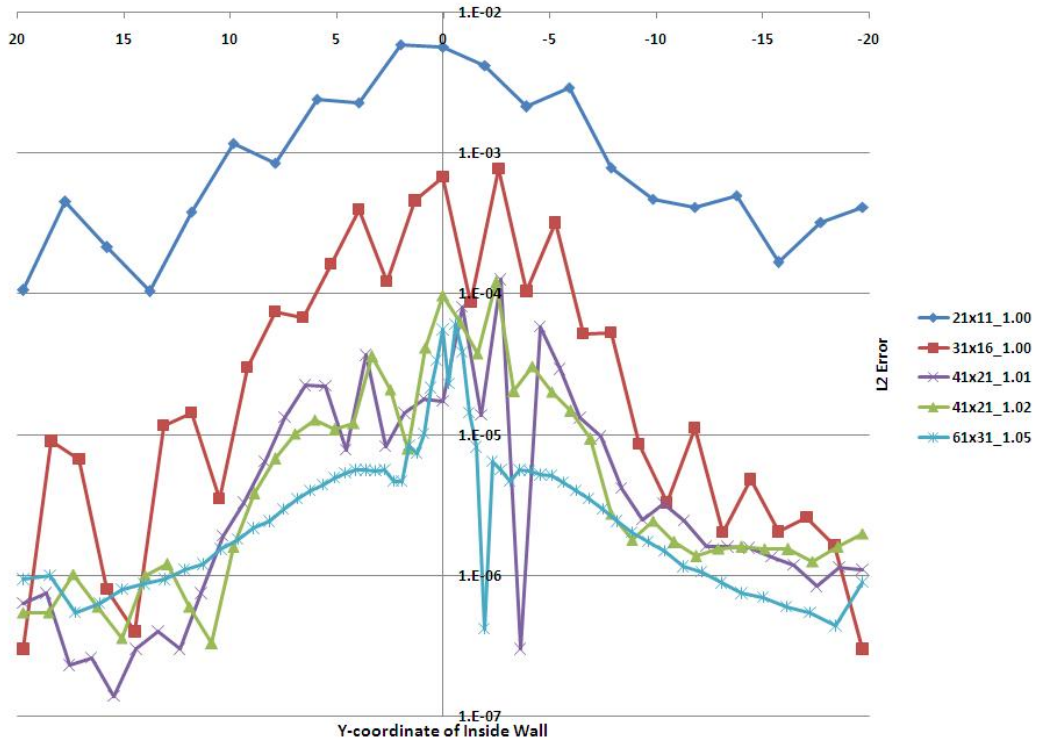

Figure 8-25: **Inside Wall L2 Error in Density for a Maximum Velocity of 0.50**

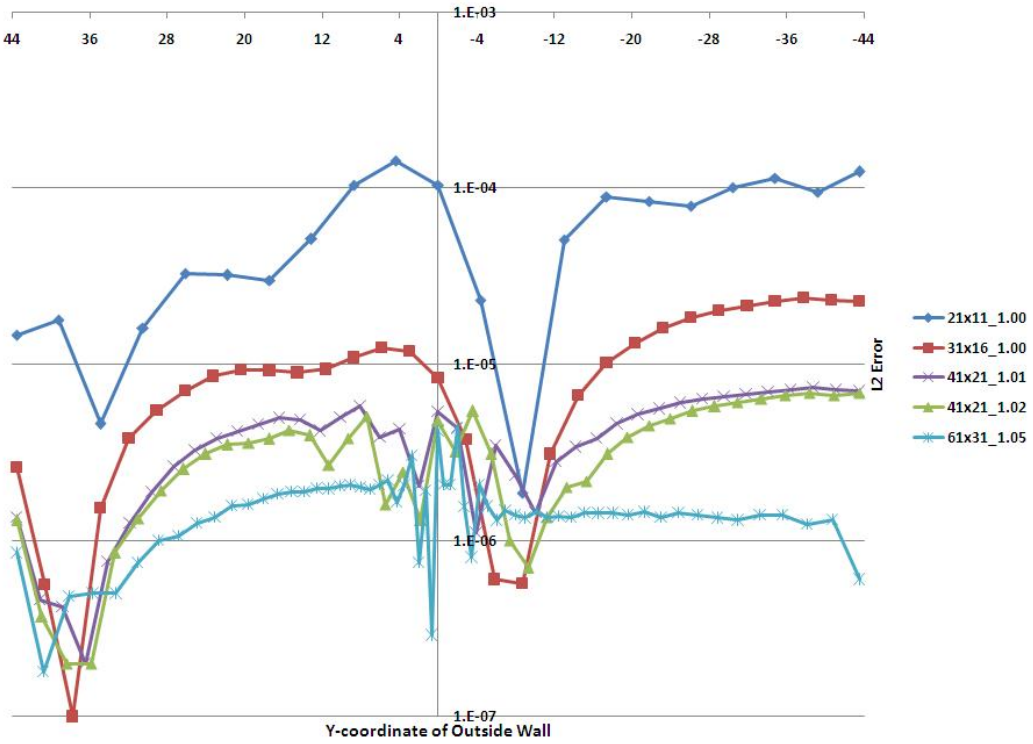

Figure 8-26: **Outside Wall L2 Error in Density for a Maximum Velocity of 0.50**

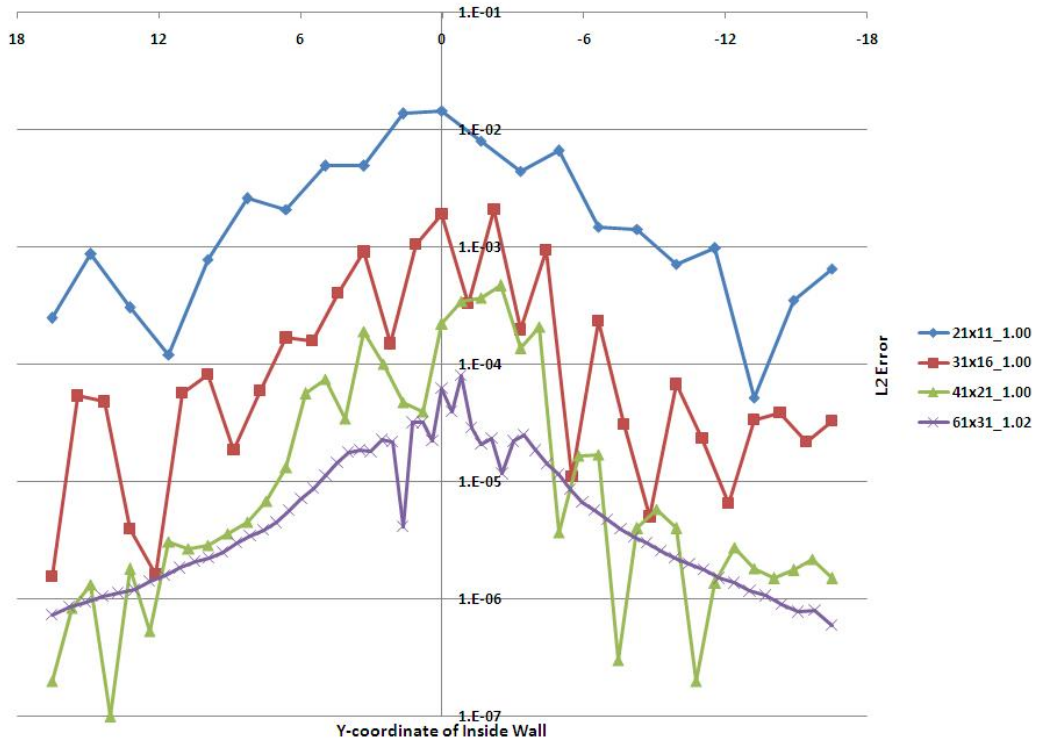

Figure 8-27: **Inside Wall L2 Error in Density for a Maximum Velocity of 0.60**

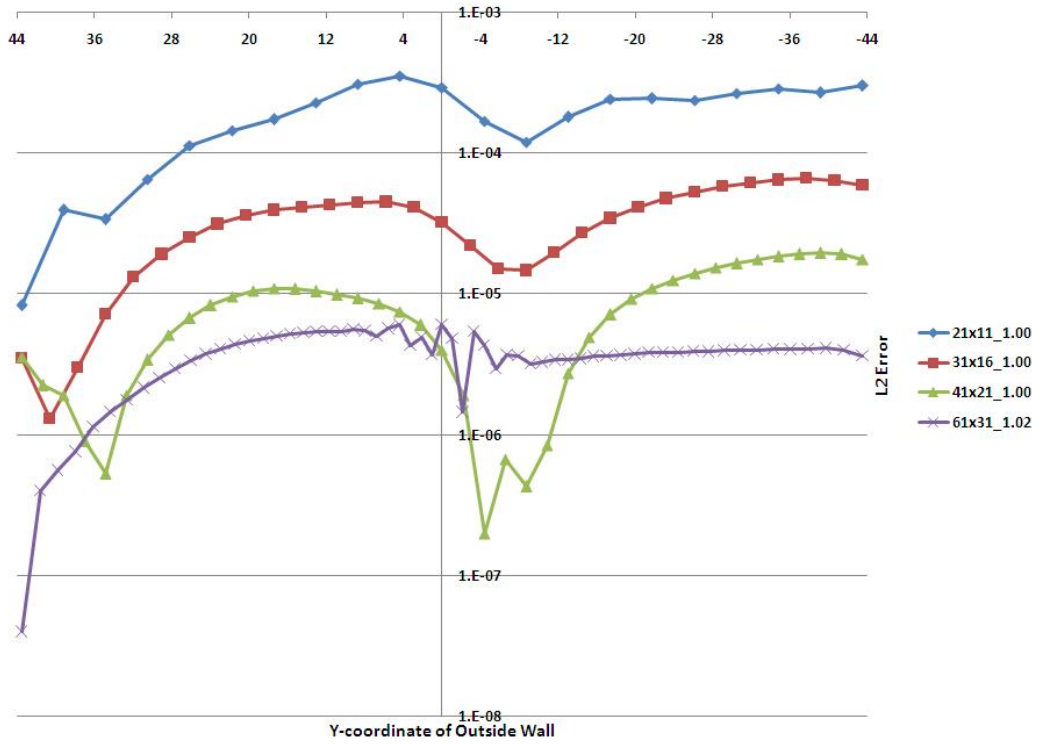

Figure 8-28: **Outside Wall L2 Error in Density for a Maximum Velocity of 0.60**

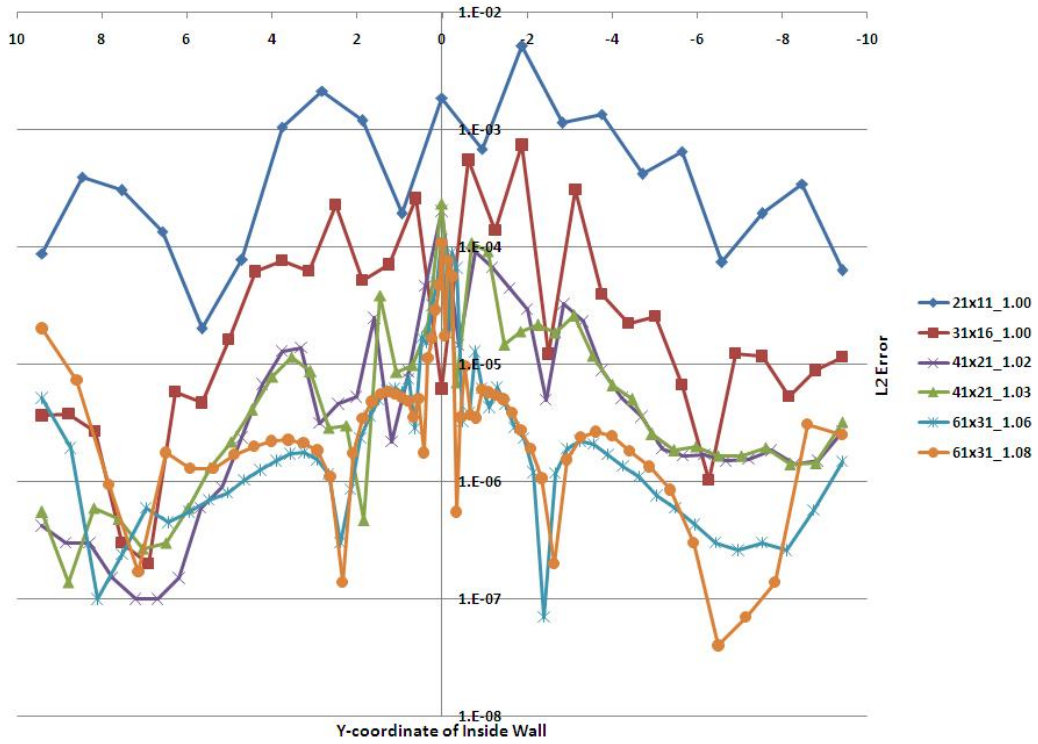

Figure 8-29: **Inside Wall L2 Error in Density for a Maximum Velocity of 0.70**

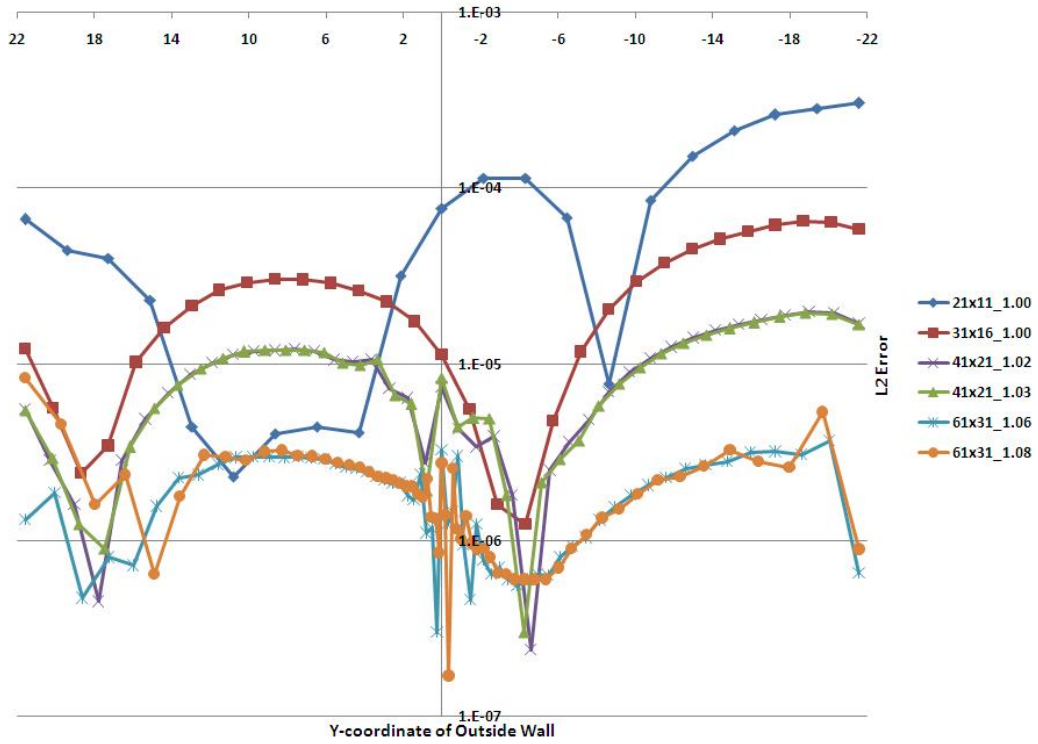

Figure 8-30: **Outside Wall L2 Error in Density for a Maximum Velocity of 0.70**

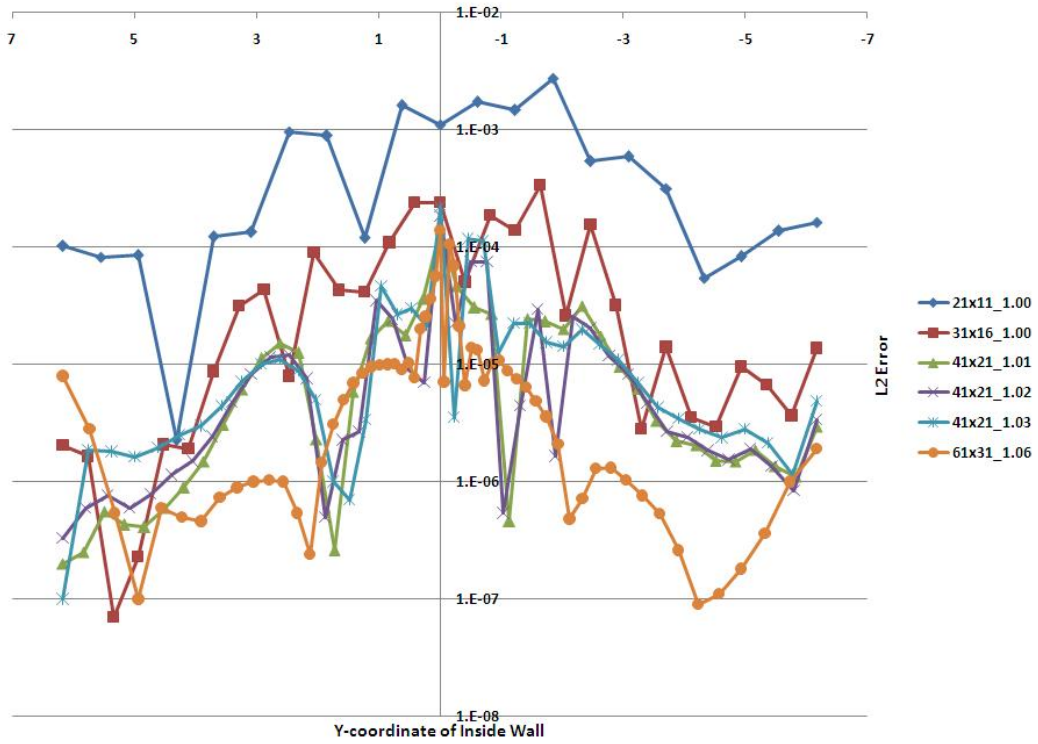

Figure 8-31: **Inside Wall L2 Error in Density for a Maximum Velocity of 0.80**

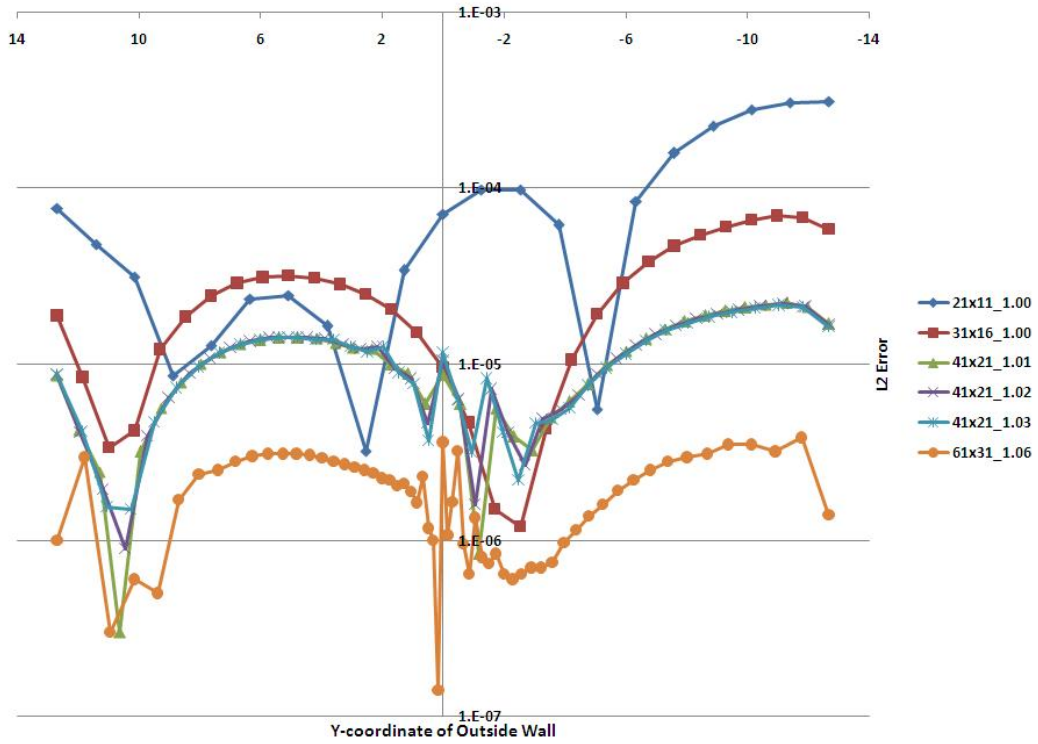

Figure 8-32: **Outside Wall L2 Error in Density for a Maximum Velocity of 0.80**

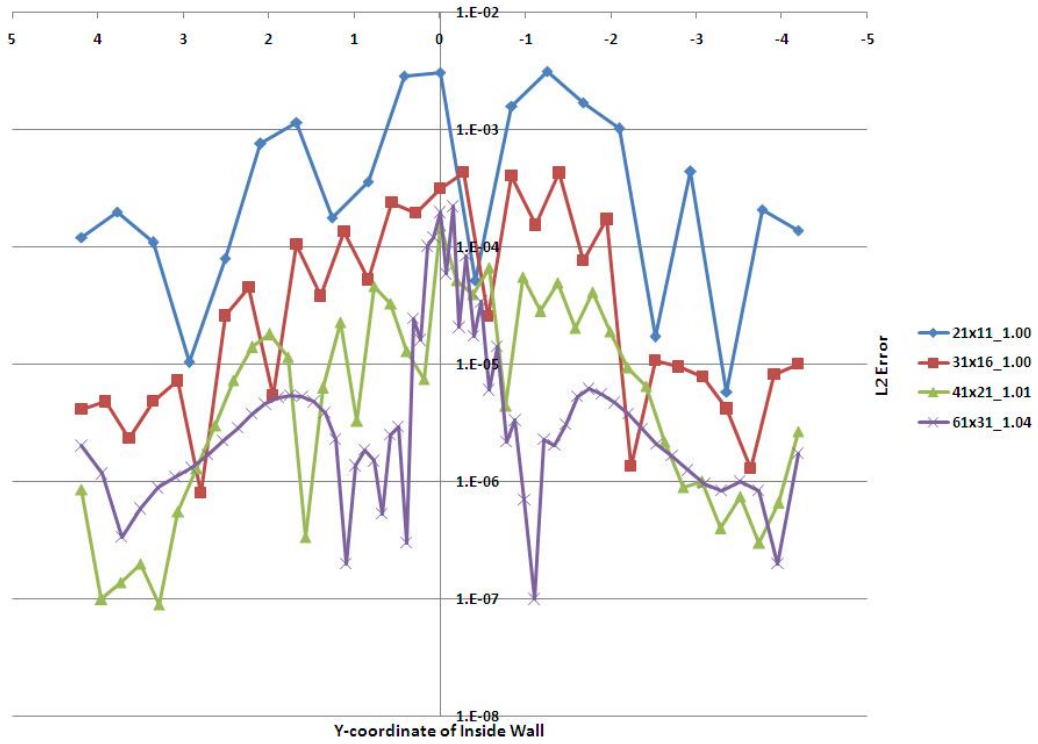

Figure 8-33: **Inside Wall L2 Error in Density for a Maximum Velocity of 0.95**

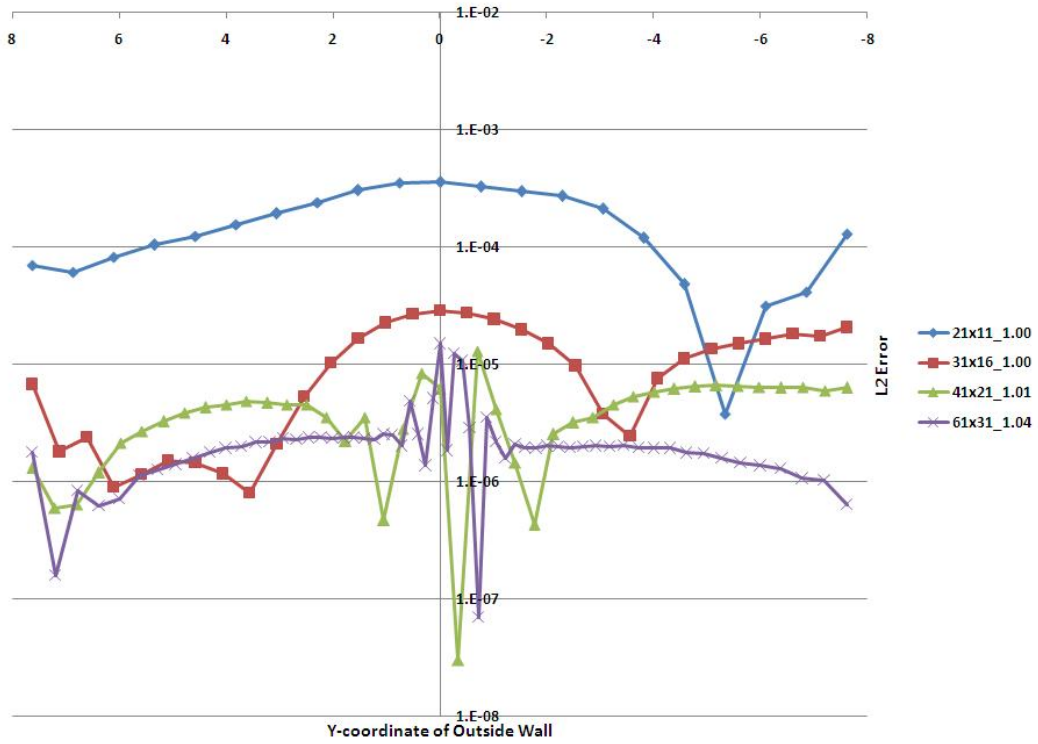

Figure 8-34: **Outside Wall L2 Error in Density for a Maximum Velocity of 0.95**

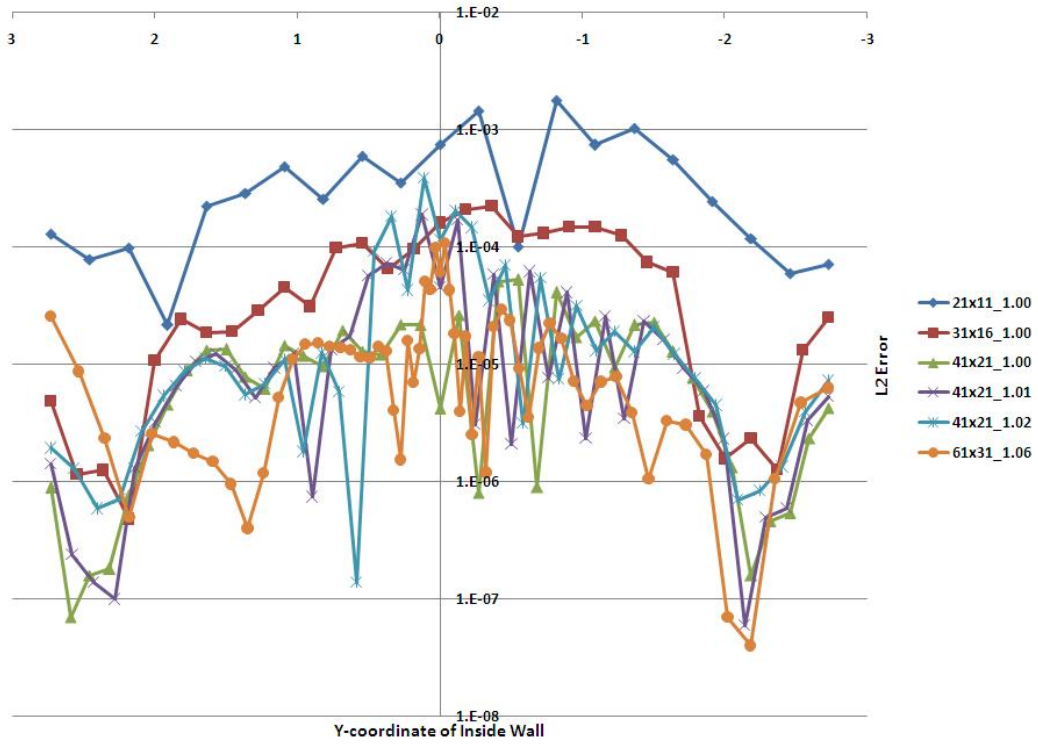

Figure 8-35: **Inside Wall L2 Error in Density for a Maximum Velocity of 1.05**

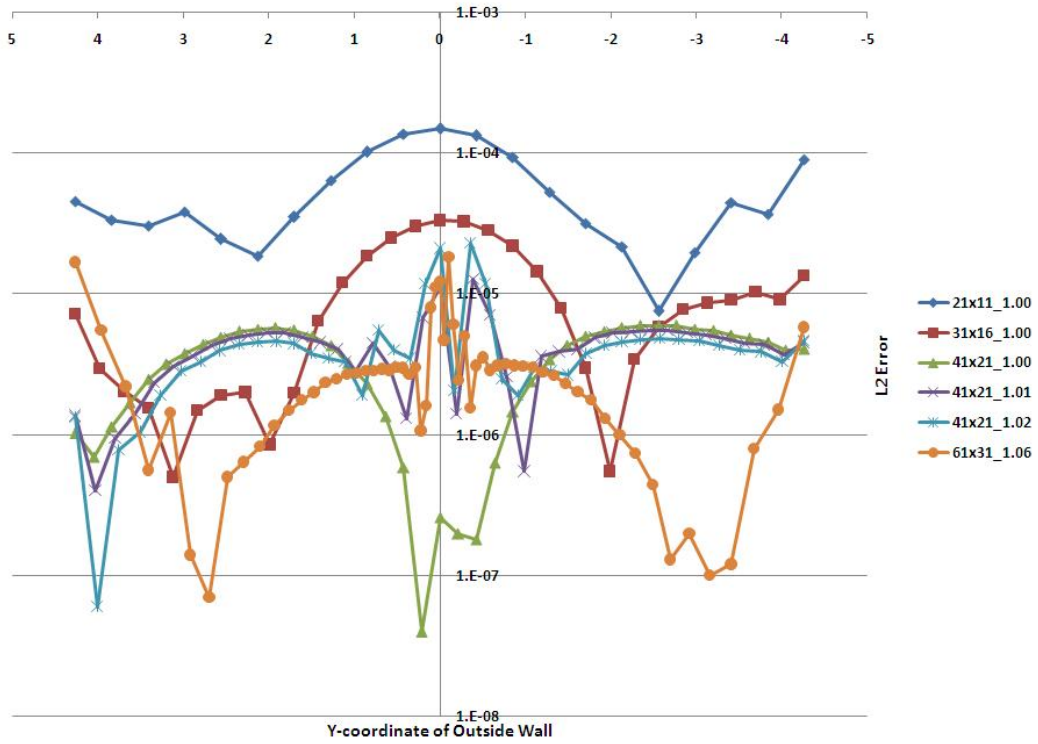

Figure 8-36: **Outside Wall L2 Error in Density for a Maximum Velocity of 1.05**

Chapter 9

Conclusions and Future Work

9.1 Conclusions

In the present work, the Giles non-reflecting boundary conditions have been extended to Curvilinear co-ordinates for wall-bounded flows, with non-orthogonal grids and curved boundary geometries. In addition to the non-reflecting boundary conditions, wall boundary conditions have been derived and implemented for inflow/outflow-wall corners. The wall corner conditions were sufficient to eliminate the flow through wall at inflow and outflow corners of the Ringleb flow test cases. However, Cartesian Giles boundary conditions with the wall corner conditions could not solve the corner problem and eventually caused the flow solution to diverge. Two-dimensional Curvilinear Giles boundary conditions were derived from the Curvilinear form of the linearized Euler equations using a similar approach to that of the Cartesian Giles boundary conditions. Additional terms that were not present in the chain rule form of Cartesian Giles boundary conditions were present in the Curvilinear bound-

ary conditions. These additional terms all contained the factor $(\xi_x\eta_x + \xi_y\eta_y)$ which becomes zero for an orthogonal grid. The Curvilinear boundary conditions, when implemented without the additional terms, displayed the same corner problem that was encountered with the chain rule form of Cartesian Giles boundary conditions, proving the significance of the additional orthogonal terms. In order to completely eliminate flow through the wall and obtain the correct solution at the corners, the Curvilinear boundary conditions with the additional terms and the wall conditions were required.

The Curvilinear Giles boundary conditions along with the wall conditions were successfully tested on various Ringleb flow geometries. However, a long-term instability was noticed for all the Ringleb flow cases beyond certain grid density. This was eliminated by stretching the grid towards the inflow and outflow boundaries. Converged solutions were obtained for all the test cases with acceptable L2 errors.

9.2 Recommendations for Future Work

The significance of the Curvilinear form of the Giles non-reflecting boundary conditions in solving problems with non-orthogonal grids and non-planar boundaries was shown through this effort. A three-dimensional Curvilinear extension to the Giles boundary conditions is currently being developed. The present work provides a guideline for developing compatibility conditions at interfaces of different kinds of boundaries. Following a similar approach, compatibility conditions could be developed for other types of boundary corners such as a Giles-Giles interface or an inflow/outflow interface. The issue of long-term instability observed with denser grids could further be investigated by quantifying the frequency of the instability and identifying its dependence on various flow, geometry, and grid parameters. The effect of various spatial discretization schemes on the long-term instability is of interest.

Appendix A

Ringleb Flow Contours

Flow contours of the analytical solution of a Ringleb flow domain with kmax = 0.80, kmin = 0.30, and $\overline{q} = 0.20$, on a 61x31 grid are provided here.

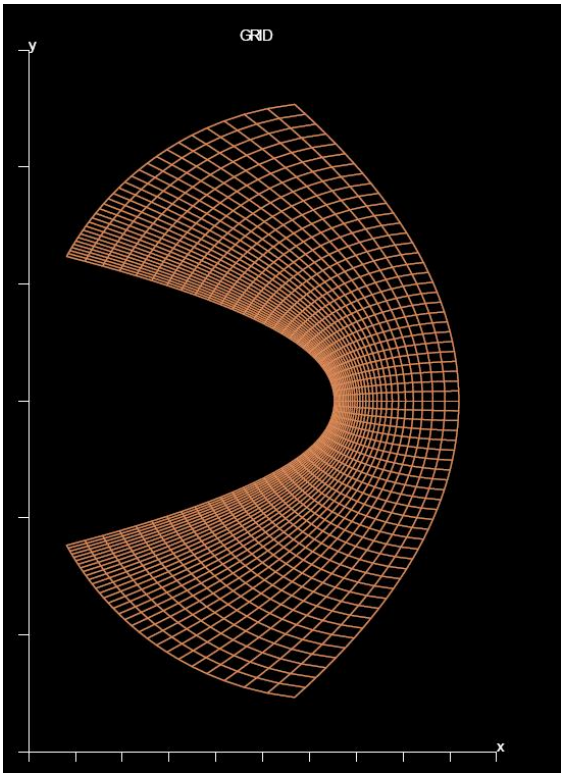

Figure A-1: **61x31 Grid for a Maximum Velocity = 0.80**

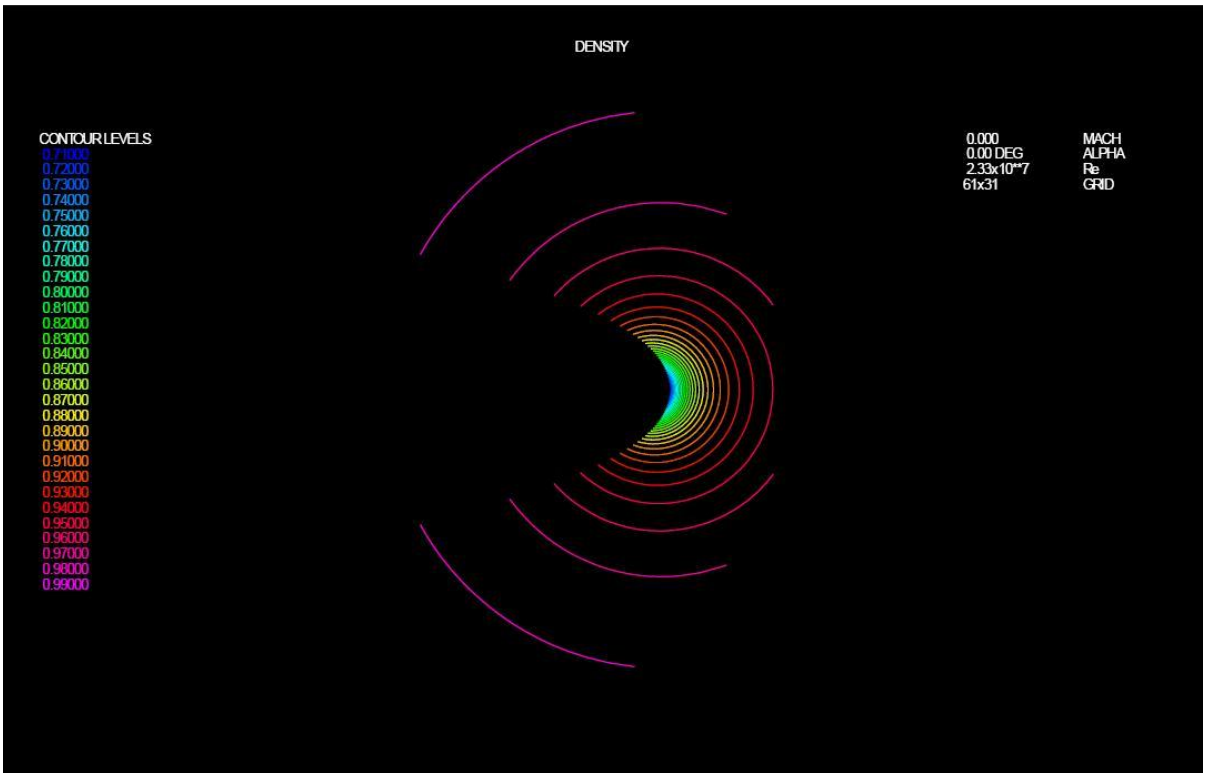

Figure A-2: **Density Contours for a Maximum Velocity = 0.80**

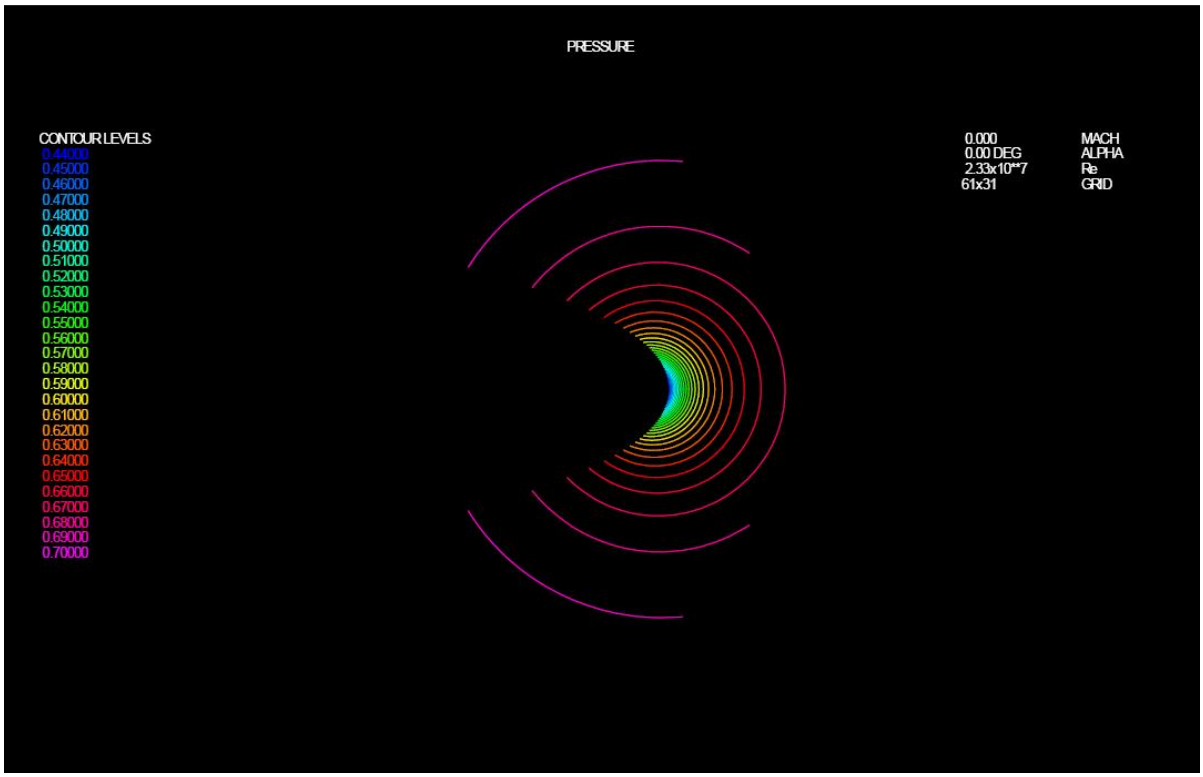

Figure A-3: **Pressure Contours for a Maximum Velocity = 0.80**

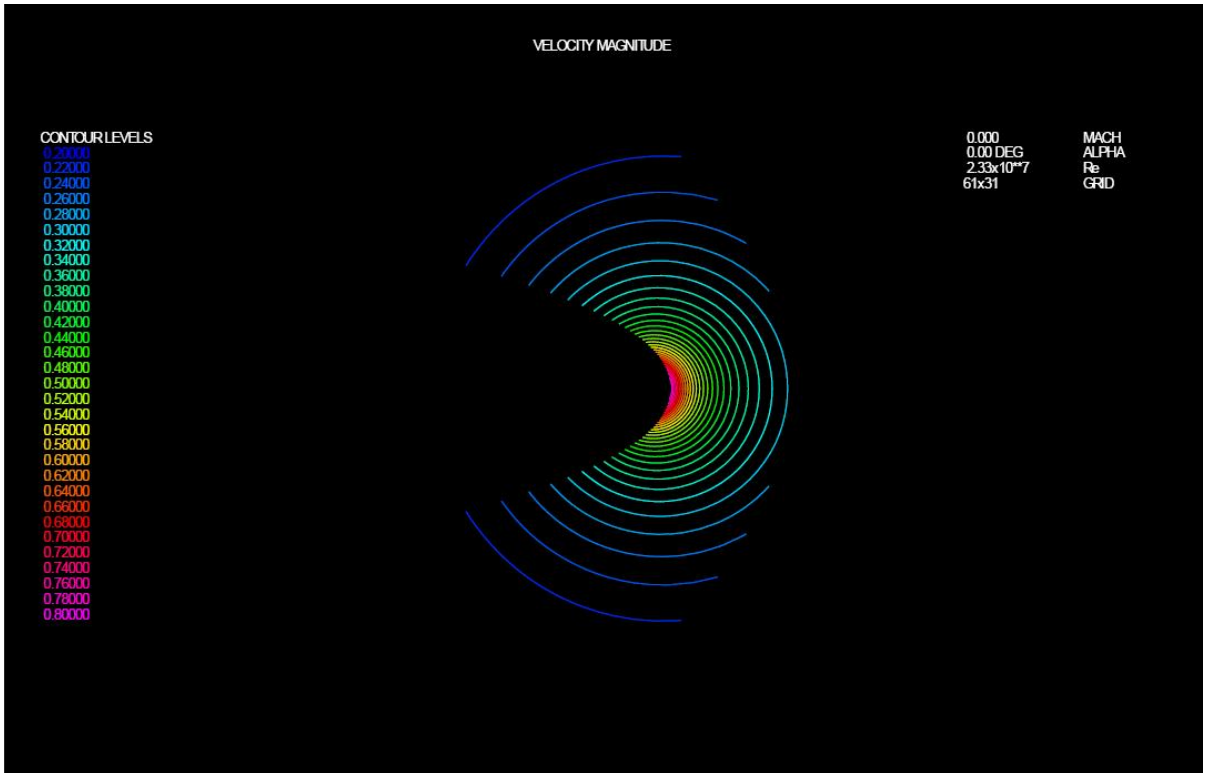

Figure A-4: **Velocity Contours for a Maximum Velocity = 0.80**

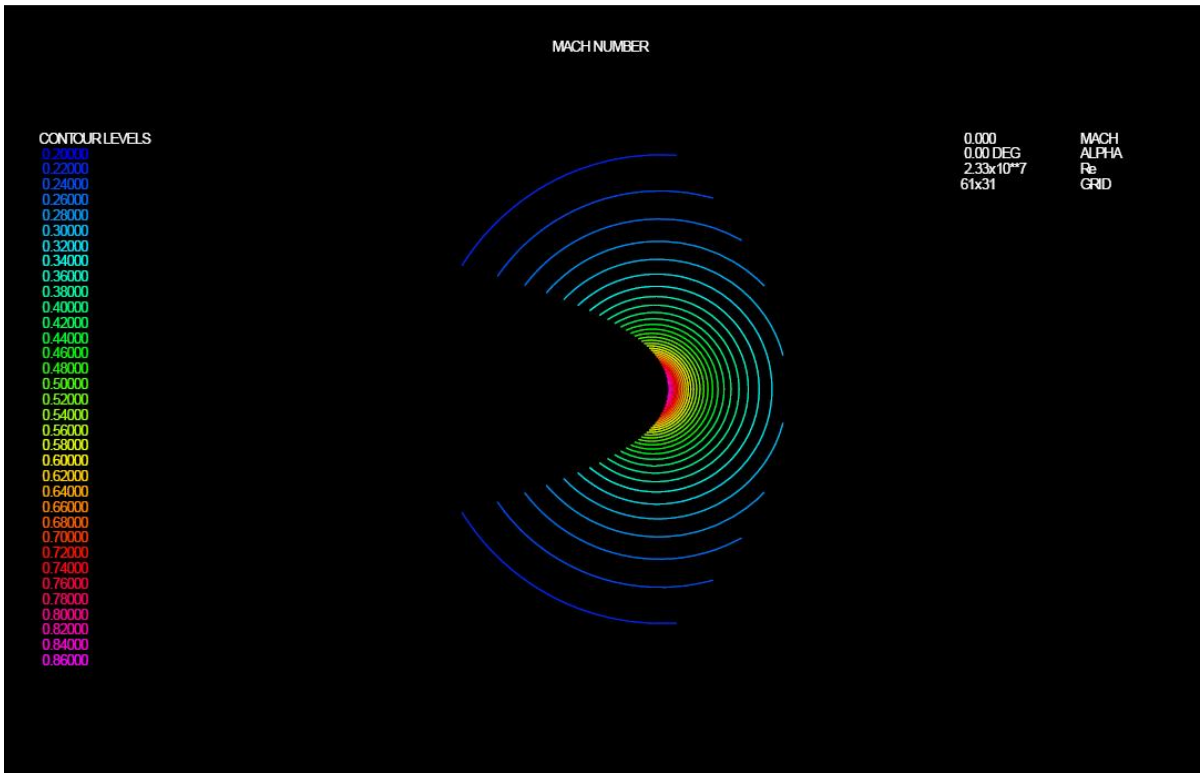

Figure A-5: **Mach number Contours for a Maximum Velocity = 0.80**

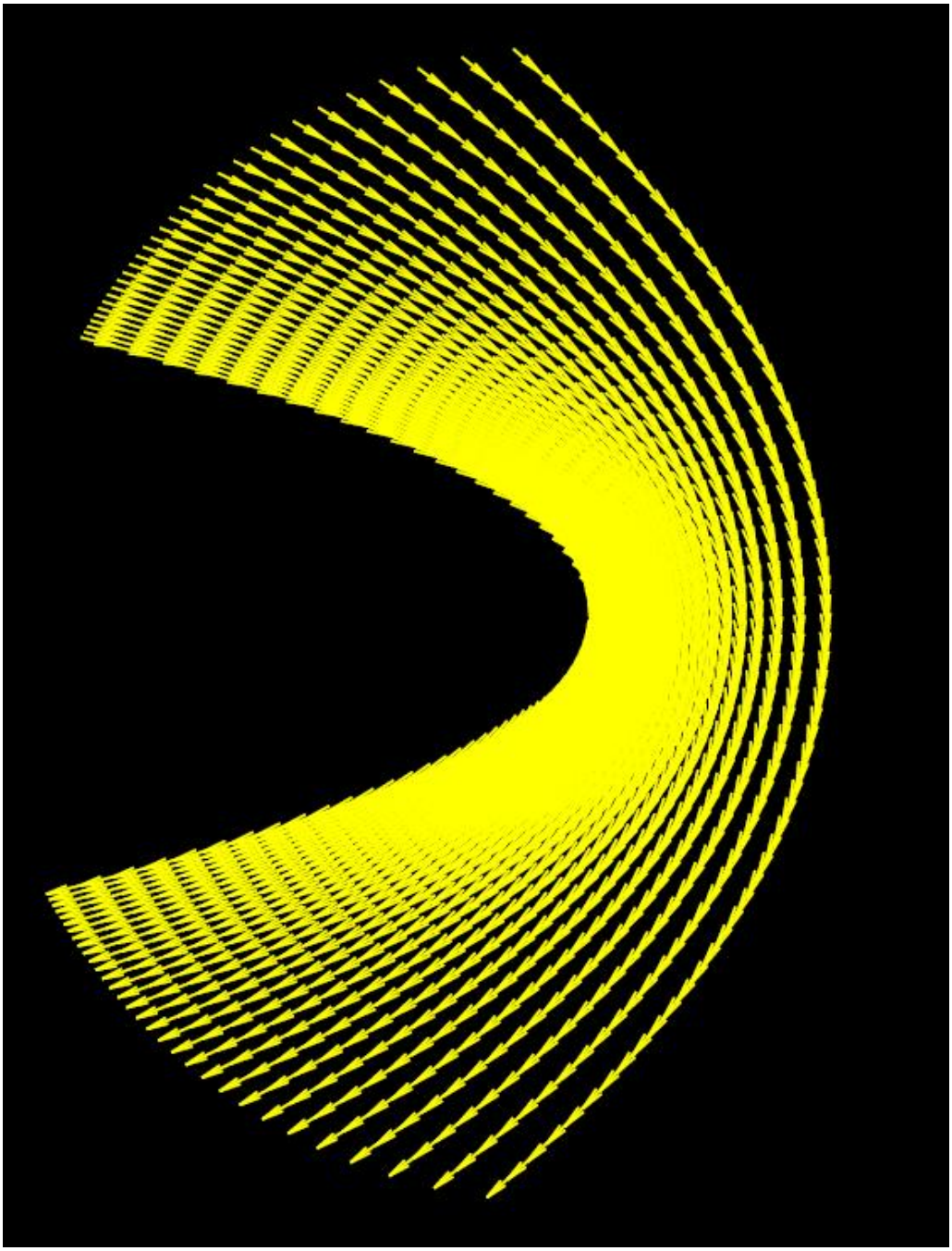

Figure A-6: **Velocity Vectors for a Maximum Velocity = 0.80**

Bibliography

[1] Kevin W. Thompson, Time Dependent Boundary Conditions for Hyperbolic Systems. *Journal of Computational Physics*, 68:1-24, 1986.

[2] Kevin W. Thompson, Time-Dependent Boundary Conditions for Hyperbolic Systems, II. *Journal of Computational Physics*, 89:439-461, 1990.

[3] H.-O. Kreiss, Initial Boundary Value Problems for Hyperbolic Systems. *Communications on Pure and Applied Mathematics*, 23:277-298, 1970.

[4] Initial-Boundary Value Problems for Linear Hyperbolic Systems. *SIAM Review*, 28:177-217, 1986.

[5] Dan Givoli, Non-reflecting Boundary Conditions. *Journal of Computational Physics*, 94:1-29, 1991.

[6] Hagstrom T., Radiation Boundary Conditions for the Numerical Simulation of Waves. *Acta Numerica*, 8:47106, 1999.

[7] Tam, C. K. W., Computational Aeroacoustics: Issues and Methods. *AIAA Journal*, 33:17881796, 1995.

[8] Tam, C. K. W., Advances in Numerical Boundary Conditions for Computational Aeroacoustics. *Journal of Computational Acoustics*, 6:377402, 1998.

[9] Sanjiva K. Lele, Computational aeroacoustics: A review. *AIAA-1997-18, Aerospace Sciences Meeting and Exhibit, 35th, Reno, NV, Jan 609, 1997*

[10] Semyon V. Tsynkov, Numerical Solution of Problems on Unbounded Domains: A Review. *Applied Numerical Mathematics*, 27:465532, 1998.

[11] Tim Colonius, Modeling Artifical Boundary Conditions for Compressible Flow. *Annu. Rev. Fluid Mech.*, 36:315-345, 2004.

[12] Ray Hixon, Radiation and Wall Boundary Conditions for Computational Aeroacoustics: A Review. *International Journal of Computational Fluid Dynamics*, 18(6):523-531, Aug 2004

[13] Mirela Caraeni, Laszlo Fuchs, Investigation of Nonreflective Boundary Conditions for Computational Aeroacoustics. *AIAA Journal*, 44(9):1932-1940, 2006.

[14] Bayliss, A. and Turkel, E., Radiation Boundary Conditions for Wave-like Equations. *Communications on Pure and Applied Mathematics*, 33:707725, 1980.

[15] Bayliss, A. and Turkel, E., Far Field Coundary Conditions for Compressible Flows. Journal of Computational Physics, 48:182199, 1982.

[16] Bayliss, A. and Turkel, E., Outflow Boundary Conditions for Fluid Dynamics. *SIAM Journal on Scientific and Statistical Computing*, 3:250259, 1982.

[17] Higdon, R.L., Absorbing Boundary Conditions for Difference Approximations to the Multidimensional Wave Equation. *Mathematics of Computation*, 47:437459, 1986.

[18] Higdon, R.L., Numerical Absorbing Boundary Conditions for the Wave Equation. *Mathematics of Computation*, 49:6590, 1987.

[19] Hagstrom, T. and Hariharan, S.I., Accurate Boundary Conditions for Exterior Problems in Gas Dynamics. *Mathematics of Computation*, 51:581597, 1988.

[20] Hagstrom, T. and Hariharan, S.I., Progressive wave expansions and open boundary problems. *In: Engquist, B. and Kriegsmann, G.A., Eds, Computational Wave Propagation (Springer, New York) 86, IMAVolumes in Mathematics and its Applications*, 86:2343, 1997.

[21] Hagstrom, T. and Goodrich, J., Experiments with Approximate Radiation Boundary Conditions for Computational Aeroacoustics. *Applied Numerical Mathematics*, 27:385402, 1998.

[22] Hagstrom, T. and Hariharan, S.I., A Formulation of Asymptotic and Exact Boundary Conditions Using Local Operators. *Applied Numerical Mathematics*, 27:403, 1998.

[23] Hariharan, S.I. and Hagstrom, T., Far Field Expansion for Anisotropic Wave Equations. *Journal of Computational Acoustics*, 2:283294, 1990.

[24] Roe, P.L., Remote Boundary Conditions for Unsteady Multidimensional Computations. *Computers and Fluids* 17:221231, 1989.

[25] Tam, C.K.W. and Dong, Z., Radiation and Outflow Boundary Conditions for Direct Computation of Acoustic and Flow Disturbances in a Nonuniform Mean Flow. *Journal of Computational Acoustics*, 4:175201, 1996.

[26] Tam, C.K.W., Kurbatskii, K.A. and Fang, J., *In: Tam, C.K.W. and Hardin, J.C., eds, Numerical Boundary Conditions for Computational Aeroacoustics Benchmark Problems, NASA CP-3352: Second Computational Aeroacoustics Workshop on Benchmark Problems*, pp 191219, 1997.

[27] Dong, T.Z., On Boundary Conditions for Acoustic Computations in Non-uniform Mean Flows. *Journal of Computational Acoustics*, 5, 297315, 1997.

[28] Berenger J. P., A Perfectly Mathced Layer for the Absorption of Electromagnetic Waves. *Journal of Computational Physics*, 114:185-200, 1994.

[29] Berenger J. P., Three-dimensional Perfectly Mathced Layer for the Absorption of Electromagnetic Waves. *Journal of Computational Physics*, 127:363-379, 1996.

[30] Hu F. Q., On Absorbing Boundary Conditions for Linearized Euler Equations by a Perfectly Matched Layer. *Journal of Computational Physics*, 129:201-219, 1996.

[31] Hesthaven J. S., On the Analysis and Construction of Perfectly Matched Layers for the Linearized Euler Equations. *Journal of Computational Physics*, 142:129-147, 1998.

[32] Hu F. Q., On Perfectly Matched Layer as an Absorbing Boundary Condition. *AIAA paper 96-1664*, 1996.

[33] Hayder M., Hu F. Q., and Hussaini Y. M., Toward Perfectly Absorbing Boundary Conditions for Euler Equations. *AIAA paper 97-2075*, 1997.

[34] Abarbanel S., Gottlieb D., A Mathematical Analysis of the PML Method. *Journal of Computational Physics*, 134:357-363, 1997.

[35] Qi Q., Geers T. L., Evaluation of the Perfectly Matched Layer for Computational Acoustics. *Journal of Computational Physics*, 139:166-183, 1998.

[36] Abarbanel S., Gottlieb D., Hesthaven J. S., Well-posed Perfectly Matched Layers for Advective Acoustics. *Journal of Computational Physics*, 154:266-283, 1999.

[37] Tam C. K. W., Auriault L., and Cambulli F., Perfectly Matched Layer as an Absorbing Boundary Condition for the Linearized Euler Equations in Open and Ducted Domains. *Journal of Computational Physics*, 144:213-234, 1998.

[38] Hu F., A Stable, Perfectly Matched Layer for Linearized Euler Equations in Unsplit Physical Variables. *Journal of Computational Physics*, 173:455480, 2001.

[39] Hu F., A Perfectly Matched Layer Absorbing Boundary Condition for Linearized Euler Equations with a Non-uniform Mean Flow. *Journal of Computational Physics*, 208:469492, 2005.

[40] Bjorn Engquist, Andrew Majda, Absorbing Boundary Conditions for the Numerical Simulation of Waves. *Mathematics of Computation*, 31(139):629:651, 1977.

[41] Andrew Majda, Stanley Osher, Reflection of Singularities at the Boundary. *Communications on Pure and Applied Mathematics*, 28:479-499, 1975.

[42] L. Nirenberg, Lectures on Linear Partial Differential Equations. *C. B. M. S Regional Conference Series in Mathematics*, 17, 1973.

[43] M. E. Taylor, Reflection of Singularities of Solutions to Systems of Differential Equations. *Communications on Pure and Applied Mathematics*, 28:457-478, 1975.

[44] Rodman, Laura C., The Application of Nonreflecting Boundary Conditions to 2-D Unsteady Computations on Curvilinear Grids. *AIAA-1990-1587, Fluid Dynamics, Plasma Dynamics and Lasers Conference*, 1990.

[45] G. W. Hedstrom, Nonreflecting Boundary Conditions for Nonlinear Hyperbolic Systems. *Journal of Computational Physics*, 30:222-237, 1979.

[46] M.B. Giles, Non-reflecting boundary conditions for Euler equation calculations. *AIAA Journal*, 28(12):2050-2058, 1990.

[47] M. B. Giles, Non-Reflecting Boundary Conditions for the Euler Equations. *Technical Report TR-88-1, MIT Computational Fluid Dynamics Laboratory*, 1988.

[48] L. N. Trefethen, L. Halpern, Well-posedness of One-way Wave Equations and Absorbing Boundary Conditions. *Mathematics of computation*, 47:421-435, 1986.

[49] M. B. Giles, UNSFLO: A Numerical Method for Calculating Unsteady Stator/Rotor Interaction. *Technical Report TR-86-6, MIT Computational Fluid Dynamics Laboratory*, 1986.

[50] A. Saxer and M.B. Giles, Quasi-3D Nonreflecting Boundary Conditions for Euler Equation Calculations. *AIAA Journal of Propulsion and Power*, 9(2):263-271, 1993.

[51] Marius C. Banica, Ian D. J. Dupree, R. Stewart Cant, Non-reflective Boundary Conditions for Non-uniform Velocity Inlet and Outlet Flows. *inter.noise 2006, Honolulu, Hawaii*, 114, Dec 2006.

[52] J. Oliger and A. Sundström, Theoretical and Practical Aspects of some Initial-boundary Value Problems in Fluid Dynamics. *SIAM Journal on Applied Mathematics*, 35(3): 419-446, 1978.

[53] J. C. Strikwerda, Initial Boundary Value Problems for Incompletely Parabolic Systems. *Communications on Pure and Applied Mathematics*, 30:797822, 1977.

[54] T. J. Poinsot and S. K. Lele, Boundary Conditions for Direct Simulations of Compressible Viscous Flow. *Journal of Computational Physics*, 101:104-129, 1992.

[55] P. Dutt, Stable Boundary Conditions and Difference Schemes for Navier-Stokes Equations. *SIAM Journal on Numerical Analysis*, 25(2):245-267, 1988.

[56] D. Rudy and J. Strikwerda, A Non-reflecting Outflow Boundary Condition for Subsonic Navier-Stokes Calculations. *Journal of Computational Physics*, 36:55-70, 1980.

[57] D. Rudy and J. Strikwerda, Boundary Conditions for Subsonic Navier-Stokes Calculations. *Computers and Fluids*, 9:327-228, 1981.

[58] J. Nordström, Accurate Solutions of the Navier-Stokes Equations despite Unknown Outflow Boundary Data, *Journal of Computational Physics*, 120:184-205, 1995a.

[59] J. Nordström, The use of Characteristic Boundary-conditions for the Navier-Stokes Equations. *Computers and Fluids*, 24(5):609-623, 1995.

[60] J. Nordström, M. H. Carpenter, Boundary and Interface Conditions for High-order Finite Difference Methods Applied to the Euler and Navier-Stokes Equations. *Journal of Computational Physics*,148:621645, 1999.

[61] G. B. Whitman, Linear and Nonlinear Waves. *John Wiley and Sons*, 1974.

[62] J. Mathews and R. L. Walker, Mathematical Methods of Physics. *W. A. Benjamin Inc.*, 1970.

[63] F. Collino, High Order Absorbing Boundary Conditions for Wave Propagation Models, Straight Line Boundary and Corner Cases. *Proceedings of the 2nd In-*

ternational Conference on Mathematical and Numerical Aspects of Wave Propagation, SIAM,161-171, 1993.

[64] C. W. Rowley, T. Colonius, Discretely Non-reflecting Boundary Conditions for Linear Hyperbolic Systems. *Journal of Computational Physics*, 157:500-538, 2000.

[65] Tam C. K. W., Dispersion-Relation-Preserving Finite Difference Schemes for Computational Acoustics. *Journal of Computational Physics*, 107:262-281, 1993.

[66] Ringleb, F., Exacte Losung der Differentialgleichung einer Adiabatischen Gasstromung. *ZAMM*, 20:185-198, 1940.

[67] Champan, C. J., High Speed Flow. *Cambridge University Press*, pp. 206, 2006

[68] Bonhaus, Daryl L., A Higher Order Finite Element Method for Viscous Compressible Flows. *Dissertation, Virginia Polytechnic Institute and State University*, pp 32-33.

[69] Hixon, R., Prefactored Small-Stencil Compact Schemes. *Journal of Computational Physics*,165:522-541, 2000.

[70] Satav, V., Validation of Wall Boundary Conditions Implemented in the BASS Code for Complex Wall Geometries. *M. S. Thesis, University of Toledo*, December 2004.

[71] Kennedy, C. A. and Carpenter, M. H., Several New Numerical Methods

for Compressible Shear-Layer Simulations. *Applied Numerical Mathematics*, 14:397-433, 1994.

[72] Hixon, R., Nallasamy, M., Sawyer, S., and Dyson, R., Unsteady Validation of a Mean Flow Boundary Condition for Computational Aeroacoustics. *AIAA Paper 2004-0521, Reno, NV*, 2004

[73] Hixon, R., Mankbadi, R. R., and Scott, J. R., Validation of a High-Order Prefactored Compact Code on Nonlinear Flows with Complex Geometries. *AIAA Paper 2001-1103, Reno, NV*, 2001.

[74] Hixon, R., Shih, S.-H., and Mankbadi, R. R., Evaluation of Boundary Conditions for the Gust-Cascade Problem. *Journal of Propulsion and Power*, 16:72-78, 2000.

[75] Tam, C. K. W. and Dong, Z., Wall Boundary Conditions for High-Order Finite-Difference Schemes in Computational Aeroacoustics. *Theoretical and Comp. Fluid Dynamics*,6:303-322, 1994.

[76] Hixon, R., Curvilinear Wall Boundary Conditions for Computational Aeroacoustics. *AIAA Paper 99-2395, Los Angeles, CA.*, 1999.

[77] Hixon, R., Nallasamy, M., and Sawyer, S., A Method for the Implementation of Boundary Conditions in High-Accuracy Finite-Difference Schemes. *AIAA Paper 2005-0608, Reno, NV*, 2005.